ECO-PHYSIOLOGICAL AND MOLECULAR MANIPULATION OF LEAF-LEVEL
PRIMARY AND SECONDARY METABOLISM BY ARTHROPOD HERBIVORY

BY

PAUL DAVID NABITY

DISSERTATION

Submitted in partial fulfillment of the requirements
for the degree of Doctor of Philosophy in Plant Biology
in the Graduate College of the
University of Illinois at Urbana-Champaign, 2012

Urbana, Illinois

Doctoral Committee:

      Professor Evan H. DeLucia, Chair
      Professor May R. Berenbaum
      Assistant Professor Andrew D.B. Leakey
      Professor Raymond E. Zielinski

ABSTRACT

Arthropod herbivory fundamentally alters ecosystem function and challenges agricultural productivity because herbivores alter photosynthesis. Feeding removes tissues and resources for growth but often introduces unseen physiological costs mediated by a reallocation in resources from growth to defense or by alterations to primary and secondary metabolism. The type of feeding damage depends on the mouthparts of the herbivore and, in part, determines the magnitude and mechanism by which photosynthesis is altered. However, there is a lack of understanding of these effects across model systems to evaluate conserved mechanisms of plant responses to herbivory. Documenting these responses from the observed and manipulated eco-physiological level down to the level of the gene can provide mechanistic understanding of how photosynthesis changes under herbivory and, ultimately, what initiates the reallocation of resources from primary to secondary metabolism (i.e., plant defense). Understanding the connections between genotype and phenotype can enhance our knowledge of ecosystem function amidst a rapidly changing climate by elucidating resource-driven trade-offs, and, as a result, forms the basis for this dissertation.

Plant responses to herbivory depend on the plant under attack and the attacking agent, but variability in the methods by which the interaction is observed makes it difficult to distinguish trends. As such, I synthesized the available literature in a review that elucidated four mechanisms for the alteration of photosynthesis at the leaf level. Arthropods sever vasculature, alter sink/source relationships, release autotoxic chemicals, or initiate a trade-off of resources from photosynthesis to defense in remaining leaf tissue. This review is presented in Chapter 2 and establishes the framework for the following chapters in which I investigate these mechanisms.

Because Earth is experiencing rapid environmental change, I surveyed leaf-level response of model forest species to multiple damage types when grown under predicted climate change conditions in Chapter 3. Elevated CO_2 attenuated damage for all damage types. As a result, the changing climate will, in part, attenuate the negative effects of herbivory on leaf-level photosynthesis. A common theme in this study and others is that damage to remaining leaf tissue from defoliation declines with time across species; however, contrary examples exist where inducible processes interact more with photosynthesis. Therefore I examined how inducible defense signaling and metabolite production altered photosynthesis in Chapter 4. I found that wound signaling immediately impaired electron transport, and defense synthesis correlated with sustained reductions in photosynthesis. Taken together, these data indicate a conserved mechanism underlying defense signaling modulates the trade-off from using resources for growth to defense.

As the preceding chapters suggest, hidden physiological costs can reduce photosynthesis relative to the damage type. Insect parasites of plants may influence leaf and canopy-level processes through the manipulation of sink/source dynamics by an unknown mechanism. In Chapter 5 I reexamined the grape-phylloxera system to reveal that the gall-forming insect parasite phylloxera induces functional stomata and globally reconfigures plant metabolism at the genomic level to enhance insect fitness. Although insect-induced stomata are rare in nature, the transcriptional pattern of gall formation is likely conserved among insect parasites and facilitates the galling habit by increasing competitive sink strength of the insect.

The following chapters provide a framework for assessing how arthropod herbivores alter leaf function across damage type and plant species. By characterizing mechanisms within model

systems, I believe I have uncovered some of the physiological costs of herbivory that modulate resource-driven trade-offs in nature.

ACKNOWLEDGMENTS

This dissertation is the culmination of thoughts and effort from many people. I thank my advisor Evan DeLucia for his guidance, patience, and exceptional foresight. He allowed me unbounded freedom to seek answers to many questions and nurtured my development into a plant biologist. I also thank May Berenbaum. She opened her lab to me and stimulated my inner entomologist with endless ideas. Together Evan and May provided balance in every way. I am grateful to the other members of my committee for their advice and friendship: Andrew Leakey was especially insightful on my experimental approaches and data presentation whereas Ray Zielinski allowed me unlimited access to his microscope and offered exceptionally reassuring conversations on my progress and development as a scientist.

I am especially grateful for the friendship and instruction in teaching I found in Carol Augspurger. I now consider myself a field biologist and will always look forward to the next field trip with friends, family, or students. I thank Tom Jacobs, too, as he has profound insight into plant development and provided me with many thought-provoking discussions. I thank Art Zangerl for the short time I knew him for he provided the structural framework of the model used in Chapter 2, and whimsical, yet rational, insight for how to maintain balance in academia.

Thank you to members of the DeLucia lab for your fun times and encouraging words: Krista Anderson-Teixeira, Damla Bilgin, Chris Black, Clare Casteel, Sarah Davis, John Drake, Ben Duval, Mike Masters, Saber Miresmailli, Olivia Niziolek, Lisa Raetz, Jorge Zavala.

Thank you to the members of the GEGC for lasting friendships, advice, and baked goods: Sharon Gray, Kat Grennan, Melinda Laborg, Anna Locke, Cody Markelz, Don Ort, David Rosenthal, Rebecca Slattery. Thank you to the PBAGS, GEEB, and Ian Kirwan for friendships and social distractions. Thank you to Mike Hillstrom, John Couture, and Rick Lindroth for

TABLE OF CONTENTS

CHAPTER 1

INTRODUCTION

BACKGROUND

Herbivory fundamentally alters ecosystem function and challenges agricultural productivity. Globally, herbivores may consume 18% of primary production in terrestrial ecosystems (Cyre and Pace 1993) but, in the absence of crop protection, reduce agricultural yield >60% (Oerke and Dehne 1997, Oerke 2006). Herbivore damage is typically assessed through visual survey; however, this approach assumes that the remaining leaf tissue functions normally. Recent assessments of this remaining tissue using non-invasive techniques reveal a range of nonvisible effects of herbivory that may double photosynthetic reductions to the individual plant and thereby contribute to substantial underestimates of losses in productivity (Zangerl et al. 2002, Aldea et al. 2006b, Patankar et al 2011, Pinkard et al. 2011).

The manner in which herbivores feed largely determines the magnitude of reductions in productivity (Zvereva et al. 2010, Patankar et al. 2011) and can be linked to damage-specific alterations of photosynthetic capacity (Welter 1989). Tissue consumption by defoliators removes photosynthetic leaf area whereas photosynthate extraction by piercing-sucking insects alters uptake and movement of carbon within the plant (see Welter 1989). The direct impact of herbivory on photosynthesis is well characterized, but remaining tissues also respond to the type of damage with varying degrees of photosynthetic reduction; minimal defoliation reduces photosynthesis four-fold in remaining leaf tissue in some species (Zangerl et al. 2002), whereas similar damage reduces photosynthesis in remaining tissues equal to the area removed in other species (Aldea et al. 2006b). Understanding these effects on photosynthesis among damage types and within model systems where genomic information is readily accessible may help link the

observed global genomic down-regulation of photosynthetic genes (Bilgin et al. 2010) to

reductions in growth. Moreover, this damage-specific alteration of photosynthesis links

herbivore-specific elicitors to the magnitude and type of plant response (Halitschke et al. 2011,

Heil et al. 2012) in determining the damage to remaining leaf tissue, including the ultimate

fitness cost.

Selection is greatest for plants to optimize resource use when attacked by herbivores to

avoid greater costs to fitness (e.g., Rhoades 1979, Herms and Mattson 1992) but the mechanisms

that regulate these trade-offs are less well understood. The direct loss of tissues reduces potential

growth and tissues adjacent to feeding damage also may reduce photosynthesis and thereby

contribute to reductions in productivity (Aldea et al. 2006b, Chapters 2-4). But beyond this

damage, feeding elicits interactive hormone signaling that induces defenses and initiates the

trade-off between using resources for growth or defense. The defense response is often specific

to the herbivore-plant interaction (Walling 2000), but the generic response to chewing herbivores

is the elicitation of the wound-signaling pathway. This pathway initiates defenses that vary in

their resource requirements for synthesis and fitness costs (Kessler et al. 2004). Gene expression

and proteomic surveys of herbivory have implicated candidate mechanisms regulating the switch

from growth to defense (Heidal and Baldwin 2004, Giri et al. 2006, Maserti et al. 2010, Chen et

al. 2011), but the functional physiology linking how defense synthesis alters resource supply

(i.e., photosynthesis) is only beginning to be understood (Zangerl et al. 1997, Zangerl et al. 2002,

Tang et al. 2009, Halitschke et al. 2011).

Among damage types galling endoparasites are unique in that their feeding behavior

induces variable morphologies that interact with photosynthesis across scales. For example, gall

damage may reduce canopy photosynthesis up to 60% in mature trees and thereby reduce

ecosystem productivity (Patankar et al. 2011). At finer scales, galls reduce photosynthesis in gall tissues (e.g., Welter 1989) but can increase and decrease photosynthesis of remaining tissues (Retuerto et al. 2004, Dorchin et al. 2006). This variability in response may reflect the complex nature of the galling habit, a lack of understanding how it is mechanistically regulated, or the competitive nature of sinks within plants. Galls directly compete for mobilized nutrients with meristems or developing reproductive structures that function as natural plant sinks, but also compete with intra- or interspecific induced sinks. This competitive environment drives gall evolution (Inbar et al. 2004) and favors the strongest sink (Larson and Whitham 1997, Compson et al. 2011). There appears to be a genetic basis for manipulating sink-source relationships and thereby altering photosynthesis in remaining leaf tissue (Compson et al. 2011) but there is a lack of understanding underlying how insect parasites initiate and maintain control over photosynthesis.

Human activities are rapidly changing the chemistry of the atmosphere and the associated increase in carbon dioxide (~ 2 µl l^{-1} yr^{-1}; www.esrl.noaa.gov/gmd/ccgg/trends/) generally enhances photosynthesis of forest ecosystems (Saxe et al. 1998; Leakey et al. 2009; Lindroth 2010). Despite this enhancement, indirect modifications of the herbivore community and changes in host plant chemistry (Hillstrom 2010, Lindroth 2010) increase damage rates by herbivores in forests elevated CO_2 levels (Couture et al. 2011). Because increased CO_2 stimulates photosynthesis and may reduce transpiratory loss by appressing stomatal aperture, the predicted increases in atmospheric CO_2 may modulate the effect of herbivory on photosynthesis; however, this scenario remains to be tested.

Non-invasive imaging technologies are powerful tools for making high-resolution, spatially resolved measurements of component processes of photosynthesis in damaged leaf

tissues (Oxborough 2004, Aldea et al. 2006a). Chlorophyll fluorescence is highly correlated with the rate of CO_2 uptake in intact leaves (Genty et al. 1989, Baker and Oxborough 2005, Tang et al. 2006) and relates directly to carbon assimilation, an ecologically important trait. Thermography allows for mapping changes in temperature associated with variation in heat flux across leaf surfaces (Jones 1999, Omasa and Takayama 2003) and can be calibrated to visualize changes in stomatal conductance (Jones 2004, Bajons et al. 2005, Grant et al. 2006). The application of these techniques is advancing our understanding of how herbivory alters remaining tissues by revealing hidden costs associated with herbivory. Of the few systems examined with these technologies (*Pastinaca sativa* L., *Glycine max* L., *Arabidopsis thaliana* L. Heynh., various hardwood trees), new insight into the mechanisms regulating herbivore impact on leaves and ultimately ecosystems has been revealed; however, the vast number of plant-insect interactions warrant further study to identify conserved plant responses that link trade-offs between photosynthesis and fitness.

OVERVIEW

How do we assess the effects of herbivory on leaf-level processes to investigate hidden physiological costs to photosynthesis?

To assess how different damage types alter photosynthesis, I conducted a literature review (Chapter 2) that examined novel and emerging technologies applied to the study of plants. These processes aim to elucidate dynamic, in-vivo, and previously undocumented alterations of leaf-level photosynthesis. Four mechanisms emerged to account for how arthropods alter photosynthesis in remaining undamaged tissue, henceforth termed *propagated damage*: 1) Severing vasculature alters leaf hydraulics, and, subsequently, water and nutrient

transport in the xylem. 2) Insect feeding can be subtle enough to avoid outright cell rupture and, by extracting photosynthate, alters sink/source relationships within and among leaves. 3) Defense-induced autotoxicity occurs when the rupture of cells releases generically biocidal compounds that disrupt homeostatic mechanisms vital for plant function. 4) Defense-induced down-regulation of photosynthesis occurs when insect attack, or even the perception of attack, induces a myriad of defense-related secondary metabolites while concomitantly reducing the expression of photosynthesis-related genes. These themes were subsequently investigated across several model species and within environmental context to increase understanding of the mechanisms regulating the observed responses.

How will a rapidly changing climate alter these leaf-level effects in the future?

Human activities are rapidly altering atmospheric chemistry, including the concentration of CO_2, which directly impacts leaf-level photosynthesis and water use efficiency. Therefore, in Chapter 3 I examined how the effect of elevated CO_2 alters leaf function across damage types using a model hardwood tree species at the aspen Free Air Concentration Enrichment (FACE) site in Rhinelander, Wisconsin. Chlorophyll fluorescence decreased for all damage types in damaged tissue and in adjacent undamaged tissues whereas the thermal signature of tissues depended on the herbivore's mode of feeding. Elevated CO_2 attenuated the magnitude of damage for all damage types at the leaf level.

How will plant defense response modulate the effects of herbivory on photosynthesis?

Herbivores reduce plant fitness by inducing defenses that reprogram plant metabolism through a reallocation of resources to defense. This fitness cost cannot be explained by the

synthesis of metabolites alone and suggests hidden costs to photosynthesis (Chapter 2). To elucidate the photosynthetic mechanisms by which defense induction reduces photosynthesis, I investigated the physiological and molecular crosstalk occurring with herbivore-elicited jasmonic acid (JA) defenses in Chapter 4. Using plants with impaired JA-signaling (and therefore reduced plant defenses), I determined that the act of JA signaling impairs photosynthetic electron transport and ultimately prolongs the suppression of photosynthesis. As a result, JA signaling involves a complex network where electron donors facilitate reductions in downstream carbon assimilation upon induction of JA dependent defenses.

How does gall formation alter leaf development and reduce photosynthesis?

Feeding by some insects increases cell proliferation and differentiation into protective enclosures i.e., galls, with specialized morphologies and biochemistries hypothesized to serve the developing parasite (Stone and Schonrogge 2003). To test this extended phenotype hypothesis and characterize the mechanisms underlying arthropod manipulation of sink/source association within a leaf (Chapter 2) I examined leaf gall formation by phylloxera in its coevolved, economically and culturally valued grape host. I determined that phylloxera globally controls leaf carbon metabolism by inducing functional stomata where none typically occur, and by transforming the transcriptional pattern of the leaf into a carbon sink. This physiological and genomic control over carbon uptake and metabolism provides the most extensive evidence in support of the extended phenotype to date.

LITERATURE CITED

Aldea M, Frank TD, DeLucia EH. 2006a. A method for quantitative analysis of spatially variable physiological processes across leaf surfaces. Photosynthesis Research 90: 161–172.

Aldea M, Hamilton JG, Resti JP, Zangerl AR, Berenbaum MR, Frank TD, DeLucia EH 2006b. Comparison of photosynthetic damage from arthropod herbivory and pathogen infection in understory hardwood samplings. Oecologia 149: 221–232.

Bajons P, Klinger G, Schlosser V. 2005. Determination of stomatal conductance by means of infrared thermography. Infrared Physics and Technology 46: 429–439.

Bilgin DD, Zavala JA, Zhu J, Clough SJ, Ort DR, DeLucia EH. 2010. Biotic stress globally down-regulates photosynthesis genes. Plant Cell and Environment. 33: 1597-1613.

Baker NR, Oxborough K. 2005. Chlorophyll fluorescence as a probe of photosynthetic productivity. Chlorophyll a fluorescence – A signature of photosynthesis. Papageorgiou GC and Govindjee (eds.) Springer: 65-82.

Chen Y, Pang Q, Dai S, Wang Y, Chen S, Yan X. 2011. Proteomic identification of differentially expressed proteins in *Arabidopsis* in response to methyl jasmonate. Journal of Plant Physiology 168: 995-1008.

Compson ZG, Larson KC, Zinkgraf MS, Whitham TG. 2011. A genetic basis for the manipulation of sink-source relationships by the galling aphid *Pemphigus batae*. Oecologia 167: 711-721.

Couture JJ, Meehan TD, Lindroth RL. 2011. Atmospheric change alters foliar quality of host trees and performance of two outbreak insect species. Oecologia 168: 863-876.

Cyr H, Pace ML. 1993. Magnitude and patterns of herbivory in aquatic and terrestrial ecosystems. Nature 361: 148–150.

Dorchin N, Cramer MD, Hoffmann JH. 2006. Photosynthesis and sink activity of wasp-induced galls in *Acacia pycnantha*. Ecology 87: 1781–1791.

Genty B, Briantais JM, Baker NR. 1989. The relationship between the quantum yield of photosynthetic electron transport and quenching of chlorophyll fluorescence. Biochimica et Biophysica Acta 990: 87–92.

Giri AP, Wunsche H, Mitra S, Zavala JA, Muck A, Svatos A, Baldwin IT 2006. Molecular interactions between the specialist herbivore *Manduca sexta* (Lepidoptera, Sphingidae) and its natural host *Nicotiana attenuata*. VII. Changes in the plant's proteome. Plant Physiology 142: 1621–1641.

Grant OM, Caves MM, Jones HG. 2006. Optimizing thermal imaging as a technique for detecting stomatal closure induced by drought stress under greenhouse conditions. Physiologia Plantarum 127: 507–518.

Halitschke R, Hamilton JG, Kessler A. 2011. Herbivore-specific elicitation of photosynthesis by mirid bug salivary secretions in the wild tobacco Nicotiana attenuata. New Phytologist 191: 528-535.

Heidel AJ, Baldwin IT. 2004. Microarray analysis of salicylic acid- and jasmonic acid-signaling in responses of *Nicotiana attenuata* to attack by insects from multiple feeding guilds. Plant, Cell and Environment 27: 1362–1373.

Heil M, Ibarra-Laclette E, Adame-Alvarez RM, Martinez O, Ramirez-Chavez E, Molina-Torres J, Herrera-Estrella L. 2012. How plants sense wounds: damaged-self recognition is based on plant derived elicitors and induces octodecanoid signaling. PLoS One 7: e30537.

Herms DA, Mattson WJ. 1992. The dilemma of plants: to grow or defend. Quarterly Review of Biology 67:283-334.

Hillstrom ML. 2010. Effects of elevated carbon dioxide and ozone on forest insect abundance, diversity, and community composition. PhD dissertation, University of Wisconsin, Madison.

Inbar M, Wink M, Wool D. 2004. The evolution of host plant manipulation by insects: molecular and ecological evidence from gall-forming aphids on *Pistacia*. Molecular Phylogenetics and Evolution 32: 504-511.

Jones H. 1999. Use of thermography for quantitative studies of spatial and temporal variation of stomatal conductance over leaf surfaces. Plant, Cell and Environment 22: 1043–1055.

Jones HG. 2004. Application of thermal imaging and infrared sensing in plant physiology and ecophysiology. Advances in Botanical Research Incorporating Advances in Plant Pathology 41: 107–163.

Kessler A, Halitschke R, Baldwin IT. 2004. Silencing the jasmonate cascade: induced plant defenses and insect populations. Science 305: 665-668.

Larson KC, Whitham TG. 1997. Competition between gall aphids and natural plant sinks: plant architecture affects resistance to galling. Oecologia 109: 575-582.

Leakey ADB, Ainsworth EA, Bernacchi CJ, Rogers A, Long SP, Ort DR. 2009 Elevated CO_2 effects on plant carbon, nitrogen, and water relations: six important lessons from FACE. Journal of Experimental Botany 60: 2859–2876.

Lindroth RL. 2010. Impacts of elevated atmospheric CO_2 and O_3 on forests: phytochemistry, trophic interactions, and ecosystem dynamics. Journal of Chemical Ecology 36: 2-21.

Maserti BE, Del Carratore R, Della Croce CM, Podda A, Migheli Q, Froelicher Y, Luro F, Morillon R, Ollitrault P, Talon M, Rossignol M. 2010. Comparative analysis of proteome changes induced by the two-spotted spider mite *Tetranychus urticae* and methyl jasmonate in citrus leaves. Journal of Plant Physiology. 168: 392-402.

Oerke EC. 2006. Crop losses to pests. Journal of Agricultural Science 144: 31-43.

Oerke EC, Dehne HW. 1997. Global crop production and the efficacy of crop protection – current situation and future trends. European Journal of Plant Pathology 103: 203–215.

Omasa K, Takayama K. 2003. Simultaneous measurement of stomatal conductance, non-photochemical quenching, and photochemical yield of photosystem II in intact leaves by thermal and chlorophyll fluorescence imaging. Plant Cell Physiology 44: 1290–1300.

Oxborough K. 2004. Imaging of chlorophyll a fluorescence: theoretical and practical aspects of an emerging technique for the monitoring of photosynthetic performance. Journal of Experimental Botany 55: 1195–1205.

Patankar R, Thomas SC, Smith SM. 2011. A gall-inducing arthropod drives declines in canopy photosynthesis. Oecologia 167: 701-709.

Pinkard EA, Battaglia M, Roxburgh S, O'Grady AP. 2011. Estimating forest net primary production under changing climate: adding pests into the equation. Tree Physiology 31: 686-699.

Retuerto R, Fernandez-Lema B, Rodriguez-Roiloa S, Obeso JR. 2004. Increased photosynthetic performance in holly trees infested by scale. Functional Ecology 18: 664–669.

Rhoades DF. 1979. Evolution of plant chemical defense against herbivores In: Rosenthal G, Janzen D, eds. Herbivores: their interaction with secondary plant metabolites. Academic Press, New York, pp 353.

Saxe H, Ellsworth DS, Heath J. 1998. Tree and forest functioning in an enriched CO_2 atmosphere. New Phytologist 139: 395–436.

Tang JY, Zielinski RE, Zangerl AR, Crofts AR, Berenbaum MR, DeLucia EH. 2006. The differential effects of herbivory by first and fourth instars of *Trichoplusia ni* (Lepidoptera: Noctuidae) on photosynthesis in *Arabidopsis thaliana*. Journal of Experimental Botany 57: 527–536.

Tang JY, Zielinski R, Aldea M, DeLucia EH. 2009. Spatial association of photosynthesis and chemical defense in *Arabidopsis thaliana* following herbivory by *Trichoplusia ni*. Physiologia Plantarum 137: 115-124.

Walling LL. 2000. The myriad plant responses to herbivores. Journal of Plant Growth and
        Regulation 19: 195-216.

Welter SC. 1989. Arthropod impact on plant gas exchange. In: Bernays EA, ed. Insect–plant
        interactions. Boca Raton, FL: CRC Press, 135–151.

Zangerl AR, Arntz AM, Berenbaum MR. 1997. Physiological price of an induced chemical
        defense: photosynthesis, respiration, biosynthesis, and growth. Oecologia 109: 433-441.

Zangerl AR, Hamilton JG, Miller TJ Crofts AR, Oxborough K, Berenbaum MR, et al 2002.
        Impact of folivory on photosynthesis is greater than the sum of its holes. Proceedings of
        the National Academy of Sciences of the USA 99: 1088–1091.

Zvereva EL, Lanta V, Kozlov MV. 2010. Effects of sap-feeding insect herbivores on growth and
        reproduction of woody plants: a meta-analysis of experimental studies. Oecologia 163:
        949-960.

CHAPTER 2

INDIRECT SUPPRESSION OF PHOTOSYNTHESIS ON INDIVIDUAL LEAVES BY

ARTHROPOD HERBIVORY[1]

ABSTRACT

Herbivory reduces leaf area, disrupts the function of leaves, and ultimately alters yield and productivity. Herbivore damage to foliage typically is assessed in the field by measuring the amount of leaf tissue removed and disrupted. This approach assumes the remaining tissues are unaltered, and plant photosynthesis and water balance function normally. However, recent application of thermal and fluorescent imaging technologies revealed that alterations to photosynthesis and transpiration propagate into remaining undamaged leaf tissue. This review briefly examines the indirect effects of herbivory on photosynthesis, measured by gas exchange or chlorophyll fluorescence, and identifies four mechanisms contributing to the indirect suppression of photosynthesis in remaining leaf tissues: severed vasculature, altered sink demand, defense-induced autotoxicity, and defense-induced down-regulation of photosynthesis. We review the chlorophyll fluorescence and thermal imaging techniques used to gather layers of spatial data and discuss methods for compiling these layers to achieve greater insight into mechanisms contributing to the indirect suppression of photosynthesis. We also elaborate on a few herbivore-induced gene-regulating mechanisms that modulate photosynthesis and discuss the difficult nature of measuring spatial heterogeneity when combining fluorescence imaging and gas exchange technology. Although few studies have characterized herbivore-induced indirect effects on photosynthesis at the leaf level, an emerging literature suggests that the loss of

---

photosynthetic capacity following herbivory may be greater than direct loss of photosynthetic tissues. Depending on the damage guild, ignoring the indirect suppression of photosynthesis by arthropods and other organisms may lead to an underestimate of their physiological and ecological impacts.

INTRODUCTION

Insects consume vast quantities of plant biomass each year, but simply considering the amount of tissue removed may underestimate their impact on yield and ecosystem production. On average, herbivores remove approx. 15% of primary production in terrestrial ecosystems, but complete removal is not uncommon in out-break years (Cyre and Pace 1993). Similarly, insects consume approx. 14% of total global agricultural output (Oerke and Dehne 1997). This value is relatively low because of the widespread application of pesticides. In the absence of pesticides, losses would exceed 50% for all major crops (Oerke and Dehne 1997). Herbivore damage is assessed in agricultural fields by surveying the amount of tissue removed from foliage. This approach, however, assumes that the remaining leaf tissue functions normally. Many types of insect damage affect photosynthesis in undamaged tissues, and these 'indirect' effects on photosynthesis may be considerably greater than the direct removal of leaf area (Welter 1989, Zangerl et al. 2002).

Insect herbivory, whether defoliation or by feeding on specific tissues (e.g. phloem or xylem), triggers a complex and interacting array of molecular and physiological responses in plants. These responses potentially reduce the photosynthetic capacity in remaining leaf tissues to a greater extent than the direct removal of photosynthetic surface area. For example, the removal of only 5% of the area of an individual *Pastinaca sativa* L. leaf by caterpillars reduced

photosynthesis by 20% in the remaining foliage (Zangerl et al. 2002), and the decline in photosynthesis in the remaining leaf tissue of a *Quercus alba* L. sapling was equal to the decrease in photosynthesis associated with the actual removal of leaf tissue (Aldea et al. 2006b). The mechanisms reducing photosynthesis in remaining leaf tissues are multifaceted, ranging from disruptions in fluid or nutrient transport to self-inflicted reductions in metabolic processes. However, the magnitude of these effects on photosynthesis and the underlying mechanisms are highly variable, depending in large part on the type of feeding damage and the mode of defense deployed by the plant under attack.

In this review, we build upon previous evaluations of the effects of insect herbivory on photosynthesis (Welter 1989, Peterson and Higley 2001) by examining feeding-induced spatial heterogeneity in photosynthesis across individual leaves. The application of fluorescence imaging techniques (Rolfe and Scholes 1995, Baker et al. 2001) is providing new insight into how different damage guilds, including pathogens and insects, affect the component processes of photosynthesis. When combined with other imaging methods such as thermography, the use of reporter genes to follow transcription, and fluorescent dyes that track signaling compounds (e.g. Ca^{2+} ions, H_2O_2), the mechanisms responsible for altering photosynthesis in remaining tissues are being elucidated. The use of geographic image analysis as a tool for making quantitative comparisons of images representing different biological processes is discussed, as this method provides the capability to compile many layers of covariate information to reveal new mechanistic insights.

Indirect versus direct effects of herbivory on photosynthesis

Plant responses to arthropod herbivory traditionally have been assessed from the guild perspective, where different insect guilds are defined by their feeding mechanisms (Welter 1989,

Peterson and Higley 2001). These guilds (e.g. chewing damage, piercing damage, etc.) were established in an effort to recognize 'homogeneity in physiological response' between different attacking agents (arthropods) that alter plant physiological processes in a similar manner (Higley et al. 1993). Using this guild approach, Welter (1989) examined an extensive body of literature across multiple guilds and found over 50% of all plant–insect interactions resulted in a loss of photosynthetic capacity. Defoliation generally increases photosynthesis, whereas specialized cell-content feeding decreases photosynthesis. Since then, several studies have examined plant responses to different insect feeding guilds and even to different insects within guilds in an effort to develop models for predicting plant response to different feeding mechanisms (see Peterson and Higley 2001).

A review of the recent literature is not entirely consistent with the conclusions stated by Welter (1989). Feeding on specialized tissues typically reduces photosynthesis, regardless of whether the attacked component is the phloem or xylem (Haile et al. 1999, Macedo et al. 2003a, b, Heng-Moss et al. 2006), the stem (Macedo et al. 2005, 2007) or general leaf fluids (Haile and Higley 2003). There is some evidence indicating that increased photosynthesis occurs in the presence of phloem feeding, particularly when the annual photosynthesis rate is estimated (Dungan et al. 2007). In contrast, defoliation injury often does not alter photosynthetic capacity, within plant families (e.g. legumes) or between hardwoods and crops (Peterson et al. 1992, 1996, 2004); however, there are examples where defoliation reduced (Delaney and Higley 2006) or increased photosynthesis (Turnbull et al. 2007).

The removal of leaf tissue by herbivores represents a 'direct' reduction of photosynthetic capacity. The suppression of photosynthesis in remaining leaf tissue is defined by any one of a number of processes, including damage to the vasculature supplying that tissue, as an 'indirect'

effect of herbivory. Arthropods damage xylem or phloem (Welter 1989), which may alter water transport, stomatal aperture, and sucrose transport and loading, thereby reducing photosynthesis in remaining leaf tissue. Severing tissue vasculature alters leaf hydraulics, and, subsequently, nutrient or osmotica transport (Sack and Holbrook 2006). If insect feeding is subtle enough to avoid outright cell rupture, modulation of nutrients sequestered by feeding will alter plant osmotica or sink/source relationships (Girousse et al. 2005, Dorchin et al. 2006). These effects also may be mediated by the plant's response. Insect attack, or even the perception of attack, can induce a myriad of defense-related responses while concomitantly reducing the expression of photosynthesis-related genes (Kessler and Baldwin 2002). In instances where plant defenses are constitutively expressed, the release of biocidal compounds against attackers may damage photosynthetic or homeostatic mechanisms vital for plant function (e.g. Zangerl et al. 2002). Indirect effects of herbivory were assigned to four classes: severed vasculature, altered sink demand, defense-related autotoxicity, and defense-induced down-regulation of photosynthesis (Figure 2.1).

Severed vasculature alters photosynthesis and water balance

Damage to leaf venation alters leaf hydraulic conductance thereby reducing stomatal conductance and photosynthesis. In the absence of alternative pathways for water transport, the consequences of damage to venation can persist for weeks after the initial injury and lead to leaf desiccation (Sack and Holbrook 2006). Defoliation injury that severs venation indiscriminately or feeding on specific tissues may physically obstruct fluid flow with insect mouthparts (stylets) or cell fragments and alter photosynthesis and water balance in remaining leaf tissue (Reddall et al. 2004; Delaney and Higley 2006). In *Glycine max* L. (soybean) a form of defoliation (skeletonization) that removes patches of tissue reduced photosynthesis in remaining tissue on

damaged leaves and on adjacent undamaged leaflets (Peterson et al. 1998). Interestingly, soybean increased carbon uptake rates and transpiration in remaining leaf tissue when one or two leaflets were completely lost (Suwignyo et al. 1995), but when leaf area removal (no patches) occurred to only part of a leaflet, CO_2 uptake did not decrease in the remaining leaflet tissue (Peterson et al. 2004).

Aldea et al. (2005) confirmed that skeletonizing of soybean leaves by Japanese beetles substantially increased water loss from the cut edges. Damaging the inter-veinal tissue increased transpiration by 150 % for up to 4 d post-injury. While this uncontrolled water loss had no detectable effect on CO_2 exchange, severed vasculature induced a short-lived (2 d) increase in photosynthetic efficiency (ΦPSII) in undamaged tissue of damaged leaves. The increase in ΦPSII without a corresponding increase in CO_2 uptake suggests that insect damage transiently decoupled photosynthetic electron transport from carbon assimilation (Aldea et al. 2005). Severing veins and inter-veinal tissue alters the hydraulic construction of leaves by reducing resistance exponentially with increasing damage (Nardini and Salleo 2005).

The effects of defoliation on photosynthesis seem to be less predictable than damage caused by other feeding guilds. In hardwoods, leaf gall and fungal damage consistently reduced ΦPSII at distances >1 cm from the point of direct damage, whereas defoliation resulted in only highly local reductions (<1 mm) in ΦPSII (Aldea et al. 2006b). With one exception, defoliation of soybean and *Arabidopsis thaliana* L. Heynh. leaves caused only a minimal reduction in ΦPSII. When compared with the mild effect of feeding by larger 4th instar *Trichoplusia ni* (Hubner) larvae, damage by smaller 1st instars severely depressed ΦPSII, maximum photosynthetic efficiency, and nonphotochemical quenching (NPQ) in *Arabidopsis* (Tang et al. 2006). The greater perimeter-to-area ratio of the numerous small holes produced by 1st instars

compared with 4th instars may have promoted greater rates of water loss from the cut edges and a corresponding reduction in ΦPSII. That the reduction in ΦPSII could be reversed by exposing the leaf to higher concentrations of CO_2 suggests that profligate water loss near cut edges reduced ΦPSII and increased NPQ by causing localized stomatal closure in the remaining undamaged leaf tissue.

Herbivory alters sink demand

In instances where plants respond to herbivory with increased CO_2 uptake, the mechanism typically is linked to compensation or an increase in the sink demand within the leaf. An extensive literature exists on photosynthetic compensation for arthropod herbivory (see Trumble et al. 1993); yet recent examples have highlighted previously uncharacterized compensatory responses. For some gall-forming insects, gall tissue itself increases photosynthesis relative to uninjured tissue. In *Ilex aquifolium* L. (holly), increased ΦPSII and electron transport rate enhanced photosynthesis (Retuerto et al. 2004) whereas a reduction in respiration in *Acacia pycnantha* Benth. galls contributed to an increase in net photosynthesis (Dorchin et al. 2006). While phloem feeding increased whole-canopy photosynthesis in beech trees, perhaps through a reduction in photosynthate build-up, the mechanism remains unclear and may be as simple as herbivore preference for hosts with higher rates of photosynthesis (Dungan et al. 2007).

In other galls of hardwoods, feeding damage reduced photosynthesis and altered water balance. Gall formation in red maple, pignut hickory, and black oak reduced ΦPSII, but increased NPQ, indicating a down-regulation of the PSII reaction centers in the area around galls (Aldea et al. 2006b). A sharp reduction in leaf temperature near galls suggests that transpiration was greater and fluid and nutrient transport increased near the point of damage (Macfall et al.

17

1994). In contrast to gall-forming insects, a leaf-mining moth that lives enclosed within leaf tissue of *Malus communis* Lamk (apple) trees, reduced carbon assimilation rates by decreasing transpiration (Pincebourd et al. 2006); however, the effects of this guild on plant physiology have yet to be evaluated using fluorescence and thermal imaging.

Defoliation also may increase photosynthesis by altering sink demand, but concerns over what and how remaining tissues were measured have been noted (Welter 1989). By enclosing severed edges within gas exchange cuvettes or measuring treatment effects on leaves where adjacent leaves were removed (within-plant controls), the data may not accurately describe plant responses specific to the herbivory treatment. Despite these potential limitations, data suggest that defoliation, as well as removal of reproductive and other vegetative sinks, may improve photosynthesis in remaining leaf tissue by increasing carboxylation efficiency and the rate of RuBP regeneration (Layne and Flore 1992, Holman and Oosterhuis 1999, Thomson et al. 2003, Ozaki et al. 2004, Turnbull et al. 2007).

Plant responses induce autotoxicity

Plants invest in defenses differently depending upon taxa, habitat, and resource availability (Fine et al. 2006), and many chemical defenses are known for both model plant systems and across less-studied taxa (Coley and Barone 1996, Berenbaum and Zangerl 2008). Plants run the risk of autotoxicity because of the biocidal properties of many secondary compounds. Although in vivo studies of autotoxicity are limited, photosynthesis may be severely reduced for some species. For example, wild parsnip (*Pastinaca sativa*) contains an arsenal of defense compounds including furanocoumarins, which are photoactivated and biocidal against a variety of organisms (Arnason et al. 1991). Furanocoumarins are contained in oil tubes under positive pressure and bleed profusely from the wounding site (Gog et al. 2005). When herbivores

sever these tubes, the release of furanocoumarins reduces ΦPSII and gas exchange at considerable distances from the actual point of insect damage (Zangerl et al. 2002, Gog et al. 2005).

The autotoxic effect of defensive compounds on photosynthesis is highly species specific. Essential oils derived from parsley (*Petroselinum crispum* Mill), wild parsnip, and rough lemon (*Citrus jambhiri* Lush.) reduce ΦPSII when applied to leaves of conspecifics; however, oils from parsley affected a 2-fold greater area than the other species (Gog et al. 2005). Baldwin and Callahan (1993) fed nicotine to two species of tobacco (*Nicotiana sylvestris* Speg. & Comes, *N. glauca* Graham) that naturally synthesized this alkaloid as a defense (Kessler and Baldwin 2002), and to two other solanaceous species lacking nicotine (*Datura stramonium* L., *Solanum lycopersicum* L.). Photosynthetic rates declined in both species that synthesize nicotine but only in one that did not (*S. lycopersicum*). Priming plants with nicotine (simulated damage) prior to being fed reduced photosynthetic rates more than in damaged-unfed plants, linking nicotine toxicity to the reduction in photosynthesis. Reduced photosynthesis, in part, reduced total growth and fitness. Subsequently, plants producing nicotine constitutively or upon the induction of defense are likely to endure autotoxicity and reductions in fitness.

Defense-induced down-regulation of photosynthesis-related genes

Jasmonates play a central role in regulating plant defense responses to herbivores. The mechanism by which herbivore-induced jasmonate synthesis promotes global reprogramming of defense gene expression and the regulation of this response have been reviewed recently (Howe and Jander 2008). While jasmonates induce defenses, they also inhibit growth and photosynthesis (Giri et al., 2006, Zavala and Baldwin 2006, Yan et al. 2007).

19

Transcriptional analysis of plant–herbivore interactions revealed that photosynthesis-related genes are down-regulated after attack (e.g. Hui et al. 2003, Reymond et al. 2004); however, few studies have demonstrated the effects of herbivore attack on photosynthesis at the proteome and physiological levels. Attack by herbivores or pathogens reduces transcription of the primary enzyme responsible for carbon fixation, ribulose-1,5-bisphosphate carboxylase/oxygenase (RuBisCO; Hermsmeier et al. 2001, Hahlbrock et al. 2003, Hui et al. 2003). Using two-dimensional electrophoresis, Giri et al. (2006) observed that herbivory reduced the abundance of RuBisCO activase (RCA) in *N. attenuata* Torr. ex S. Watson. RCA modulates the activity of RuBisCO (Portis 1995), a key regulatory enzyme of photosynthetic carbon assimilation, by facilitating the removal of sugar phosphates (ribulose bisphosphate) that prevent substrate binding and carbamylation of the protein's active site.

The regulation of RCA content may optimize plant performance during attack. Reducing RCA protein and transcript levels by gene silencing, similar to elicited plants, decreases both net photosynthetic rates and nitrate assimilation in *N. attenuata*; these reductions in photosynthesis and nitrogen assimilation, in turn, reduced the rate of biomass accumulation (Giri et al. 2006). Since nitrogen and carbon metabolism are linked, crosstalk between signaling pathways that regulate nitrogen assimilation and carbon metabolism is expected (Schachtman and Shin 2007). Either genetic or environmental manipulations that decrease photosynthesis also inhibit nitrate assimilation (Matt et al. 2002). These studies suggest that herbivore-induced reductions in RCA protein explain, at least in part, the decrease in photosynthetic rates in attacked leaves.

Partial defoliation of individual leaves by herbivores largely increases evapotranspiration via enhanced water loss from cut edges and produces leaf dehydration (Aldea et al. 2005), which not only reduces photosynthesis by causing stomata to close, but also by initiating senescence

signaling (Lim et al. 2007). A number of genes are induced by endogenous abscisic acid (ABA) in response to dehydration through the synthesis of the regulating transcription factors MYC and MYB (Yamaguchi-Shinozaki and Shinozaki 2006). Both MYC and MYB function as cis-acting elements that regulate transcription of dehydration-related genes (Abe et al. 1997). Transgenic plants overproducing MYC and MYB had higher osmotic stress tolerance, and microarray analysis indicated the presence of ABA- and jasmonic acid (JA)-inducible genes (Abe et al. 2003). In addition, AtMYC2 is a transcription factor that in *Arabidopsis* functions in JA and JA – ethylene-regulated defense responses (Anderson et al. 2004, Boter et al. 2004, Lorenzo et al. 2004). It has been suggested that crosstalk occurs on AtMYC2 between ABA- and JA-responsive gene expression at the MYC recognition sites in the promoters, and that AtMYC2 is a common transcription factor of ABA and JA pathways in *Arabidopsis* (Yamaguchi-Shinozaki and Shinozaki 2006).

The lipoxygenase pathway is differentially induced depending on the attacking agent (Heidel and Baldwin 2004, De Vos et al. 2005, Kempema et al. 2007), and the initiation of jasmonate signaling reduces photosynthesis and vegetative growth. Plants treated with methyl jasmonate develop shorter petioles than control plants (Cipollini 2005), and *Arabidopsis* mutants that accumulate higher JA concentrations have shorter petioles than wild-type (Bonaventure et al. 2007); these effects of JA on plant growth are modulated by the gene JASMONATE-ASSOCIATED1 (JAS1) (Yan et al. 2007). Moreover, herbivore-induced JA signaling suppresses regrowth and contributes to apical dominance (Zavala and Baldwin 2006). It has been suggested that the slower growth and down-regulation of photosynthetic-related genes by herbivore elicitation may be required to free-up resources for defense-related processes (Baldwin 2001). Herbivore attack produced rapid changes in sink–source relations and increased the allocation of

sugars to roots in *N. attenuata* plants; this process is regulated by the b-subunit of SnRK1 (SNF1-related kinase) protein kinase, but is independent of jasmonate signaling (Schwachtje et al. 2006). It is not clear whether the change in carbon allocation affects photosynthetic rate, per se, but growth reduction would affect leaf expansion and total plant photosynthesis.

Imaging methods applied to damaged leaves

Chlorophyll fluorescence provides a non-invasive probe that quantifies the component processes related to photosynthetic electron transport and correlates with photosynthetic capacity measured by gas exchange. There are several comprehensive discussions of the theory behind calculating fluorescence parameters and how imaging has been applied to leaf-level physiology (Lenk et al. 2007), aided in crop production practices (Baker and Rosenqvist 2004), or has been used to screen for stressors and circadian rhythms (Chaerle et al. 2007). High-resolution spatial maps of primary photosynthetic processes, including estimates of the rate of electron transport through PSII, energization of the thylakoid membrane, and the quantum efficiency of PSII, not only provide direct estimates of the magnitude of damage but also provide insight into underlying mechanisms (Baker et al. 2001, Oxborough 2004, 2005).

The mechanisms governing the spatial patterns of photosynthesis following herbivory can be explored further by examining the spatial correspondence of other processes. The ability to collect spatially resolved data for a wide range of molecular, physiological and biophysical processes is increasing dramatically (Chaerle and Van Der Straeten 2000; Table 2.1). The damage to water-conducting xylem by chewing insects may generate localized water limitations (Tang et al. 2006). Insofar as these water limitations or other localized changes in leaf chemistry affect stomatal conductance, thermal imaging offers a powerful tool for mapping changes in temperature associated with variation in latent heat flux across leaf surfaces (Jones 1999, Omasa

and Takayama 2003). With proper calibration, thermal maps can be converted directly into maps of stomata conductance (Jones 2004, Bajons et al. 2005, Grant et al. 2006). However, because of intrinsic properties of thermal cameras as well as lateral heat transfer within leaves (Jones 2004), the resolution of thermal images typically is lower than fluorescence images.

The spatial pattern of other components of the photosynthetic machinery, including chlorophyll content and engagement of the xanthophyll cycle (Lichtenthaler et al. 1996, Gamon et al. 1997, Gitelson et al. 2005) are readily mapped with hyperspectral imaging (Chaerle and Van Der Straeten 2000, Schuerger et al. 2003), though this has not yet been applied to variation within single leaves. The construction of transgenic plants with the promoter region of a gene of interest connected to a 'reporter gene' permits monitoring of the spatial distribution of transcription, and markers for various organelles, subcellular structures, protein motility and the cellular environment (e.g. pH; Dixit et al. 2006). Genes for firefly luciferase or β-glucuronidase (de Ruijter et al. 2003) have been useful in this regard (Jefferson et al. 1987, Greer et al. 2002); intrinsically fluorescent proteins, such as green, blue and yellow fluorescent proteins, may be more useful partners for in vivo imaging studies because of their high quantum yield (Dixit et al. 2006).

In addition to the use of various tracers and dyes for mapping the movement of water, labeling defense compounds (reactive oxygen species) and following transmembrane signals (Ca^{+2}), measurement of beta emissions from carbon isotopes by autoradiography provides a powerful technique for tracking the movement of carbohydrates and emitted from the former are short lived and more powerful, thus reducing the logistical problems of handling radioactive waste and providing the capability of penetrating thick plant tissues (Minchin and Thorpe 2003).

A wealth of information about how herbivory affects photosynthesis and other aspects of leaf physiology could be obtained by applying complementary imaging methods and, if they are applied to the same leaf in one experiment, could provide deeper insight into the mechanisms by which herbivory reduces photosynthesis in the remaining leaf tissue. Combining different images with different resolution is, however, challenging. One approach is to construct simple regressions between the values in aggregate pixels in one image with aggregate pixels in another image. West et al. (2005) applied this approach to an examination of the effect of stomatal patchiness (thermal image) on photosynthesis (fluorescence image). Deeper insight can be gained by applying methods of geographical image analysis to physiological data (Omasa and Takayama 2003, Leinonen and Jones 2004, Aldea et al. 2006a). By registering and re-sampling images taken with different instruments, multiple images can be aligned precisely and expressed at a common resolution. Once aligned, new maps are generated that represent the composite information derived from the original separate images (Aldea et al. 2006a). The 'image map' of *A. thaliana* damaged by *T. ni* larvae (Figure 2.2) revealed that immediately near holes, ΦPSII was greatly reduced and the gene coding for cinnamate-4-hydroxylase (C4H) was strongly induced (red areas). C4H is the first cytochrome P450 monooxygenase in the phenylpropanoid pathway and its induction near damaged areas suggests that a reorientation of metabolism toward defense may have contributed to the loss of photosynthetic efficiency near the cut edges. At greater distances from the edge, other factors contribute to the reduction in quantum efficiency as values of dark-adapted F_v/F_m and C4H expression are low.

Limitations to measuring gas exchange simultaneously with imaging

One of the major limitations to estimating herbivore-induced effects on photosynthesis is correctly characterizing CO_2 diffusion and uptake within the leaf. Gas exchange measurements

typically are used to generate a relationship between photosynthetic assimilation and internal [CO_2] – the A/C_i response curve. This relationship assumes leaves have homogenous distribution of chloroplasts (for light absorption) and of stomata (for gas exchange; von Caemmerer 2000). Heterogeneity across remaining leaf tissues caused by herbivory may compromise the utility of the A/C_i response curve. In addition, gas exchange chambers enclosing leaves reduce internal CO_2 where gaskets overlay leaf area through shading-induced stomatal closure (Pieruschka et al. 2006). Diffusion of CO_2 may also occur laterally, with respect to morphology, and may diffuse 2 mm in homobaric and up to 1 mm in heterobaric (compartmentalized) leaves (Pieruschka et al. 2006, Morison et al. 2007). Heterogeneity in photosynthesis caused by non-uniform CO_2 uptake, in addition to lateral diffusion of CO_2 within leaves, will interact with heterogeneity induced by feeding damage when scales are similar. For example, defoliation damage may reduce ΦPSII within a distance of 1–2 mm (Aldea et al. 2005, 2006b); however, CO_2 diffusion through cut edges into damaged tissues and adjacent undamaged tissues, may increase C_i and alleviate the suppression or even enhance photosynthesis.

CONCLUSIONS

In many cases, arthropod damage reduces photosynthesis to a greater extent than would be predicted by the direct loss of leaf tissue. With the use of new imaging technologies we are beginning to understand how photosynthesis and water balance are modulated in undamaged tissue following herbivory. Connecting these alterations in physiology to changes in gene transcription and hormonal signaling will increase our ability to estimate whole-plant responses to herbivory and will improve our estimates of the impact of herbivory on higher levels of biological organization, such as yield loss and assessments of overall ecosystem productivity.

Indirect alterations of photosynthesis have been identified across multiple plant systems and can be categorized by plant responses. Severed vasculature increases transpiration, reduces ΦPSII, and reduces NPQ, whereas sink demands of galls enhance transpiration. Photosynthesis is greatly reduced through the release of toxic secondary compounds or defenses elicited by herbivore attack. Even the initiation of these defenses triggers down-regulation of photosynthetic component processes or proteins. Despite these characterized indirect effects, investigations are lacking for some damage types (e.g. specialized cell content feeders) and their subsequent interactions with primary and secondary metabolite pools.

While we are closer to elucidating the mechanisms responsible for herbivore-induced alterations in photosynthesis and related processes in undamaged tissues, a complete understanding of how the indirect suppression of photosynthesis propagates away from the point of damage remains unknown. Genomic analyses of plants challenged by arthropods have revealed a trend for down-regulation of photosynthesis-related genes, but a closer look at transcriptional changes between and within feeding guilds has identified differential regulation of defense genes and overlap among damage guilds. A universal response to herbivory is the induction of the lipoxygenase pathway, but attacking agents differentially induce this pathway and corresponding jasmonate concentrations (Heidel and Baldwin 2004, De Vos et al. 2005, Kempema et al. 2007). Differences in concentrations of defense signaling molecules may lead to differential down-regulation of photosynthesis genes. Already, the overlap in the magnitude of down-regulation has been noted between caterpillars and general cell content feeders compared with aphids (Voelckel et al. 2004), leading to species-specific regulation of different metabolic pathways (e.g. nitrogen metabolism by aphids). Subsequently, within plant mechanisms

underlying the indirect effect, and not the direct effect, may drive physiological responses in

future plant–insect interactions.

LITERATURE CITED

Abe H, Yamaguchi-Shinozaki K, Urao T, Iwasaki T, Hosokawa D, Shinozaki K. 1997. Role of *Arabidopsis* MYC and MYC homologs in drought- and abscisic acid-regulated gene expression. The Plant Cell 9: 1859–1868.

Abe H, Urao T, Ito T, Seki M, Shinozaki K, Yamaguchi-Shinozaki K. 2003. *Arabidopsis* AtMYC2 (bHLH) and AtMYB2 (MYB) function as transcriptional activators in abscisic acid signaling. The Plant Cell 15: 63–78.

Aldea M, Hamilton JG, Resti JP, Zangerl AR, Berenbaum MR, DeLucia EH. 2005. Indirect effects of insect herbivory on leaf gas exchange in soybean. Plant, Cell and Environment 28: 402–411.

Aldea M, Frank TD, DeLucia EH. 2006a. A method for quantitative analysis of spatially variable physiological processes across leaf surfaces. Photosynthesis Research 90: 161–172.

Aldea M, Hamilton JG, Resti JP, Zangerl AR, Berenbaum MR, Frank TD, DeLucia EH 2006b. Comparison of photosynthetic damage from arthropod herbivory and pathogen infection in understory hardwood samplings. Oecologia 149: 221–232.

Arnason JT, Philogene BJR, Towers GHN. 1991. Phototoxins in plant-insect interactions. In: Rosenthal GA, Berenbaum MR, eds. Herbivores: their interactions with secondary plant metabolites. New York, NY: Academic Press, 317–341.

Anderson JP, Badruzsaufari E, Schenk PM, Manners JM, Desmond OJ, Ehlert C, Maclean DJ, Ebert PR, Kazan K 2004. Antagonistic interaction between abscisic acid and jasmonate-ethylene signaling pathways modulates defense gene expression and disease resistance in *Arabidopsis*. The Plant Cell 16: 3460–3479.

Bajons P, Klinger G, Schlosser V. 2005. Determination of stomatal conductance by means of infrared thermography. Infrared Physics and Technology 46: 429–439.

Baker NR, Rosenqvist E. 2004. Applications of chlorophyll fluorescence can improve crop production strategies: an examination of future possibilities. Journal of Experimental Botany 55: 1607–1621.

Baker NR, Oxborough K, Lawson T, Morison JIL. 2001. High resolution imaging of photosynthetic activities of tissues, cells and chloroplasts in leaves. Journal of Experimental Botany 52: 614–621.

Baldwin IT. 2001. An ecologically motivated analysis of plant-herbivore interactions in native tobacco. Plant Physiology 127: 1449–1458.

Baldwin IT, Callahan P. 1993. Autotoxicity and chemical defense: nicotine accumulation and carbon gain in solanaceous plants. Oecologia 94: 534–541.

Berenbaum MR, Zangerl AR. 2008. Facing the future of plant-insect interaction research: le retour a la 'raison d'etre' Plant Physiology 146: 804–811.

Bonaventure G, Gfeller A, Proebsting WM, Hoerstensteiner S, Chetelat A, Martinoia E, Farmer EE 2007. A gain of function allele of TPC1 activates oxylipin biogenesis after leaf wounding in *Arabidopsis*. The Plant Journal 49: 889–898.

Boter M, Ruiz-Rivero O, Abdeen A, Prat S. 2004. Conserved MYC transcription factors play a key role in jasmonate signaling both in tomato and *Arabidopsis*. Genes and Development 18: 1577–1591.

Buschmann C, Langsdorf G, Lichtenthaler HK. 2000. Imaging of the blue, green and red fluorescence emission of plants: an overview. Photosynthetica 38: 483–491.

von Caemmerer S. 2000. Biochemical models of leaf photosynthesis. Victoria, Australia: CSIRO Publishing.

Canny MJ. 1990. Tansley review no. 22 – what becomes of the transpiration stream? New Phytologist 114: 341–368.

Chaerle L, Van Der Straeten D. 2000. Imaging techniques and the early detection of plant stress. Trends in Plant Science 5: 495–501.

Chaerle L, Leinonen I, Jones HG, Van Der Straeten D. 2007. Monitoring and screening plant populations with combined thermal and chlorophyll fluorescence imaging. Journal of Experimental Botany 58: 773–784.

Cipollini D. 2005. Interactive effects of lateral shading and jasmonic acid on morphology, physiology, seed production, and defense traits in *Arabidopsis thaliana*. International Journal of Plant Science 166: 955–959.

Clearwater MJ, Clark CJ. 2003. In vivo magnetic resonance imaging of xylem vessel contents in woody lianas. Plant, Cell and Environment 26: 1205–1214.

Coley PD, Barone JA. 1996. Herbivory and plant defenses in tropical forests. Annual Review of Ecology and Systematics 27: 305–335.

Cyr H, Pace ML. 1993. Magnitude and patterns of herbivory in aquatic and terrestrial ecosystems. Nature 361: 148–150.

Delaney KJ, Higley LG. 2006. An insect countermeasure impacts plant physiology: midrib vein cutting, defoliation and leaf photosynthesis. Plant, Cell and Environment 29: 1245–1258.

De Vos M, Van Zaanen W, Koornneef A, Korzelius JP, Dicke M, Van Loon LC, Pieterse CMJ 2005. Herbivore-induced resistance against microbial pathogens in *Arabidopsis*. Plant Physiology 142: 353–363.

Dixit R, Cyr R, Gilroy S. 2006. Using intrinsically fluorescent proteins for plant cell imaging. The Plant Journal 45: 599–615.

Dorchin N, Cramer MD, Hoffmann JH. 2006. Photosynthesis and sink activity of wasp-induced galls in *Acacia pycnantha*. Ecology 87: 1781–1791.

Dungan RJ, Turnbull MH, Kelly D. 2007. The carbon costs for host trees of a phloem-feeding herbivore. Journal of Ecology 95: 603–613.

Fine PVA, Miller ZJ, Mesones I, Irazuzta S, Appel HM, Stevens MHH, Saaksjarvi I, Schultz JC, Coley PD 2006. The growth-defense tradeoff and habitat specialization by plants in Amazonian forests. Ecology 87: 150–162.

Fryer MJ, Oxborough K, Mullineaux PM, Baker NR. 2002. Imaging of photo-oxidative stress responses in leaves. Journal of Experimental Botany 53: 1249–1254.

Gaff DF, O-Ogola O. 1971. The use of nonpermeating pigments for testing the survival of cells. Journal of Experimental Botany 22: 756–758.

Gamon JA, Surfus JS. 1999. Assessing leaf pigment content and activity with a reflectometer. New Phytologist 143: 105–117.

Gamon JA, Serrano L, Surfus JS. 1997. The photochemical reflectance index: an optical indicator of photosynthetic radiation use efficiency across species, functional types, and nutrient levels. Oecologia 112: 492–501.

Genty B, Briantais JM, Baker NR. 1989. The relationship between the quantum yield of photosynthetic electron transport and quenching of chlorophyll fluorescence. Biochimica et Biophysica Acta 990: 87–92.

Girousse C, Moulia B, Silk W, Bonnemain JL. 2005. Aphid infestation causes different changes in carbon and nitrogen allocation in alfalfa stems as well as different inhibitions of longitudinal and radial expansion. Plant Physiology 137: 1474–1484.

Giri AP, Wunsche H, Mitra S, Zavala JA, Muck A, Svatos A, Baldwin IT 2006. Molecular interactions between the specialist herbivore *Manduca sexta* (Lepidoptera, Sphingidae) and its natural host *Nicotiana attenuata*. VII. Changes in the plant's proteome. Plant Physiology 142: 1621–1641.

Gitelson AA, Vina A, Ciganada V, Rundquist DC, Arkebauer TJ. 2005. Remote estimation of canopy chlorophyll content in crops. Geophysical Research Letters 32: 1–4.

Gog L, Berenbaum MR, DeLucia EH, Zangerl AR. 2005. Autotoxic effects of essential oils on photosynthesis in parsley, parsnip, and rough lemon. Chemoecology 15: 115–119.

Grant OM, Caves MM, Jones HG. 2006. Optimizing thermal imaging as a technique for detecting stomatal closure induced by drought stress under greenhouse conditions. Physiologia Plantarum 127: 507–518.

Greer LFIII, Szalay AA. 2002. Imaging of light emission from the expression of luciferases in living cells and organisms: a review. Luminescence 17: 43–74.

Gussoni M, Greco F, Vezzoli A, Osuga T, Zetta L. 2001. Magnetic resonance imaging of molecular transport in living morning glory stems. Magnetic Resonance Imaging 19: 1311–1322.

Hahlbrock K, Bednarek P, Ciolkowski I, Hamberger B, Heise A, Liedgens H, Logeman E, Nurnberger T, Schmelzer E, Somssich IE, Tan J 2003. Non-self recognition, transcriptional reprogramming, and secondary metabolite accumulation during plant/pathogen interactions. Proceedings of the National Academy of Sciences of the USA 100: 14569–14576.

Haile FJ, Higley LG. 2003. Changes in soybean gas-exchange after moisture stress and spider mite injury. Environmental Entomology 32: 433–440.

Haile FJ, Higley LG, Ni X, Quisenberry SS. 1999. Physiological and growth tolerance in wheat to Russian wheat aphid (Homoptera: Aphididae) injury. Environmental Entomology 28: 787–794.

Heidel AJ, Baldwin IT. 2004. Microarray analysis of salicylic acid- and jasmonic acid-signaling in responses of *Nicotiana attenuata* to attack by insects from multiple feeding guilds. Plant, Cell and Environment 27: 1362–1373.

Heng-Moss T, Macedo T, Franzen L, Baxendale F, Higley L, Sarath G. 2006. Physiological responses of resistant and susceptible buffalograsses to *Blissus occiduus* (Hemiptera: Blissidae) feeding. Journal of Economic Entomology 99: 222–228.

Hermsmeier D, Schittko U, Baldwin IT. 2001. Molecular interactions between the specialist herbivore *Manduca sexta* (Lepidoptera: Sphingidae) and its natural host *Nicotiana attenuata*. I. Large-scale changes in the accumulation of growth- and defense-related plant mRNAs. Plant Physiology 125: 683–700.

Higley LG, Browde JA, Higley PM. 1993. Moving toward new understandings of biotic stress and stress interactions. In: Buxton DR, ed. International crop science I. Madison, WI: Crop Science Society of America, 749–754.

Holman EM, Oosterhuis DM. 1999. Cotton photosynthesis and carbon partitioning in response to floral bud loss due to insect damage. Crop Science 39: 1347–1351.

Howe GA, Jander G. 2008. Plant immunity to insect herbivores. Annual Review of Plant Biology 59: 41–66.

Hui DQ, Iqbal J, Lehmann K, Gase K, Saluz HP, Baldwin IT. 2003. Molecular interactions between the specialist herbivore *Manduca sexta* (Lepidoptera: Sphingidae) and its natural host *Nicotiana attenuata*. V. Microarray analysis and further characterization of large-scale changes in herbivore-induced mRNAs. Plant Physiology 131: 1877–1893.

Jefferson RA, Kavanagh TA, Bevan MW. 1987. GUS fusions: b-glucuronidase as a sensitive and versatile gene fusion marker in higher plants. EMBO Journal 6: 3901–3907.

Jones H. 1999. Use of thermography for quantitative studies of spatial and temporal variation of stomatal conductance over leaf surfaces. Plant, Cell and Environment 22: 1043–1055.

Jones HG. 2004. Application of thermal imaging and infrared sensing in plant physiology and ecophysiology. Advances in Botanical Research incorporating Advances in Plant Pathology 41: 107–163.

Kawachi N, Sakamoto K, Ishii S, Fujimaki S, Suzui N, Ishioka NS, Matsuhashi S 2006. Kinetic analysis of carbon-11-labeled carbon dioxide for studying photosynthesis in a leaf using positron emitting tracer imaging system. Transactions of Nuclear Science 53: 2991–2997.

Kempema LA, Cui X, Holzer FM, Walling LL. 2007. *Arabidopsis* transcriptome changes in response to phloem-feeding silverleaf whitefly nymphs: similarities and distinctions in responses to aphids. Plant Physiology 143: 849–865.

Kessler A, Baldwin IT. 2002. Plant responses to insect herbivory: the emerging molecular analysis. Annual Review of Plant Biology 53: 299–328.

Layne DR, Flore JA. 1992. Photosynthetic compensation to partial leaf area reduction in sour cherry. Journal of American Society for Horticultural Science 117: 279–286.

Leiononen I, Jones HG. 2004. Combining thermal and visible imagery for estimating canopy temperature and identifying plant stress. Journal of Experimental Botany 55: 1423–1431.

Lenk S, Chaerle L, Pfundel EE, Langsdorf G, Hagenbeek D, Lichtenthaler HK, Van Der Straetan D, Buschmann C 2007. Multispectral fluorescence and reflectance imaging at the leaf level and its possible applications. Journal of Experimental Botany 58: 807–814.

Lichtenthaler HK, Gitelson A, Lang M. 1996. Non-destructive determination of chlorophyll content of leaves of a green and an aurea mutant of tobacco by reflectance measurements. Journal of Plant Physiology 148: 483–493.

Lim PO, Kim HJ, Nam HG. 2007. Leaf senescence. Annual Review of Plant Biology 58: 115–136.

Lorenzo O, Chico JM, Sanchez-Serrano JJ, Solano R. 2004. JASMONATEINSENSITIVE1 encodes a MYC transcription factor essential to discriminate between different jasmonate-regulated defense responses in *Arabidopsis*. The Plant Cell 16: 1938–1950.

Macedo TB, Bastos CS, Higley LG, Ostlie KR, Madhavan S. 2003a. Photosynthetic responses of soybean to soybean aphid (Homoptera: Aphididae) injury. Journal of Economic Entomology 96: 188–193.

Macedo TB, Higley LG, Ni X, Quisenberry S. 2003b. Light activation of Russian wheat aphid-elicited physiological responses in susceptible wheat. Journal of Economic Entomology 96: 194–201.

Macedo TB, Peterson RKD, Weaver DK, Morrill WL. 2005. Wheat stem sawfly, *Cephus cintus* Norton, impact on wheat primary metabolism: an ecophysiological approach. Environmental Entomology 34: 719–726.

Macedo TB, Weaver DK, Peterson RKD. 2007. Photosynthesis in wheat at the grain filling stage is altered by the wheat stem sawfly (Hymenoptera: Cephidae) injury and reduced water availability. Journal of Entomological Science 42: 228–238.

Macfall JS, Spaine P, Doudrick R, Johnson GA. 1994. Alterations in growth and water transport processes in fusiform rust galls of pine, determined by magnetic-resonance microscopy. Phytopathology 84: 288–293.

Maffei M, Bossi S, Spiteller D, Mithofer A, Boland W. 2004. Effects of feeding *Spodoptera littoralis* on lima bean leaves. I. Membrane potentials, intracellular calcium variations, oral secretions, and regurgitated components. Plant Physiology 134: 1–11.

Matt P, Krapp A, Haake V, Mock HP, Stitt M. 2002. Decreased Rubisco activity leads to dramatic changes of nitrate metabolism, amino acid metabolism and the levels of phenylpropanoids and nicotine in tobacco antisense RBCS transformants. The Plant Journal 30: 663–677.

Minchin PEH, Thorpe MR. 2003. Using Plant Biology 30: 831 – 841.

Morison JIL, Lawson T, Cornic G. 2007. Lateral CO2 diffusion inside dicotyledonous leaves can be substantial: quantification in different light intensities. Plant Physiology 145: 680–690.

Nardini A, Salleo S. 2005. Water stress-induced modifications of leaf hydraulic architecture in sunflower: co-ordination with gas exchange. Journal of Experimental Botany 56: 3093–3101.

Oerke E-C, Dehne H-W. 1997. Global crop production and the efficacy of crop protection – current situation and future trends. European Journal of Plant Pathology 103: 203–215.

Omasa K, Takayama K. 2003. Simultaneous measurement of stomatal conductance, non-photochemical quenching, and photochemical yield of photosystem II in intact leaves by thermal and chlorophyll fluorescence imaging. Plant Cell Physiology 44: 1290–1300.

Oxborough K. 2004. Imaging of chlorophyll a fluorescence: theoretical and practical aspects of an emerging technique for the monitoring of photosynthetic performance. Journal of Experimental Botany 55: 1195–1205.

Oxborough K. 2005. Using chlorophyll a fluorescence imaging to monitor photosynthetic performance. In: Govindjee, Papageorgiou GC, eds. Chlorophyll fluorescence: a signature of photosynthesis. Dordrecht: Kluwer Academic Press, 409–428.

Ozaki K, Saito H, Yamamuro K. 2004. Compensatory photosynthesis as a response to partial debudding in ezo spruce, *Picea jezoensis*, seedlings. Ecological Research 19: 225–231.

Peterson RKD, Higley LH. 2001. Biotic stress and yield loss. Boca Raton, FL: CRC Press.

Peterson RKD, Danielson SD, Higley LG. 1992. Photosynthetic responses of alfalfa to actual and simulated alfalfa weevil (Coleoptera: Curculionidae) injury. Environmental Entomology 21: 501–507.

Peterson RKD, Higley LG, Spomer SM. 1996. Injury by *Hyalaphora cecropia* (Lepidoptera: Saturniidae) and photosynthetic responses of apple and crabapple. Environmental Entomology 25: 416–422.

Peterson RKD, Higley LG, Haile FJ, Barrigossi JAF. 1998. Mexican bean beetle (Coleoptera: Coccinelidae) injury affects photosynthesis of *Glycine max* and *Phaseolus vulgaris*. Environmental Entomology 27: 373–381.

Peterson RKD, Shannon CL, Lenssen AW. 2004. Photosynthetic responses of legume species to leaf-mass consumption injury. Environmental Entomology 33: 450–456.

Pieruschka R, Schurr U, Jensen M, Wolff WF, Jahnke S. 2006. Lateral diffusion of CO_2 from shaded to illuminated leaf parts affects photosynthesis inside homobaric leaves. New Phytologist 169: 779–787.

Pincebourd S, Frak E, Sinoquet H, Regnard JL, Casas J. 2006. Herbivory mitigation through increased water-use efficiency in a leaf-mining moth-apple tree relationship. Plant, Cell and Environment 29: 2238–2247.

Portis AR. 1995. The regulation of rubisco by rubisco activase. Journal of Experimental Botany 46: 1285–1291.

Reddall A, Sadras VO, Wilson LJ, Gregg PC. 2004. Physiological responses of cotton to two-spotted spider mite damage. Crop Science 44: 835–846.

Retuerto R, Fernandez-Lema B, Rodriguez-Roiloa S, Obeso JR. 2004. Increased photosynthetic performance in holly trees infested by scale. Functional Ecology 18: 664–669.

Reymond P, Bodenhausen N, Van Poecke RMP, Krishnamurthy V, Dicke, M, Farmer EE. 2004. A conserved transcript pattern in response to a specialist and a generalist herbivore. The Plant Cell 16: 3132–3147.

Rolfe SA, Scholes JD. 1995. Quantitative imaging of chlorophyll fluorescence. New Phytologist 131: 69–79.

de Ruijter NCA, Verhees J, van Leewen W, van der Krol AR. 2003. Evaluation and comparison of GUS, LUC and GFP reporter system for gene expression studies in plants. Plant Biology 5: 103–115.

Sack L, Holbrook NM. 2006. Leaf hydraulics. Annual Review of Plant Biology 57: 361–381. Schachtman DP, Shin R. 2007. Nutrient sensing and signaling: NPKS. Annual Review of Plant Biology 58: 47–69.

Schuerger AC, Capelle GA, Di Benedetto JA, Mao C, Thai CN, Evans MD, Richards JT, Blank TA, Stryjewski EC. 2003. Comparison of two hyperspectral imaging and two laser-induced fluorescence instruments for detection of zinc stress and chlorophyll concentration in bahia grass (*Paspalum notatum* Flugge.). Remote Sensing of Environment 84: 572–588.

Schwachtje J, Minchin PEH, Jahnke S, van Dongen JT, Schittko U, Baldwin IT. 2006. SNF1-related kinases allow plants to tolerate herbivory by allocating carbon to roots. Proceedings of the National Academy of Sciences of the USA 103: 12935–12940.

Suwignyo RA, Nose A, Kawamitsu Y, Tsuchiya M, Wasano K. 1995. Effects of manipulations of source and sink on carbon exchange rate and some enzymes of sucrose metabolism in leaves of soybean [*Glycine max* (L.) Merr.]. Plant Cell Physiology 36: 1439–1446.

Tang JY, Zielinski RE, Zangerl AR, Crofts AR, Berenbaum MR, DeLucia EH. 2006. The differential effects of herbivory by first and fourth instars of *Trichoplusia ni* (Lepidoptera: Noctuidae) on photosynthesis in *Arabidopsis thaliana*. Journal of Experimental Botany 57: 527–536

Thomson VP, Cunningham SA, Ball MC, Nicotra AB. 2003. Compensation for herbivory by *Cucumis sativus* through increased photosynthetic capacity and efficiency. Oecologia 134:

Thorpe MR, Ferrieri A, Herth MM, Ferrieri RA. 2007. C-imaging: methyl jasmonate moves in both phloem and xylem, promotes transport of jasmonate, and of photoassimilate even after proton transport is decoupled. Planta 226: 541–551.

Trumble JT, Kolodny-Hirsch DM, Ting IP. 1993. Plant compensation for arthropod herbivory. Annual Reviews of Entomology 38: 93–119.

Turnbull TL, Adams MA, Warren CR. 2007. Increased photosynthesis following partial defoliation of field-grown *Eucalyptus globulus* is not caused by increased leaf nitrogen. Tree Physiology 27: 1481–1492.

Voelckel C, Weisser WW, Baldwin IT. 2004. An analysis of plant-aphid interactions by different microarray hybridization strategies. Molecular Ecology 13: 3187–3195.

Welter SC. 1989. Arthropod impact on plant gas exchange. In: Bernays EA, ed. Insect–plant interactions. Boca Raton, FL: CRC Press, 135–151.

West JD, Peak D, Peterson JQ, Mott KA. 2005. Dynamics of stomatal patches for a single surface of *Xanthium strumarium* L. leaves observed with fluorescence and thermal images. Plant, Cell and Environment 28: 633–641.

Yamaguchi-Shinozaki K, Shinozaki K. 2006. Responses and tolerance to dehydration and cold stresses. Annual Review of Plant Biology 57: 781–803.

Yan Y, Stolz S, Chetelat A, Reymond P, Pagni M, Dubugnon L, Farmer EE 2007. A downstream mediator in the growth repression limb of the jasmonate pathway. The Plant Cell 19: 2470–2483.

Zangerl AR, Hamilton JG, Miller TJ Crofts AR, Oxborough K, Berenbaum MR, DeLucia EH. 2002. Impact of folivory on photosynthesis is greater than the sum of its holes. Proceedings of the National Academy of Sciences USA 99: 1088–1091.

Zavala JA, Baldwin IT. 2006. Jasmonic acid signaling and herbivore resistance traits constrain regrowth after herbivore attack in *Nicotiana attenuata*. Plant, Cell and Environment 29: 1751–1760.

TABLES

Table 2.1. Representative physiological and molecular processes readily visualized *in vivo* using various imaging methods. Where appropriate, the excitation and measurements wavelengths are noted (Wavelength: excitation/measurement). Modified from Aldea et al. (2006a).

Parameter		Process	Wavelength	Reference
Photosynthesis	F_v/F_m	Maximum quantum efficiency of PSII	470/700	Genty et al. 1989; Rolfe and Scholes 1995;
	NPQ	Non-photochemical energy dissipation		Oxborough 2004
	F_{PSII}	Quantum yield of electron transport		
Water & energy status	Thermal	Transpiration, conductance	None/ >1200	Jones 1999; Omasa and Takayama 2003
	MRI	Water transport	X-rays/microwaves	Gussoni et al. 2001, Clearwater and Clark 2003
	Tracers		Depends on tracer	Gaff & O-Ogoloa 1971; Canny 1990
Leaf pigments	NDVI	Chlorophyll content	<700/750,704	Gamon and Surfus 1999
	Red/Green	Anthocyanin content	<700/600-699, 500-599	
	PRI	Xanthophyll cycle	<700/531, 570	
Molecular interactions	GFP	Gene expression, protein motility,	485/509	Buschmann et al. 2000; Dixit et al. 2006
and cell environment	RFP	organelle location, cellular pH	490, 520, 563/583	
	BFP		UV/440	
Defense compounds	Dyes	Reactive oxygen species, Ca^{+2}	400 - 700	Fryer et al. 2002; Maffei et al. 2004
Metabolites	Beta emission	Carbohydrate/metabolite transport	autoradiography	Minchin and Thorpe 2003; Thorpe et al. 2007

Figure 2.1. Conceptual model of the direct effect of herbivory (removal of leaf area) and the indirect effects of herbivore damage to foliage on photosynthesis in the remaining leaf tissues. The concept underlying this figure was developed by Dr. Arthur Zangerl.
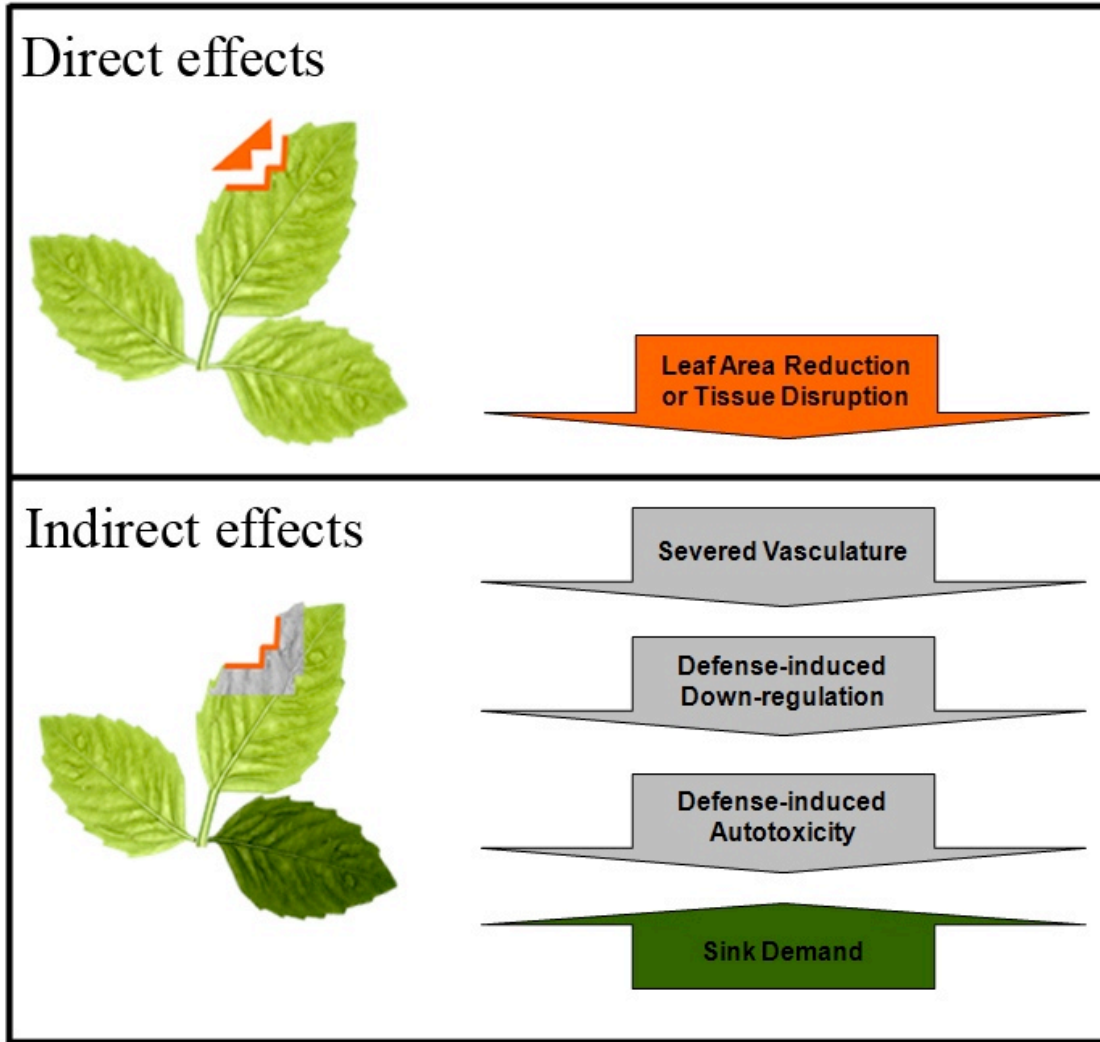
Figure 2.2. False color images of the location of damage classes surrounding holes in an *Arabidopsis thaliana* leaf exposed to herbivory by *Trichoplusia ni* larvae. Transgenic plants carried a cinnamate-4-hydroxylase (C4H) promoter and β-glucuronidase (GUS) reporter gene fusion. In *A. thaliana*, enzymes in the phenylpropanoid pathway may contribute to defense against pathogens; C4H is constitutively expressed in the veins of undamaged leaves and induced by wounding near the site of damage. The image was constructed by combining independent images of the same leaf of chlorophyll fluorescence (ΦPSII) and GUS staining for C4H activity using geographic image analysis software. The false-color scale bars indicate the mean value of ΦPSII for each damage class. The veins shown in blue and purple were classes that were excluded from analysis because their high level of GUS staining was not related to herbivory. Data were generously provided by Dr. Jennie Tang.
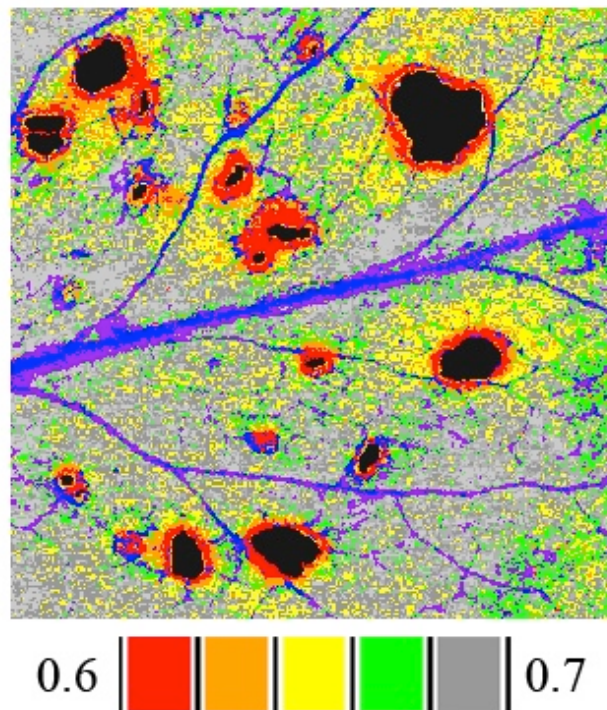
CHAPTER 3[2]

ELEVATED CO$_2$ INTERACTS WITH HERBIVORY TO ALTER CHLOROPHYLL FLUORESCENCE AND LEAF TEMPERATURE IN *BETULA PAPYRIFERA* AND *POPULUS TREMULOIDES*

ABSTRACT

Herbivory may influence ecosystem properties including productivity and diversity, but recent evidence suggests that damage by herbivores modulates potential productivity specific to damage type. Because productivity is linked to photosynthesis at the leaf-level, which in turn is influenced by atmospheric CO$_2$ concentrations, we investigated how different herbivore damage types alter component processes of photosynthesis under ambient and elevated atmospheric CO$_2$. We examined spatial patterns in chlorophyll fluorescence and temperature of leaves damaged by leaf-chewing, gall-forming, and leaf-folding insects in aspen trees and by leaf-chewing insects in birch trees under ambient and elevated CO$_2$ at the Aspen Free-Air CO$_2$ Enrichment (FACE) site in Wisconsin. Both defoliation and gall damage suppressed the operating efficiency of photosystem II (ΦPSII) in remaining leaf tissue yet the distance that damage propagated was marginally attenuated under elevated CO$_2$. Elevated CO$_2$ also increased leaf temperatures, which reduced the cooling effect of gall formation and freshly chewed leaf tissue. These results provide mechanistic insight into how different damage types influence the remaining, visibly undamaged leaf tissue and suggest that elevated CO$_2$, coupled with warming climate may reduce the effects of herbivory on electron transport controlling photosynthesis.

INTRODUCTION

Arthropod herbivory alters ecosystem productivity, especially in outbreak years (Cyr and Pace 1993), and recent evidence suggests that the manner of feeding (e.g., chewing, phloem feeding) may alter how herbivory affects productivity (Zvereva et al. 2010, Patankar et al. 2011). Reductions in productivity result, in part, from damage-specific alterations of photosynthetic capacity. Direct tissue consumption (loss of photosynthetic area) by defoliators and direct cellular disruption or altered osmotic potential (extracted photosynthate) by piercing-sucking insects differentially affect photosynthesis (see Welter 1989). Insect feeding also selectively impairs remaining leaf tissue through direct and indirect alterations of leaf physiology (Nabity et al. 2009). Within the few systems (*P. sativa*, *G. max*, *A. thaliana*, various hardwood trees) evaluated thus far, the general response is a suppression of leaf photosynthesis beyond the area of arthropod feeding.

As arthropod herbivores feed, tissue damage may suppress photosynthesis in remaining tissues by severing vasculature (Aldea et al. 2006; Tang et al. 2006), altering sink/source relationships (Dorchin et al. 2006), autotoxicity (Gog et al. 2005), and defense-induced down-regulation of photosynthetic genes (Bilgin et al. 2010). Remaining tissues also may respond to the type of damage with varying degrees of physiological impairment; a 5% reduction in leaf area by a chewing herbivore resulted in a 20% reduction in photosynthetic capacity of remaining parsnip leaf tissue (Zangerl et al. 2002), whereas damage to understory hardwood trees reduced photosynthesis in remaining tissues equal to the area removed (Aldea et al. 2006). Understanding these effects on physiology among damage types and within model systems where genomic information is readily accessible may help link the observed global genomic down-regulation of

photosynthetic genes (Bilgin et al. 2010) to physiological impairment in visibly unaltered remaining leaf tissues.

Atmospheric carbon dioxide is rising steadily ($\sim$2 μl l^{-1} yr^{-1}; www.esrl.noaa.gov/gmd/ccgg/trends/) and generally enhances photosynthesis of forest ecosystems (Saxe et al. 1998; Leakey et al. 2009; Lindroth 2010). Despite this enhancement, elevated CO_2 levels also increase damage rates by herbivores in aspen and birch (Couture et al. 2011). This increase in damage typically coincides with increased abundance of phloem-feeding herbivores and decreased chewing and galling herbivore abundance in field sites fumigated with CO_2 (Hillstrom and Lindroth 2008; Hillstrom 2010). Because increased CO_2 stimulates photosynthesis and reduces stomatal conductance thereby improving leaf water status, the predicted increases in atmospheric CO_2 may modulate the effect of herbivory on photosynthesis. The propagation of fungal damage beyond visible lesions into remaining, visibly undamaged tissues is reduced under elevated CO_2 (McElrone et al. 2010); however, there are no examinations of how herbivores may alter photosynthesis of trees grown under future CO_2 concentrations.

Chlorophyll fluorescence imaging is a powerful tool for making high-resolution, spatially-resolved measurements of component processes of photosynthesis in damaged leaf tissues (Oxborough 2004, Aldea et al. 2006). Measurement of the quantum efficiency of photosystem II (ΦPSII) is particularly useful in this regard because it is highly correlated with the rate of CO_2 uptake in intact leaves (Genty et al. 1989, Baker and Oxborough 2005, Tang et al. 2006) and relates directly to carbon assimilation, an ecologically important trait. Using this approach, Aldea et al. (2006) identified spatial patterns in fluorescence and thermal images with some degree of host specificity; defoliation typically reduces ΦPSII in remaining leaf tissue

along cut edges whereas some gall formers reduce ΦPSII well beyond visible feeding damage. However, no studies have investigated how arthropod herbivory affects remaining leaf tissue under elevated CO_2 or among herbivore damage types within one plant species to minimize the variabilty introduced by species. The objective of this research was to determine if elevated CO_2 modulates the effect of herbivory on the spatial pattern of photosynthesis as indicated by variation in ΦPSII in two tree species growing under otherwise natural environmental conditions. Because elevated CO_2 may enhance photosynthesis, water use efficiency, and alter the production of secondary chemicals, we hypothesized that elevated CO_2 will attenuate the effects of herbivore damage. We tested this hypothesis at the Aspen Free Air CO_2 Enrichment (FACE) site in northern Wisconsin. We utilized aspen trees of a single clone to minimize genetic variability and examined multiple insect herbivores inflicting three different damage types.

MATERIALS AND METHODS

Experimental Design

Research was conducted during the summers of 2008-2009 at the Aspen Free-Air CO_2 Enrichment (Aspen FACE) site in north-central Wisconsin, USA (W 89.5°, N 45.7°). This 32-ha site contained 12, 30-m diameter plots of the following treatment combinations: ambient, elevated CO_2 (ambient + 200 μl l^{-1}), elevated O_3 (1.5 x ambient), and elevated CO_2 plus elevated O_3. Three plots were designated for each fumigation treatment and blocked from north to south across the site. Only ambient and elevated CO_2 plots were used for this experiment.

Each plot contained five aspen (*Populus tremuloides* Michx.) genotypes in addition to birch (*Betula papyrifera* Marsh.) and sugar maple (*Acer saccharum* Marsh.); however, we examined only one aspen genotype and birch. We selected aspen genotype 216 for our study

because it responds strongly to CO_2 enrichment (Noormets et al. 2001). Aspen genotype 216 and birch were used during 2008 and only aspen was examined again in 2009. For both aspen and birch, defoliation damage of unknown age and herbivore source was examined in 2008. In addition, two other insect damage types were evaluated on aspen: skeletonizing damage by larval sawflies (*Phyllocolpa* sp.) where feeding occurs within the folded edges of leaves and leaves galled by midge flies (*Harmandia* sp; see Figure 3.1). To control for time after chewing damage occurred we conducted a 24h feeding trial of gypsy moth (*Lymantria dyspar* L.) on aspen. In each plot, three branches with full sun exposure on three different trees were enclosed in fine mesh bags; each bag contained 20-30 undamaged leaves on determinant shoots. Ten fifth instar larvae were placed in each bag and allowed to feed overnight. Measurements of chlorophyll fluorescence and leaf temperature were made the following day.

To assess how elevated CO_2 alters the effects of herbivore damage, we identified leaves from each tree species within each plot for each damage type and randomly selected four leaves for each species/damage type combination. All leaves were on determinant shoots. The spatial patterns of temperature and photosynthetic electron transport were measured by thermography and chlorophyll fluorescence, respectively. Data from these cohorts represented subsamples for each plot and were subsequently pooled by plot (n=3).

Thermography

To quantify the effects of herbivory on the spatial pattern of water loss, thermal images of each damage type were taken using an infrared camera (ThermaCAM Infrared Camera, FLIR Systems, Portland, OR, USA). Branchlets were excised and rapidly transported back to a nearby field laboratory. Individual leaves were then excised from branchlets under degassed water, their petioles were placed in a water-filled 2-ml tube, and allowed to equilibrate to steady state, light-

adapted conditions (150 μmol m^{-2}s^{-1} PFD at 25ºC). Excised leaves were imaged at constant light

and temperature (150 μmol m^{-2}s^{-1} PFD at 25ºC) and at ambient CO_2.

Chlorophyll Fluorescence

To quantify the effect of different damage types on the efficiency of primary

photochemistry, the spatial pattern of the operating efficiency of photosystem II (ΦPSII) was

measured with an imaging chlorophyll fluorometer (Walz Imaging PAM, Walz GmbH,

Effeltrich, Germany). Branchlets and leaves were collected and maintained in a field laboratory

under the conditions described above. Leaves were allowed to equilibrate to environmental

conditions within the field laboratory until a steady state was reached. This occurred when the

fluorescent yield (continuously monitored by the camera) no longer fluctuated in false-color

pixel intensity thereby indicating stability in electron transport across the leaf surface. Once

steady state was reached, fluorescense was recorded for a 2x3 cm area of leaf surface centered on

the herbivore damage. ΦPSII was calculated from an initial image of minimum fluorescence in a

light adapted state (F') and an image of fluorescence following a 1-s saturating pulse (ca. 2500

μmol m^{-2}s^{-1}; F'$_m$) using the formula: ΦPSII= (F'$_m$ – F')/F'$_m$. Although the leaves selected in this

experiment were from the sunlight canopy and typically were exposed to higher ambient light

conditions, the assessment of pulse amplitude modulated (PAM) fluorescence was made under

low irradiance to optimize the imaging device at its highest resolution and to enhance the

correlation between fluorescence and photosynthetic rate (Longstaff et al. 2002). Light-adapted

fluorescence was used over dark-adapted fluorescence because the former provides a more

accurate quantification of quantum yield, and therefore a stronger proxy for photosynthesis

(Baker 2009).

The entire process of collecting tissue from the canopy, allowing leaves to reach steady state temperature and fluorescence yield, and imaging both thermal and ΦPSII spatial patterns spanned < 30min per leaf.

Image Analysis

True-color reflected-light images were taken with a digital camera (PowerShot SD1000, Canon, Lake Success, New York) for each leaf using a camera mounted a fixed distance from the leaf and with a standard within each image to accurately calculate leaf area. The total leaf area in pixels was calculated for each false-color fluorescence and thermal image using the appropriate software (ImagingWin v2.32, Heinz Walz GmbH, Effeltrich, Germany; ThermaCam Quick Report, FLIR Systems, Portland, OR, USA). This area in pixels was then compared to the calculated leaf area to quantify the number of false-color pixels occurring in visibly damaged tissue (the galled region, the leaf fold, or the approximate leaf area defoliated), regions of undamaged tissue (of equivalent thermal of fluorescent signature as undamaged control leaves), and regions in-between where visible damage ceased but altered fluorescence or thermal signatures occurred (hereafter "propagated damage"). This process allowed accurate calculation of the true dimensions covered by each false-color pixel. False-color pixels were then counted for each region and converted to distances/areas. Propagated damage was quantified as any pixel intensity deviating >5% from undamaged tissue within the same leaf. Because chewing herbivores remove tissue, there is minimal visible damage (a cut edge); therefore, we calculated propagated damage as the distance of pixels from the cut edge that deviated > 5% from undamaged tissue within the same leaf.

Reflectance Measurement

To further explore possible mechanisms for how physiological damage may propagate from developing galls spectral reflectance was measured on galls, visibly undamaged tissue on the same leaf, and adjacent undamaged leaves. Galls were selected because of the greater alteration in thermal spatial patterns than other damage types and because the damaged tissue remained on the leaf over time (24h defoliation damage resulted in a great alteration of thermal spatial patterns but this effect was not sustained in older tissue). Leaf reflectance was measured in June 2009 on undamaged and galled leaves excised from equivalent nodes on determinate shoots in both elevated CO_2 and ambient plots. Four leaves for each damage type were removed from branchlets from different trees and combined for a single average of each damage type for each plot (n=3). Leaves were irradiated by an internal tungsten halogen light source in a field laboratory as previously described and upwelling irradiance (300 to 1100 nm) was recorded using a portable spectroradiometer (UniSpec Spectral Analysis System, PP Systems, Haverhill, MA, USA). The spectroradiometer was equipped with a visible/near infrared detector of <10 nm Raleigh resolution and 3.3nm bin size (<0.3 nm accuracy). Measurements were taken in a field laboratory with the fiber optic probe pointed downward to measure upwelling irradiance under ambient conditions. Prior to each measurement, a reference scan was performed by pointing the probe downward on a white reference standard (PP Systems, Haverhill, MA, USA).

Reflectance data (R) were used to calculate the photochemical reflectance index, water index, and normalized difference vegetation index. The photochemical reflectance index (PRI) was calculated as $(R_{531}-R_{570}) / (R_{531}+R_{570})$; this index responds to the composition of xanthophyll pigments and correlates with ΦPSII and net CO_2 assimilation (Gamon et al. 1997). The water index (WI) measures tissue water content and was calculated as R_{900}/R_{970} (Penuelas et al., 1997).

The normalized difference vegetation index $NDVI_{750}$ assesses foliar chlorophyll content and was calculated as $(R_{750}-R_{705}) / (R_{750}+R_{705})$ (Sims and Gamon 2002).

Data Analysis

This study employed a split plot design with blocking where whole plot treatments consisted of CO_2 level (ambient and elevated) and subplot consisted of damage type (defoliation, gall, leaf fold, undamaged). We analyzed aspen separately from birch because damage to the two tree species was produced by different insects, and thus treatments of herbivore type were asymmetrically applied. The model for each analysis used was: $Y_{ijkl} = \mu + B_i + C_j + e_{ij} + D_k + CD_{jk} + e_{ijk}$; where fixed effects included CO_2 level (C_j), damage type (D_k), and their interaction term (CD_{jk}). Block (B_i), whole plot error (e_{ij}), and subplot error (e_{ijk}) were random effects. Only aspen was examined again in 2009. Analysis of variance (ANOVA; PROC MIXED, SAS v.9.2, SAS Institute, Cary, NC) was used for all comparisons. Because low replication (n=3) increases the probability for type II errors but increasing a increases the probability for type I errors (Filion et al. 2000), we reported P-values $0.05 \leq 0.10$ as marginally significant and ≤ 0.05 as significant.

RESULTS

Arthropod damage altered ΦPSII and leaf surface temperature in visibly damaged tissue and reduced ΦPSII of remaining tissues adjacent to feeding damage; however, the extent that damage propagated into remaining leaf tissue depended on the type of injury (Figure 3.1, Tables 3.1 and 3.2). Defoliation and gall formation increased the spatial heterogeneity of leaf temperature and ΦPSII, but skeletonizing damage by larval sawflies did not. Defoliation reduced ΦPSII ~5-7% for ~1mm from chewed edges and increased temperature of the chewed edge in both aspen and birch (Figures 3.2 and 3.3). Aspen leaves with 24h larval gypsy moth defoliation

damage responded with larger reductions in ΦPSII efficiency (~14%) and enhanced evaporative cooling along the chewed edge; propagated damage reduced temperature ~0.5$°$C up to 4mm away from damage (Table 3.1). At its maximum, gall damage reduced ΦPSII >10% relative to undamaged tissues, but the distance that damage (defined as pixels deviating >5% from undamaged tissue on the same leaf) propagated into remaining leaf tissue was small (0.3±0.1mm). Gall damage enhanced evaporative cooling and reduced temperature by 1.2±0.2$°$C; this cooling effect propagated 2.5±0.2mm into adjacent non-galled tissues. Gall damage reduced the spectral reflectance for all wavelengths between 400 and 700 nm with the exception of a peak near 550 (i.e. xanthophylls). Gall damage also reduced PRI and increased water content (WI; Table 3.3).

Elevated CO_2 reduced the distance that defoliation damage in birch and 24h defoliation damage in aspen altered ΦPSII in adjacent tissues. (Table 3.2, Figure 3.2). Elevated CO_2 also reduced the cooling effect of gall formation on remaining leaf tissue (Figure 3.3). Although birch responded to ambient and elevated CO_2 with similar leaf temperatures and damage propagation distances quantitatively comparable to those of aspen, these effects were not statistically resolved. Elevated CO_2 also marginally reduced potential chlorophyll content of undamaged leaves (NDVI; Table 3.3).

DISCUSSION

Arthropod herbivory increased the spatial heterogeneity of photosynthesis and water use in remaining leaf tissue across tree species, but it did so in a damage-specific manner. Although background levels of herbivory typically are low (<16%) with the exception of outbreak years, even low levels may alter biomass (Wolf et al. 2008, Patankar et al. 2011). Our data indicated

that fresh defoliation damage immediately impaired ΦPSII in remaining aspen tissues and that this reduction in ΦPSII attenuated with time (Table 3.2, Figure 3.2). Older damage also reduced ΦPSII and transpiration in remaining tissues suggesting that the leaf never completely recovered from the original herbivore attack (Tables 3.1 and 3.2, Figure 3.2). Another common damage type, gall formation, reduced ΦPSII but this reduction was localized and did not propagate from the gall into the surrounding leaf tissue. In contrast to ΦPSII, lower leaf temperatures indicated that transpiration was enhanced in undamaged leaf tissue surrounding galls (Figure 3.2). Because as little as a 0.5ºC change in leaf surface temperature can indicate a 10% shift in stomatal conductance (Jones 1999) and ΦPSII correlates strongly with photochemistry (Genty and Meyer 1994), these subtle alterations in remaining leaf tissue may alter carbon gain at larger scales. When summed at the leaf-level, the area of apparently healthy tissue but with lower ΦPSII can be equal to the area with visible herbivore damage (Aldea et al. 2006, Zangerl et al. 2002). Thus, relying on visible damage may underestimate the effect of herbivory on photosynthesis and plant productivity.

Elevated CO_2 increased leaf temperature in aspen which, in turn, interacted with damage type to reduce the cooling effect of immediate defoliation damage and gall formation. Although the values of birch leaf temperature under ambient and elevated CO_2 were similar to aspen, the effect of CO_2 was not statistically resolvable at the low replication common among FACE sites (Filion et al. 2000). Elevated CO_2 reduced the distance that damage to ΦPSII propagated into remaining tissue in birch and 24h defoliation in aspen. These results support the hypothesis that elevated CO_2 can mitigate the effect of herbivory on photosynthesis.

The mechanisms underlying suppressed ΦPSII and altered transpiration vary with the type of herbivore damage. Defoliation damage may sever vasculature and initiate a cooling effect

through evaporative water loss from cut tissues; however, defoliation damage may also initiate water movement from the vascular tissue into the apoplast where it evaporates at the equilibrium point between water vapor and liquid often at a distance from the cut edge (Aldea et al. 2005). In instances where no reduction in ΦPSII occurred concomitantly with an enhanced cooling effect, as with 24h defoliation damage >1mm from cut edges in aspen, apoplastic water transfer may have triggered reductions in leaf temperature without altering photosynthesis. Given that apoplastic water movement is driven by the equilibrium point between vapor and liquid, we would expect ambient temperatures and not CO_2 concentrations to influence the equilibrium point. Our results agree with this notion as 24h defoliation damage in both ambient and elevated CO_2 propagated equal distances into remaining leaf tissue. However, elevated CO_2 reduced the distance of propagated damage to ΦPSII efficiency. Spectral reflectance suggested that aspen leaves grown under elevated CO_2 had lower chlorophyll content, reduced ΦPSII, but elevated water content (Table 3.3). Thus, it is possible that the increases in leaf mass per unit area (i.e. increased thickness) in aspen species grown under elevated CO_2 (Liberloo et al. 2007) and the observed increase in water content under elevated CO_2 enhanced leaf tolerance to desiccation induced by defoliation damage. This tolerance, in turn, may have reduced the suppression of ΦPSII at cut edges.

Gall formation transforms host morphology and physiology at some cost to the host to enhance fitness of the attacking parasite (Stone and Schonrogge 2003). Leaf galls may enhance net photosynthesis by reducing respiration (Dorchin et al. 2006) yet structural and chemical changes often yield tissues deficient in photosynthetic proteins and pigments (e.g., Yang et al. 2007). Gall formation in aspen generated tissues with reduced ΦPSII and enhanced transpiration relative to undamaged tissues. Whereas other hardwood species show damage to ΦPSII

propagated away from the gall into remaining non-galled leaf tissues (e.g., *Carya glabra*; Aldea et al. 2006), aspen galls reduced ΦPSII only minimally outside of the galled structure. Higher spectral reflectance between 400 and 700 nm with the exception of a peak near 550 (i.e. xanthophylls) suggests reduced absorbance for all photosynthetically active pigments. This finding, in addition to the observed lower N content in gall tissue compared to non-galled leaf tissue of galled leaves (unpublished data) suggests a lack of photosynthetic pigment protein complexes contribute to reduced ΦPSII but that this reduction was limited to actual area occupied by the gall.

Aspen galls enhanced transpiration in gall tissues thereby reducing leaf temperatures in adjacent tissues. Because no tissues had been cut, as with defoliation damage, the movement of water to the developing gall was likely driven by evapotranspiration through stomata, the only other openings in the leaf surface. We observed increased leaf temperatures across all tissue types under elevated CO_2 in June. This result agrees with other studies on tree response to elevated CO_2 (see Wittig et al. 2007 for a synthesis) and suggests elevated CO_2 reduced stomatal aperture thereby reducing transpiration and increasing leaf temperature. Thus, it is likely that reduced stomatal aperture on galls and the surrounding leaf area attenuated the cooling effect of gall formation. Gall formation by *Harmandia* species in aspen typically occurs adjacent to major veins (pers. observation) and distorts xylem elements in other aspen species (Hyde 1922) possibly to facilitate transport to a developing sink. While the degree to which this alters the nutrient flux to the developing parasite is unknown, the increased temperature relative to ambient conditions suggests insect development may occur faster under future predicted shifts in climate.

Arthropod herbivory can reduce plant productivity by removing photosynthetic leaf area. In addition, results from this study and others (Aldea et al. 2005, 2006, Patankar et al. 2011,

Zangerl et al. 2002) indicate that in some cases damage to leaf surfaces causes a reduction in the quantum efficiency of photosystem II fluorescence (ΦPSII) which is highly correlated with the rate of carbon assimilation. These reductions of photosynthesis in remaining leaf tissue following herbivory vary with the plant species under attack as well as the herbivore (Nabity et al. 2009). The mechanisms governing this reduction in photosynthesis are not well understood but in some cases relate to disruptions in carbon and water transport. Insofar as growth under elevated CO_2 increases the rate of carbon uptake and reduces water loss by reducing stomatal conductance, it is expected that this element of global change would modulate the effect of herbivory on photosynthesis. Though measurement variation was high, growth under elevated CO_2 reduced the distance that herbivore-induced reductions in photosynthesis propagated away from the point of damage in aspen and birch, suggesting that at least for these species, elevated CO_2 may reduce the impact of herbivory on photosynthesis. Arthropod herbivory directly alters productivity and will interact with changing climate albeit with a high degree of uncertainty in hardwood forest ecosystems (Lindroth 2010).

LITERATURE CITED

Aldea M, Hamilton JG, Resti JP, Zangerl AR, Berenbaum MR, DeLucia EH. 2005. Indirect effects of insect herbivory on leaf gas exchange in soybean. Plant Cell and Environment 28: 402-411.

Aldea M, Hamilton, JG, Resti JP, Zangerl AR, Berenbaum MR, Frank TD, DeLucia EH. 2006. Comparison of photosynthetic damage from arthropod herbivory and pathogen infection in understory hardwood samplings. Oecologia 149: 221-232.

Baker NR. 2008. Chlorophyll fluorescence: a probe of photosynthesis in vivo. Annual Review of Plant Biology 59: 89-113.

Baker NR, Oxborough K. 2005. Chlorophyll fluorescence as a probe of photosynthetic productivity. In: Papageorgiou GC, Govindjee, eds. Chlorophyll a fluorescence: a signature of photosynthesis. Advances in Photosynthesis and Respiration, Vol. 19. The Netherlands: Springer, 65–82.

Bilgin DD, Zavala JA, Zhu J, Clough SJ, Ort DR, DeLucia EH. 2010. Biotic stress globally down-regulates photosynthesis genes. Plant Cell and Environment. 33: 1597-1613.

Couture JJ, Meehan TD, Lindroth RL. 2011. Atmospheric change alters foliar quality of host trees and performance of two outbreak insect species. Oecologia 168: 863-876.

Cseke LJ, Tsai CJ, Rogers A, Nelsen MP, White HL, Karnosky DF, Podila GK. 2009. Transcriptomic comparison in the leaves of two aspen genotypes having similar carbon assimilation rates but different partitioning patterns under elevated [CO_2]. New Phytologist 182: 891-911.

Cyr H, Pace ML. 1993. Magnitude and patterns of herbivory in aquatic and terrestrial ecosystems. Nature 361: 148-150.

Dorchin N, Cramer MD, Hoffmann JH. 2006. Photosynthesis and sink activity of wasp-induced galls in *Acacia pycnantha*. Ecology 87: 1781-1791.

Filion M, Dutilleul P, Potvin C. 2000. Optimum experimental design for Free-Air Carbon Dioxide Enrichment (FACE) studies. Global Change Biology 6: 843-854.

Gamon JA, Serrano L, Surfus JS. 1997. The photochemical reflectance index: An optical indicator of photosynthetic radiation use efficiency across species, functional types, and nutrient levels. Oecologia 112: 492-501.

Genty B, Meyer S. 1994 Quantitative mapping of leaf photosynthesis using chlorophyll fluorescence imaging. Australian Journal of Plant Physiology 22: 277-284.

Gog L, Berenbaum MR, DeLucia EH, Zangerl AR. 2005 Autotoxic effects of essential oils on photosynthesis in parsley, parsnip, and rough lemon. Chemoecology 15: 115-119.

Hillstrom ML, Lindroth RL. 2008. Elevated atmospheric carbon dioxide and ozone alter forest insect abundance and community composition. Insect Conservation and Diversity 1: 233–241.

Hillstrom ML. 2010. Effects of elevated carbon dioxide and ozone on forest insect abundance, diversity, and community composition. PhD dissertation, University of Wisconsin, Madison.

Hyde KC. 1922. Anatomy of a gall on *Populus trichocarpa*. Botanical Gazette 74: 186-196.

Jones HG. 1999. Use of thermography for quantitative studies of spatial and temporal variation of stomatal conductance over leaf surfaces. Plant Cell and Environment 22: 1043-1055.

Leakey ADB, Ainsworth EA, Bernacchi CJ, Rogers A, Long SP, Ort DR. 2009 Elevated CO_2 effects on plant carbon, nitrogen, and water relations: six important lessons from FACE. Journal of Experimental Botany 60: 2859–2876.

Liberloo M, Tulva I, Raim O, Kull O, Ceulemans R. 2007. Photosynthetic stimulation under long-term CO_2 enrichment and fertilization is sustained across a closed *Populus* canopy profile (EUROFACE). New Phytologist 173: 537-549.

Lindroth RL. 2010. Impacts of elevated atmospheric CO_2 and O_3 on forests: phytochemistry, trophic interactions, and ecosystem dynamics. Journal of Chemical Ecology 36: 2-21.

Longstaff BJ, Kildea T, Runcie JW, Cheshire A, Dennison WC, Hurd C Kana T, Raven JA, Larkum AW. 2002. An in situ study of photosynthetic oxygen exchange and electron transport rate in the marine macroalga *Ulva lactuca* (Chlorophyta). Photosynthesis Research 74: 281-293.

McElrone AJ, Hamilton JG, Krafnick AJ, Aldea M, Knepp RG, DeLucia EH. 2010. Combined effects of elevated CO_2 and natural climatic variation on leaf spot diseases of redbud and sweetgum trees. Environmental Pollution 158: 108-114.

Nabity PD, Zavala JA, DeLucia EH. 2009. Indirect suppression of photosynthesis on individual leaves by arthropod herbivory. Annals of Botany 103: 655-663.

Noormets A, McDonald EP, Dickson RE, Kruger EL, Sober A, Isebrands JG, Karnosky DF. 2001. The effect of elevated carbon dioxide and ozone on leaf- and branch-level photosynthesis and potential plant-level carbon gain. Trees 15: 262-270.

Oxborough K. 2004 Imaging of chlorophyll a fluorescence: theoretical and practical aspects of an emerging technique for the monitoring of photosynthetic performance. Journal of Experimental Botany 55: 1195–1205.

Patankar R, Thomas SC, Smith SM. 2011. A gall-inducing arthropod drives declines in canopy photosynthesis. Oecologia 167: 701-709.

Penuelas J, Pinol J, Ogaya R, Filella I. 1997. Estimation of plant water concentration by the reflectance water index WI (R_{900}/R_{970}). International Journal of Remote Sensing 18: 2869-2875.

Saxe H, Ellsworth DS, Heath J. 1998. Tree and forest functioning in an enriched CO_2 atmosphere. New Phytologist 139: 395–436.

Sims DA, Gamon JA. 2002. Relationship between pigment content and spectral reflectance across a wide range of species, leaf structures and developmental stages. Remote Sensing Environment 81: 337-354.

Stone GN, Schonrogge K. 2003. The adaptive significance of insect gall morphology. Trends in Ecology and Evolution 18: 512-522.

Tang JY, Zielinski RE, Zangerl AR, Crofts AR, Berenbaum MR, DeLucia EH. 2006. The differential effects of herbivory by first and fourth instars of *Trichoplusia ni* (Lepidoptera: Noctuidae) on photosynthesis in *Arabidopsis thaliana*. Journal of Experimental Botany 57: 527-536.

Welter SC. 1989. Arthropod impact on plant gas exchange. In: Bernays EA (ed) Insect-plant Interactions. CRC Press, Boca Raton, FL, pp 135-151.

Wittig VE, Ainsworth EA, Long SP. 2007. To what extent do current and projected increases in surface ozone affect stomatal conductance of trees? A meta-analytic review of the last three decades of experiments. Plant Cell and Environment 30: 1150-1162.

Wolf A, Kozlov MV, Callaghan TV. 2008. Impact of non-outbreak insect damage on vegetation in northern Europe will be greater than expected during a changing climate. Climate Change 87: 91-106.

Yang CM, Yang MM, Huang MY, Hsu JM, Jane WN. 2007. Lifetime deficiency of photosynthetic pigment-protein complexes CP1, A1, AB1, and AB2 in two cecidomyiid galls derived from *Machilus thumbergiii* leaves. Photosynthetica 45: 589-593.

Zangerl AR, Hamilton JG, Miller TJ Crofts AR, Oxborough K, Berenbaum MR, DeLucia EH. 2002. Impact of folivory on photosynthesis is greater than the sum of its holes. Proceedings of the National Academy of Sciences USA 99: 1088-1091.

Zvereva EL, Lanta V, Kozlov MV. 2010. Effects of sap-feeding insect herbivores on growth and reproduction of woody plants: a meta-analysis of experimental studies. Oecologia 163: 949-960.

TABLES

Table 3.1. Mean (±SE) leaf temperature for damaged and undamaged tissues grown under ambient and elevated CO_2, and the distance that the change in temperature propagated into adjacent tissue (part-table A). A summary of P values for the main effects of CO_2 fumigation, different damage types, and their interaction is also included (part-table B)

Species	Damage type	Undamaged temp (°C)		Damaged temp (°C)		Propagation (mm)	
A		Ambient	Elevated	Ambient	Elevated	Ambient	Elevated
Aspen	Leaf fold	22.0±0.3	23.7±0.2	21.8±0.2	23.5±0.2	ND	ND
	Defoliation	22.0±0.3	23.9±0.2	22.3±0.3	23.9±0.3	0.5±0.03	0.3±0.05
	Gall	21.8±0.3	23.7±0.2	20.2±0.3	22.8±0.3	2.2±0.40	2.7±0.20
Birch	Defoliation	22.4±0.4	23.5±0.3	22.6±0.4	23.9±0.2	0.5±0.07	0.3±0.06
Aspen	24h Defoliation	25.3±0.2	25.0±0.2	24.6±0.2	24.4±0.2	3.9±0.30	4.4±0.40

B	Main effect	Temperature	Propagation
Aspen	CO_2	0.04	0.50
	Damage	<0.01	<0.01
	CO_2 x Damage	0.03	0.14
Birch	CO_2	0.16	0.20
	Damage	0.20	NA
	CO_2 x Damage	0.66	NA

Table 3.1. (continued)

Species	Main effect	Temperature	Propagation
Aspen	CO_2	0.49	0.33
(24h feeding exp)	Damage	<0.01	NA
	CO_2 x Damage	0.78	NA

Damage by leaf folding did not alter the spatial pattern of temperature within a leaf.
ND propagated distance was not detectable

Table 3.2. Mean (±SE) ΦPSII for damaged and undamaged tissues grown under ambient and elevated CO_2, and the distance that the change in temperature propagated into adjacent tissue (part-table A). A summary of P values for the main effects of CO_2 fumigation, different damage types, and their interaction is also included (part-table B).

Species	Damage type	Undamaged ΦPSII		Damaged ΦPSII		Propagation (mm)	
A		Ambient	Elevated	Ambient	Elevated	Ambient	Elevated
Aspen	Leaf fold	0.616±0.004	0.626±0.004	0.605±0.008	0.619±0.004	ND	ND
	Defoliation	0.615±0.003	0.611±0.006	0.568±0.005	0.569±0.005	0.81±0.05	0.73±0.05
	Gall	0.619±0.004	0.616±0.005	0.551±0.016	0.542±0.018	0.14±0.08	0.43±0.20
Birch	Defoliation	0.601±0.012	0.602±0.013	0.569±0.008	0.571±0.008	0.80±0.04	0.59±0.05
Aspen	24h Defoliation	0.609±0.008	0.619±0.006	0.525±0.007	0.523±0.008	0.94±0.03	0.86±0.02
B		Main effects		ΦPSII		Propagation (mm)	
Aspen		CO_2		0.66		0.65	
		Damage		<0.01		0.07	
		CO_2 x Damage		0.69		0.44	
Birch		CO_2		0.44		<0.01	
		Damage		0.04		NA	
		CO_2 x Damage		0.32		NA	

Table 3.2. (continued)

Species	Main effects	ΦPSII	Propagation (mm)
Aspen	CO_2	0.88	0.03
(24h feeding exp)	Damage	<0.01	NA
	CO_2 x Damage	0.98	NA

Damage by leaf folding did not alter the spatial pattern of ΦPSII within a leaf.
ND propagated distance was not detectable

Table 3.3. Reflectance indices (unitless) were calculated from the spectral reflectances of gall damage and nearby undamaged leaves grown under ambient and elevated CO_2. There was no significant difference in the indices measured near the gall on a damaged leaf and on an undamaged leaf, so only data for nearby undamaged leaves are shown. A summary of P values for the main effects of CO_2 fumigation, and damage as well as their interaction is included.

Index	Ambient CO_2		Elevated CO_2		P value		
	Aspen Leaf	Aspen Gall	Aspen Leaf	Aspen Gall	CO_2	Damage	CO_2 x Damage
PRI	0.09±0.01	-0.05±0.01	0.06±0.01	-0.04±0.01	0.89	<0.01	0.08
WI	1.03±0.00	1.10±0.01	1.03±0.00	1.10±0.02	0.98	<0.01	0.76
NDVI	0.32±0.01	0.07±0.01	0.29±0.00	0.07±0.01	0.07	<0.01	0.13

Figure 3.1. Representative true-color reflected light images (a), false-color thermal images (b), and false-color images of fluorescence (ΦPSII efficiency; c) for damage from leaf folds (*Phyllocolpa* larvae; top row), defoliation (unknown age and herbivore; second row), 24h defoliation (*Lymantria dispar*; third row), and gall (*Harmandia* sp.; bottom row) on aspen (*P. tremuloides*). All images are represented to scale with the exception that 24h defoliation damage (*) is on the same false-color scale from 20 to 26ºC.
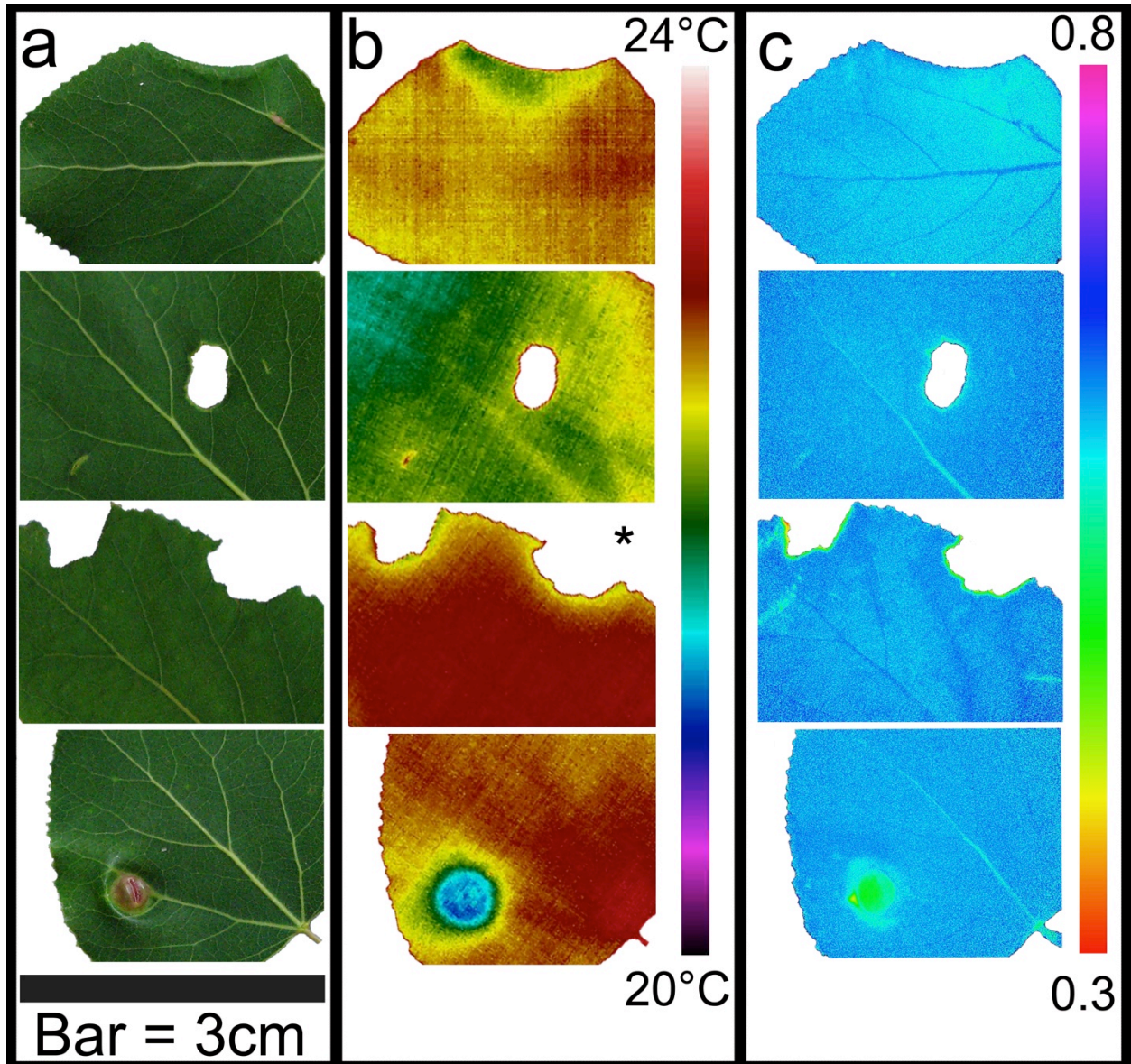
Figure 3.2. Mean (±SE) distance that damage to ΦPSII propagated into remaining tissues adjacent defoliated edges and galls (n=3 per damage type). Values for ΦPSII reduced by $> 5\%$ relative to remaining tissues were designated as damaged. Significant deviation between fumigation treatments is indicated by 'a' for $P<0.05$ or 'b' for $P<0.01$. Only aspen leaf fold damage did not propagate into remaining tissue i.e. was not detectable (ND) and therefore was not included; however, all other damage types did propagate into remaining tissues ($P<0.01$).
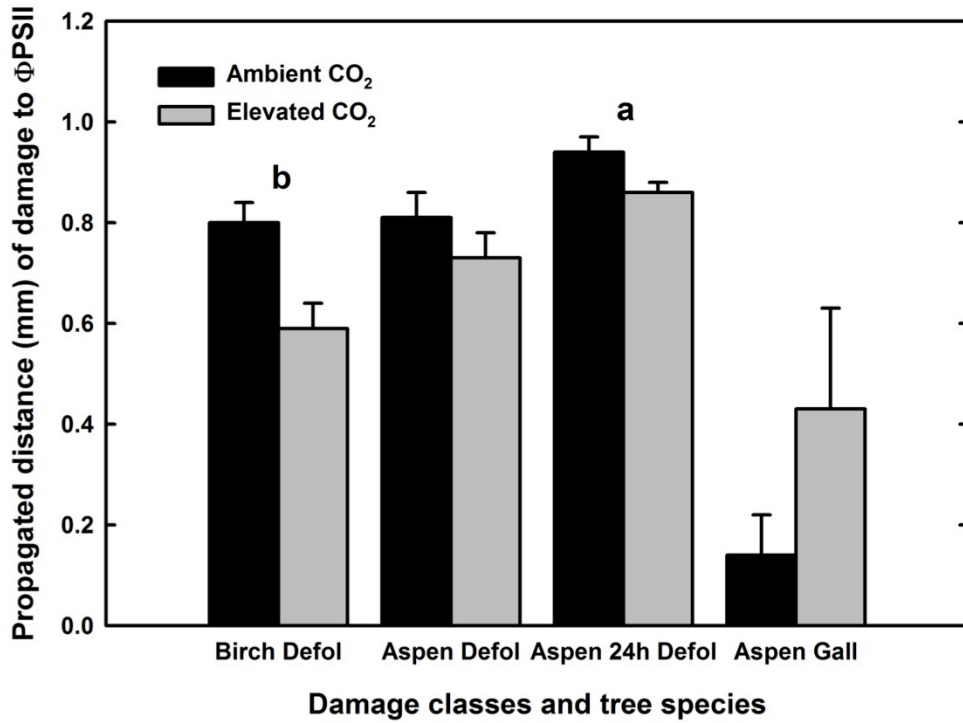
Figure 3.3 Mean (±SE) difference in leaf temperature (ΔT) between visibly damaged (d) and remaining (c) tissue within the same leaf (n=3 per damage type). Significant deviation between fumigation treatments for each damage type is indicated by 'a' for $P<0.05$ or 'b' for $P<0.01$. *Only aspen leaf fold damage did not differ in temperature from remaining tissue (i.e. ΔT did not differ from 0); however, all other damage types did ($P<0.01$).
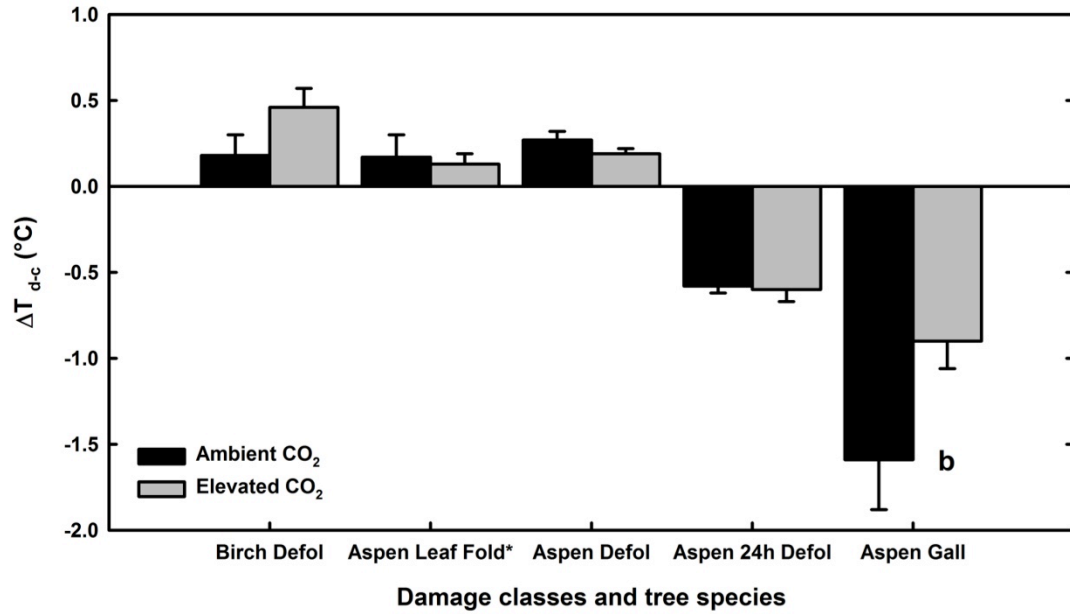
CHAPTER 4

HERBIVORE INDUCTION OF JASMONIC ACID AND CHEMICAL DEFENSES REDUCES PHOTOSYNTHESIS IN *NICOTIANA ATTENUATA*

ABSTRACT

Herbivores elicit damage-specific effects in leaf tissues that signal a shift in metabolism from growth to defense. This trade-off may account for reductions in fitness; however, the defense-induced changes in carbon assimilation that precede this reallocation in resources remain largely undetermined. Therefore, we characterized the response of photosynthesis to herbivore induction of jasmonic acid (JA)-related defenses in the model plant species *Nicotiana attenuata* to increase understanding of these mechanisms. We hypothesized that JA-induced defenses will reduce fitness by decreasing leaf photosynthesis upon attack and predicted that wild-type plants will suffer greater reductions in photosynthesis than plants lacking JA-induced defenses. We characterized gas exchange coupled to chlorophyll fluorescence imaging and measured production of defense-related metabolites immediately after attack and through recovery. Herbivore damage immediately reduced electron transport and gas exchange in wild-type plants but suppressed gas exchange for several days after attack. The sustained reductions occurred concurrently with increased defense metabolites in wild-type plants whereas lipoxygenase suppressed plants suffered minimal suppression in photosynthetic parameters and no increase in defense metabolite production. Here we identified that lipoxygenase signaling and its resulting JA-related metabolites reduce component processes of photosynthesis and contribute to reduced fitness when herbivores attack.

INTRODUCTION

Plants optimize resource use when attacked by herbivores to minimize reductions in fitness (e.g., McKey 1974) but the mechanisms that regulate these physiological trade-offs are not well understood. Feeding by arthropod herbivores reduces growth in part through the loss of photosynthetic tissue (e.g., Welter 1989), yet tissues adjacent to feeding damage also may reduce photosynthesis and thereby contribute to reductions in productivity (Aldea et al. 2006;, Nabity, et al. 2009, 2012,). Feeding also elicits the production of a complex network of hormone signaling that induces defenses and initiates the trade-off between using resources for growth or defense. The manifestation of these defenses can be specific to the herbivore-plant interaction (Walling 2000), but the generic response for chewing herbivores is the elicitation of the jasmonic acid (JA) signaling pathway. This pathway regulates both indirect and direct defenses that vary in their resource requirements and fitness costs (Kessler et al. 2004). Gene expression and proteomic surveys of JA elicitation implicate candidate mechanisms regulating the switch from growth to defense (Heidel and Baldwin 2004, Giri et al. 2006, Maserti et al. 2010, Chen et al. 2011), but the functional physiology linking how defense production alters photosynthesis is only beginning to be understood (Zangerl et al. 1997, 2002, Tang et al. 2009, Halitschke et al. 2011).

The elicitation of JA-related defenses reduces fitness across many species (Cipollini 2007, Kim et al. 2009, Kessleret al. 2011); however, in *Nicotiana attenuata* Torr. ex Watson, the type of metabolite may determine the reduction in growth and fitness. Genetic suppression of trypsin protease inhibitors (TPI) increases growth and fitness (Zavala et al. 2004) but plants silenced in nicotine production do not differ in other metabolites or measures of growth relative to wild-type plants (Steppuhn et al. 2004). As such, TPI may incur greater resource costs than

nicotine. Interestingly, the reallocation of resources to produce TPI, nicotine, or other defense compounds does not fully account for the ultimate fitness cost as plants lacking those defenses still decrease in growth and fitness when attacked by chewing herbivores (van Dam and Baldwin 2001, Zavala et al. 2004, Zavala and Baldwin 2004). This persistent reduction in fitness cannot be explained by the synthesis or lack of individual defense products and suggests that other aspects of physical damage or JA signaling reduce photosynthesis and growth-related processes.

Herbivore-altered photosynthesis in remaining tissues may yield a significant and often unaccounted for reduction in growth or fitness. When caterpillar feeding removed 5% of the leaf area of wild parsnip *Pastinaca sativa* L. leaf photosynthesis declined by 20% in the remaining foliage for at least three days as a result of ruptured oil tubes containing autotoxic terpenes (Zangerl et al. 2002, Gog et al. 2005). Defoliation in many other species that lack autotoxic defenses also reduces photosynthesis in remaining leaf tissue, but this damage can be minimal and attenuate as ruptured tissues lignify (Aldea et al. 2005, 2006, Nabity et al. 2012). In some cases, damage in remaining tissues can equal the amount of tissue consumed (Aldea et al. 2006) and effectively double fitness costs for each bite consumed. Defoliation by the tobacco hornworm *Manduca sexta* L. in *N. attenuata* reduces the operating efficiency of photosystem II (F_q'/F_m') in remaining tissue, and this indicates that electron transport may limit carbon assimilation after short term feeding (Halitschke et al. 2011). However, feeding damage by piercing sucking insects does not reduce photosynthesis, nor do these insects increase JA or nicotine levels (Heidel and Baldwin 2004, Halitschke et al. 2011, unpublished data). As such, herbivore-specific elicitors may determine the photosynthetic suppression in remaining leaf tissue and ultimate reductions in fitness (Halitschke et al. 2011). But because different defense signaling networks are induced relative to the type of herbivore attack (i.e., phloem-feeding

aphid vs. chewing larva), additional data on the how defense induction alters photosynthesis may reveal mechanisms underlying the herbivore-modulated reprogramming of plant metabolism.

The objective of this study was to characterize how induction of JA defenses by herbivore attack suppresses component processes of photosynthesis. We characterized photosynthesis immediately after attack, and through time with production of defense compounds to increase understanding of the physiological mechanisms by which growth and fitness decline with herbivory. We hypothesized that an inducible JA-related defense signaling network reduces growth and fitness by suppressing leaf photosynthesis upon attack and predict wild-type plants will suffer greater reductions in photosynthesis than plants lacking JA-related defense production.

MATERIALS AND METHODS

Plants and insects

To test how defense signaling and synthesis alter component processes of photosynthesis, we examined the physiological response of plants with and without genetically suppressed JA-defense signaling in combination with herbivory. Wild-type *Nicotiana attenuata* plants were compared to a genetically altered strain, antisense LOX3 (asLOX), in which the primary lipoxygenase initiating the JA-signaling cascade is suppressed (Halitschke and Baldwin 2003). This genetic modification results in > 25 % decrease in nicotine, up to 50 % decrease in TPI, and 45-65 % decrease in JA burst upon herbivore attack. Seeds obtained from the Max Planck Institute for Chemical Ecology (Jena, Germany) were prepared and germinated on agar in an environmental growth chamber (25 °C 16:8 L:D) following Krugel et al. (2002) and then transplanted to 2 liter pots containing soilless media (Sunshine LC1, SunGro Horticulture,

Bellevue, WA). All transplants were grown in a glasshouse with supplemental lighting ($28:22 \pm$ 2 °C, 16:8 L:D), watered when necessary, and infested >2 weeks after transplanting. Eggs of *M. sexta* were obtained from an in-house colony and, upon hatching, neonate (< 1 day old) larvae were caged on +1 source leaves as determined by Giri et al. (2006) and allowed to feed for either 1 or 3 days. These source leaves are the first fully expanded leaf of the developing rosette and were used in place of stalk leaves to test how early herbivory events contribute to lasting reductions in growth and fitness. Plants lacking herbivores were fitted with the same fine mesh cages on +1 source leaves but without insects. Larvae grew as they fed, and, after three days, were 1st instars.

Gas exchange and chlorophyll fluorescence imaging

To capture rapid responses reflecting the direct effect of leaf damage on photosynthesis, gas exchange and chlorophyll fluorescence were measured on plants following one day of herbivory. In a subsequent experiment plants were exposed to three day of herbivory to capture potential effects related to synthesis and translocation of the major direct defenses (approx. three day for TPI; Van Dam et al. 2001, approx. five day for nicotine; Shi et al. 2006). Two cohorts of plants were used in the three-day feeding experiment to provide tissue for analysis of plant metabolites. The first cohort was assessed for photosynthesis prior to harvesting at two time points: immediately after feeding and after two-day recovery time (no insect feeding). The second cohort of plants was assessed for photosynthesis immediately after feeding damage, after three-day recovery, and after seven-day recovery time following a random design blocked by time of measurement within each day. For all experiments, each genotype (n = 5) was assessed at each herbivore treatment (+ or –herbivore) under the conditions described. Immediately after measurements leaves were clipped, frozen in liquid N_2, and stored at -80 °C. Leaves examined

through time were collected at the last time point. All frozen leaf samples were ground using mortar and pestle under liquid N_2, divided into aliquots of known mass (~150 mg), and stored at -80 °C until hormone and metabolite analysis.

Gas exchange was measured with an infrared gas analysis system (LI-6400, Licor, Lincoln, NE) with a modified cuvette to allow for simultaneous chlorophyll fluorescence imaging with a CFImager (Technologica, UK). Leaves were dark-adapted (> 30 minutes), imaged after an 800 ms saturating pulse (> 6000 PAR), light adapted (at 350 PAR) for 20 minutes until gas exchange parameters stabilized, and then imaged after another saturating pulse. This allowed for images of maximal (F_m), minimal (F_o), and variable ($F_v = F_m - F_o$) fluorescence and the calculation of the maximal efficiency of photosystem II (F_v/F_m) as defined by Baker (2008). Once light-adapted steady state was achieved, gas exchange values were recorded, and images for the operating efficiency of photosystem II (F_q'/F_m') were taken.

To characterize herbivore induced spatial heterogeneity in leaf fluorescence we counted the number of pixels within each leaf that were reduced in value > 5 % for F_v/F_m and > 10 % for F_q'/F_m' images relative to the average value of undamaged leaf tissue in the same leaf. This value of undamaged tissue did not differ from average values of separate, undamaged leaves assessed concurrently with damaged leaves. We expressed the damaged area as a percentage of remaining tissue for each image type. Images were made under low irradiance to maximize electron transfer efficiency (Baker et al. 2007). This procedure optimizes the assessment of pulse amplitude modulated (PAM) fluorescence and strengthens the correlation between fluorescence and photosynthetic rate (Longstaff et al. 2002).

Plant hormones

To quantify how defense-related plant hormones interact with alterations in photosynthesis we characterized jasmonic acid (JA) and salicylic acid (SA) for individual leaves. Hormones were analyzed by high performance liquid chromatography coupled to a mass spectrometer (HPLC/MS: 2010 EV HPLC/MS, Shimadzu, Columbia, MD, USA) using a protocol modified from Wang et al. (2007). Aliquots of frozen leaf tissue were extracted with 1 mL ethyl acetate spiked with isotopically labeled internal standards for JA (200 ng ml^{-1}; ^{5}JA) and SA (50 ng ml^{-1}; ^{4}SA). Samples were vortexed for 5 minutes and centrifuged at 13000 rpm for 20 minutes at 4 °C, and then the supernatants were transferred to new tubes. Each sample was re-extracted with 0.5 ml of unlabeled ethyl acetate, shaken, and centrifuged under the same conditions. The supernatants were combined and evaporated until dryness at 30 °C under a vacuum concentrator. The dried residue was re-suspended in 0.5 mL 70 % (v/v) methanol, vortexed > 5 minutes, and centrifuged at 13000 rpm for 10 minutes, and 0.4 mL was transferred to vials for analysis by HPLC/MS

The HPLC/MS was operated in negative electro-spray ionization mode with a mobile phase of 0.05 % formic acid (solvent A) and 0.05 % formic acid in methanol (solvent B) used in gradient mode for the separation following Wang *et al*. (2007). Samples (10 μL) were injected at a flow rate of 200 μL min^{-1} onto a Luna C18 column (250 x 2 mm, 5 μ ID, Phenomenex, Torrance, CA, USA) with selected reaction monitoring of compound-specific parent ions JA = 209; ^{5}JA = 214; SA = 137; ^{4}SA = 141.

Direct defense traits

To quantify how defenses interact with alterations in photosynthesis we assayed individual leaves for trypsin protease inhibitors (TPI) and nicotine. TPI activity was determined

by radial diffusion assay (van Dam et al. 2001). Activity was normalized to protein content determined from an aliquot of ground leaf tissue extracted under 0.5 mL of 100 mM Hepes (titrated to pH 7.5 with NaOH) and assayed with the Pierce BCA protein kit (ThermoFisher Scientific, Rockford, IL). Nicotine content was analyzed by HPLC following a protocol modified from Keinanen et al. (2001). Aliquots of ground leaf samples were extracted with 1 mL 40 % methanol with 0.5 % acetic acid in H_2O, combined with 0.3 g of 1mm Zircon/Silica beads (Biospec Products Inc, Bartlesville, OK), and shaken in a Mini Beadbeater (Biospec Products Inc) for 45 seconds. Ground tissues were then vortexed for 2 hours, centrifuged at 13000 g for 10 minutes, and 0.3 mL pipetted to HPLC vials for analysis.

The same HPLC/MS was used to measure direct defense traits although a mobile phase made up of 0.25% phosphoric acid in H_2O (solvent A) and 100% acetonitrile (solvent B) was used for separation. Samples (10 μL) were injected at a flow rate of 200 μL min^{-1} onto a column (4.6 x 150 mm, 3 μ ID, Inertsil ODS3, GL Sciences Inc, Torrance, CA) and elution times and monitoring wavelengths were as in Keinanen et al. (2001).

Data analysis

Data for plant hormones and direct defense traits were analyzed with a mixed model analysis of variance (ANOVA, Proc Mixed 9.2, SAS Institute, Cary, NC) with genotype (wild-type or asLOX) and herbivore (+ or -) as fixed effects. When the initial ANOVA yielded a significant difference, post-hoc comparisons were made between least squares means (LS means). Gas exchange and chlorophyll fluorescence imaging parameters were analyzed by ANOVA when measurements corresponded with destructively harvested leaves. Gas exchange measured through time was analyzed by repeated measures ANOVA with post-hoc comparisons as described. Data describing the percentage of tissue where fluorescence was reduced relative to

undamaged leaves were log transformed prior to analysis by ANOVA. Defense metabolites were regressed against photosynthesis parameters using Proc Corr 9.2 (SAS Institute, Cary, NC). All comparisons were made at $P \le 0.05$ unless otherwise specified.

RESULTS

Herbivory rapidly altered photosynthesis, defense signaling, and metabolites synthesis in *N. attenuata* though effects were mild (Table 4.1). A brief herbivore attack – one day – caused a significant reduction in carbon assimilation and stomatal conductance (g_s) ($F = 5.36$; $df = 1,12$; $P = 0.04$, $F = 4.65$; $df = 1,12$; $P = 0.05$, respectively) but no differences were detected between genotypes. Defense-modified asLOX plants maintained lower respiration rates than wild-type plants ($F = 5.06$, $df = 1,12$, $P = 0.04$) but no interaction with herbivory was detected. JA and TPI levels increased in wild-type plants compared to asLOX plants ($F = 13.03$ $df = 1,12$ $P = 0.004$, $F = 111.2$ $df = 1,12$ $P < 0.001$, respectively), whereas nicotine content did not increase with one-day herbivory but was lower overall in asLOX plants (Table 4.1). Carbon assimilation did not correlate with any defense compounds but did correlate with propagated damage to dark-adapted electron transport ($r = -0.46$, $P = 0.04$). This propagated damage also strongly correlated with JA and TPI but not nicotine levels (JA; $r = 0.65$; $P = 0.002$, TPI; $r = 0.58$; $P = 0.007$, nicotine; $r = 0.03$; $P = 0.9$).

Longer feeding resulted in lasting reductions in photosynthesis and elicited a strong, sustained defense response. After three days of feeding insects consumed 7% of total leaf area (160 mm^2) and reduced maximal (F_v/F_m) and operating (F_q'/F_m') efficiency in electron transport in remaining tissue adjacent to feeding sites. Greater propagated damage occurred in wild-type plants than in asLOX plants (Figure 4.1). This damage in wild-type plants decreased to the levels

73

observed in asLOX plants after two-day recovery time (F_v/F_m; WT = 3.7 ± 0.2 %, asLOX = 3.7 ± 1.1 %, F_q'/F_m'; WT = 4.1 ± 0.3 %, asLOX = 2.5 ± 0.5 %,). No main effects for herbivore or genotype occurred when assessed across the entire leaf. Insects consumed equivalent amounts of leaf tissue across three-day feeding experiments for both genotypes indicating that the difference in percentage damage to remaining tissue was not related to the amount of leaf consumed.

Herbivory reduced leaf photosynthesis in both genotypes (F = 6.92; df = 1,12; P = 0.03) but interacted with genotype through time (F = 4.73; df = 1,12; P = 0.05). Thus, photosynthesis declined in wild-type plants immediately following chewing damage and for up to three days after removal of insects, whereas photosynthesis recovered immediately after insect removal in asLOX plants (Figure 4.2). Both g_s and C_i decreased after three days of feeding in damaged wild type plants but only g_s remained lower up to three days into recovery. Wild-type plants also maintained higher respiration rates through time (F = 5.06; df = 1,12; P = 0.04) with an immediate decrease in respiration in infested wild-type plants after feeding that attenuated with recovery. Gas exchange parameters for plants destructively harvested for metabolite assessment were similar to those recorded in the infestation and recovery experiment.

The effect of herbivory on plant signaling hormones and defensive chemicals was similar to the response of photosynthesis. JA levels increased immediately after three-day feeding and remained elevated after two-day recovery time in wild-type plants whereas asLOX plants maintained lower JA levels at each sample date until seven-day recovery (Figure 4.3). TPI and nicotine levels also increased after feeding; however, the level of leaf TPI remained elevated after seven-day recovery. asLOX plants did not increase in defense metabolites with herbivory. SA levels did not differ among treatments throughout the experiment (data not shown).

To determine how the defense response related to the suppression in photosynthesis we examined the correlations between gas exchange and defense response variables (Table 4.2). The amount of area consumed did not correlate with the propagated damage to F_v/F_m or F_q'/F_m', thereby reducing the likelihood that physical damage determined the suppression in electron transport. There was a lack in consistency with how CO_2 assimilation correlated with defense metabolites through time, but defense metabolites were strongly correlated with propagated damage to electron transport (Table 4.2). Carbon assimilation did not correlate with percentage reductions in electron transport suggesting that reductions in gas exchange were not largely determined by limitations in electron transport. Stomatal conductance was negatively correlated with nicotine ($r = -0.31$; $P = 0.02$) across all time points but this relationship did not occur between nicotine and other gas exchange parameters.

DISCUSSION

Chewing damage to *N. attenuata* induced JA-dependent defenses and this defense response immediately interrupted electron transport and reduced gas exchange for days following the initial herbivore attack. These data provide new insight into the proposed physiological link (Halitschke et al. 2011) between the herbivore-elicited down-regulation of photosynthetic gene expression and the resulting reductions in fitness (Voelckel and Baldwin 2004). Herbivore attack reduced growth and fitness through suppression in the component processes of photosynthesis that included 1) the removal of photosynthetic leaf area, 2) physically damaging remaining leaf tissue, and 3), down-regulating photosynthesis in remaining leaf tissue by signaling for defense. Down-regulation of photosynthesis occurs in other plant species that synthesize/release biocidal compounds with herbivory (e.g., terpenes, Zangerl et al.

2002, Gog et al. 2005); however, if JA-defense signaling reduces components of photosynthesis, then herbivore-mediated down-regulation of photosynthesis may be conserved and directly linked to the type of defense response.

Because wound signaling is transduced by the oxidation of free α-linolenic acid within the chloroplast via electron-carrying lipoxygenases (LOX3; Halitschke and Baldwin 2003) but results in downstream synthesis of JA (Gfeller et al. 2010), it is difficult to assess what components of the signaling pathway interact directly with photosynthesis. We assessed how suppressing the entire pathway altered photosynthesis and observed reductions in electron transport that were strongly correlated with JA levels and subsequently with the production of defense metabolites, albeit to a lesser degree. Prior evidence indicates wild-type *N. attenuata* has lower gene expression of light-harvesting complex (LHC) and PSII oxygen-evolving-complex polypeptides compared to asLOX plants when attacked by herbivores whereas gene expression of Rubisco small subunit and two peptides of PSII decreases more in asLOX than in wild-type plants (Halitschke and Baldwin 2003). These expression patterns suggest LOX3-signaling suppresses gene expression of transcripts related to electron transport proteins whereas gene expression for Calvin cycle and other electron transport proteins are uncoupled from LOX3-dependent signaling. In comparison with inverted repeat JASMONATE RESISTANT (JAR4/6) plants that maintain functional LOX activity but reduce amino acid conjugation of JA, asLOX plants transcriptionally up regulate components of photosystem I (StPSI-I; photosystem 1 reaction center subunit) and Rubisco (Wang et al. 2008). As a result, LOX3 signaling may interact with photosynthesis more directly than JA synthesis and the suppression of LOX3 reduces a potential physiological cost associated with defense signaling. Plants with reduced function of PsbS, a light harvesting protein that facilitates the quenching of excess energy into

dissipated heat, showed strong up-regulation of the lipoxygenase-signaling pathway (Frenkel et al. 2009); this result reinforces the link between light reaction-associated electron transport and lipoxygenase signaling. Finally, we observed reduced electron transport only under larval attack and not between undamaged genotypes thereby indicating that an interaction with larval secretions may determine the degree of photosynthetic suppression upon signaling for defense. Larval saliva dephosphorylates constitutively phosphorylated lipoxygenase in *Arabidopsis* and reduces JA synthesis/signaling (Thivierge et al. 2010); thus, the lipoxygenase-dependent reduction in photosynthesis is likely herbivore mediated. Given the oxidation that occurs upon herbivory, it will be interesting to investigate how JA-induced reactive oxygen species (ROS) modulate LHCs of photochemistry and interrupt electron transfer.

Herbivory down-regulates genes related to primary photochemistry and the Calvin cycle across many herbivore-plant interactions (Bilgin et al. 2010). However, the translation into altered protein levels is less clear. Calvin cycle enzymes increase (Maserti et al. 2010) or decrease (Chen et al. 2011) but LHC proteins generally increase. Larval attack in *N. attenuata* generates similar trends in gene expression and protein modification (Halitschke and Baldwin 2003, Giri et al. 2006). Our data indicate reduced functioning capacity in the light harvesting reactions of photochemistry, specifically when defense signaling is intact. Given this effect occurred immediately after attack and was not sustained, it is possible that reduced synthesis of key photosynthetic proteins occurs simultaneously with attenuation of degradation pathways in an effort to optimize resource allocation toward defense without sacrificing vital components of photosynthesis.

Insect herbivory reduces photosynthesis in remaining tissue (Zangerl et al. 2002, Nabity et al. 2009). We observed reduced electron transport efficiency in more remaining leaf tissue of

wild type than asLOX plants but small reductions around chewed leaf edges in asLOX plants immediately after insect attack. This result is consistent with previous data for *N. attenuata* (Halitschke et al. 2011) and surveys of chewing herbivore damage in other species (Aldea et al. 2006, Nabity et al. 2012). Given that damage propagated in both genotypes, feeding interrupted electron transport by physically disrupting tissues leading to desiccation, or introducing electron scavengers through insect oral secretions or lysed cells (e.g., glucose oxidase, ROS). Previously, 30% leaf area consumption was observed to reduce F_q'/F_m' averaged across the remaining leaf area (Halitschke et al. 2011). We did not resolve this suppression at the leaf level when 7% leaf area was consumed and saw minimal suppression in chlorophyll fluorescence restricted to cut edges when plants were allowed to recover. Our data suggest the greater reductions in F_v/F_m or F_q'/F_m' were linked to defense, but the act of wounding produces transient effects that immediately and minimally contribute to downstream reductions in CO_2 assimilation. Defoliation damage propagates further into remaining tissue immediately after feeding in other systems, but when the damaged leaf is given time to recovery, the effects of herbivory diminish (Aldea et al. 2005, Nabity et al. 2012).

The manner of feeding largely determines the degree of propagated damage; younger larvae produce more cut edges per bite relative to older larvae, significantly compromising the function of remaining tissue (Tang et al. 2006). After one day of exposure to plants neonates fed minimally (1.4% leaf area) yet doubled propagated damage (2.9%) in wild-type plants relative to three-day attack (by continuously growing neonates that developed into 1st instars) where leaf area was reduced 6.3% but only suppressed 8.1% of remaining tissue. Taken together, these results suggest that timeliness and manner of the feeding damage interact to determine the degree

of propagated damage in *N. attenuata*, and may only partly explain the proposed physiological link that reductions in F_q'/F_m' drive reductions in fitness (Halitschke et al. 2011).

Gas exchange declined immediately after feeding in wild-type plants but not in asLOX plants. While this finding agrees, in part, with Halitschke et al. (2011), we also observed stomatal limitations to CO_2 assimilation and continued suppression in wild-type plants for days after the initial attack. With the onset of herbivory, both stomatal conductance and C_i decreased thereby indicating that stomata limit CO_2 assimilation. Defoliation damage reduces stomatal conductance in many other species, often through tissue desiccation and loss in turgor associated with severed vasculature (Sack and Holbrook 2006). We also observed electron transport decreased minimally in asLOX and transiently in both genotypes suggesting the contribution of reduced electron transport to prolonged reductions in gas exchange was minimal. To this end, the sustained suppression in photosynthesis did not occur with altered C_i suggesting neither electron transport nor stomatal limitations drove the long-term reduction in CO_2 assimilation. Halitschke et al. (2011) also documented no decrease in stomatal conductance or change in C_i that, assuming transient reductions in F_q'/F_m', indicates other defense-related components alter photosynthesis.

Our one-day study suggested a combination of reduced electron transport and stomatal closure transiently reduced photosynthesis, but given three-day feeding and full defense metabolite synthesis, photosynthetic suppression was sustained through time. We observed increased levels of JA, TPI, and nicotine concurrent with reductions in gas exchange after three days of feeding. Although all defense compounds were positively correlated with the degree of propagated damage only nicotine showed consistent negative correlations with gas exchange (Table 4.2). Exogenous nicotine application suppresses photosynthesis in solanaceous plants that both do and do not synthesize nicotine (Baldwin and Callahan 1993), so it is possible that

autotoxicity interfered with carbon uptake by closing stomata, a mechanism that warrants further attention. TPI synthesis also exacts fitness costs (Zavala et al. 2004) and these may be modulated through photosynthesis; however, reported reductions in Rubisco or other Calvin cycle enzymes may be stronger drivers for decreased CO_2 assimilation (Giri et al. 2006).

LITERATURE CITED

Aldea M, Hamilton JG, Resti JP, Zangerl AR, Berenbaum MR, DeLucia EH. 2005. Indirect effects of insect herbivory on leaf gas exchange in soybean. Plant, Cell and Environment 28: 402-411.

Aldea M, Hamilton, JG, Resti JP, Zangerl AR, Berenbaum MR, Frank TD, DeLucia EH. 2006. Comparison of photosynthetic damage from arthropod herbivory and pathogen infection in understory hardwood samplings. Oecologia 149: 221-232.

Baker NR. 2008. Chlorophyll fluorescence: a probe of photosynthesis in vivo. Annual Review of Plant Biology 59: 89-113.

Baker NR, Harbinson J, Kramer DM. 2007. Determining the limitations and regulation of photosynthetic energy transduction in leaves. Plant Cell and Environment 30: 1107-1125.

Baldwin IT, Callahan P. 1993. Autotoxicity and chemical defense: nicotine accumulation and carbon gain in solanaceous plants. Oecologia 94: 534–541.

Bilgin DD, Zavala JA, Zhu J, Clough SJ, Ort DR, DeLucia EH. 2010. Biotic stress globally down-regulates photosynthesis genes. Plant Cell and Environment. 33: 1597-1613.

Chen Y, Pang Q, Dai S, Wang Y, Chen S, Yan X. 2011. Proteomic identification of differentially expressed proteins in *Arabidopsis* in response to methyl jasmonate. Journal of Plant Physiology 168: 995-1008.

Cipollini D. 2007. Consequences of the overproduction of methyl jasmonate on seed production, tolerance to defoliation, and competitive effect and response of *Arabidopsis thaliana*. New Phytologist 173: 146-153.

Frenkel M, Kulheim C, Jankanpaa HJ, Skogstrom O, Dall'Osto L, Agren J, Bassi R, Moritz T, Moen J, Jansson S. 2009. Improper excess light energy dissipation in *Arabidopsis* results in a metabolic reprogramming. BMC Plant Biology 9:12.

Gfeller A, Dubugnon L, Liechti R, Farmer EE. 2010. Jasmonate biochemical pathway. Science Signaling 3: cm3.

Giri AP, Wunsche H, Mitra S, Zavala SJA, Muck A, Svatos A, Baldwin IT. 2006. Molecular interactions between the specialist herbivore *Manduca sexta* (Lepidoptera: Sphingidae) and its natural host *Nicotiana attenuata*. VII Changes in the plant's proteome. Plant Physiology 142: 1621-1641.

Gog L, Berenbaum MR, DeLucia EH, Zangerl AR. 2005. Autotoxic effects of essential oils on photosynthesis in parsley, parsnip, and rough lemon. Chemoecology 15: 115–119.

Halitschke R, Baldwin IT. 2003. Antisense LOX expression increases herbivore performance by decreasing defense responses and inhibiting growth-related transcriptional reorganization in *Nicotiana attenuata*. The Plant Journal 36: 794-807.

Halitschke R, Hamilton JG, Kessler A. 2011. Herbivore-specific elicitation of photosynthesis by mirid bug salivary secretions in the wild tobacco *Nicotiana attenuata*. New Phytologist 191: 528-535.

Heidel AJ, Baldwin IT. 2004. Microarray analysis of salicylic acid- and jasmonic acid-signaling in responses of *Nicotiana attenuata* to attack by insects from multiple feeding guilds. Plant, Cell and Environment 27: 1362–1373.

Keinanen M, Oldham NJ, Baldwin IT. 2001. Rapid HPLC screening of jasmonate-induced increases in tobacco alkaloids, phenolics, and diterpene glycosides in *Nicotiana attenuata*. Journal of Agriculture and Food Chemistry 49: 3553-3558.

Kessler A, Halitschke R, Baldwin IT. 2004. Silencing the jasmonate cascade: induced plant defenses and insect populations. Science 305: 665-668.

Kessler A, Halitschke R, Poveda K. 2011. Herbivory-mediated pollinator limitation: negative impacts of induced volatiles on plant-pollinator interactions. Ecology 92: 1769-1780.

Kim EH, Kim YS, Park SH, Koo YJ, Choi YD, Chung YY, Lee IJ, Kim J.K. 2009. Methyl jasmonate reduces grain yield by mediating stress signals to alter spikelet development in rice. Plant Physiology 149: 1751-1760.

Krugel T, Lim M, Gase K, Halitschke R, Baldwin IT. 2002. *Agrobacterium*-mediated transformation of *Nicotiana attenuata*, a model ecological expression system. Chemoecology 12: 177-183.

Longstaff BJ, Kildea T, Runcie JW, Cheshire A, Dennison WC, Hurd C, Kana T, Raven JA, Larkum AW. 2002. An in situ study of photosynthetic oxygen exchange and electron transport rate in the marine macroalga *Ulva lactuca* (Chlorophyta). Photosynthesis Research 74: 281-293.

Lou Y, Baldwin IT. 2004. Nitrogen supply influences herbivore-induced direct and indirect defenses and transcriptional responses in *Nicotiana attenuata*. Plant Physiology 135: 496-506.

Maserti BE, Del Carratore R, Della Croce CM, Podda A, Migheli Q, Froelicher Y, Luro F, Morillon R, Ollitrault P, Talon M., Rossignol M. 2010. Comparative analysis of proteome changes induced by the two-spotted spider mite *Tetranychus urticae* and methyl jasmonate in citrus leaves. Journal of Plant Physiology. 168: 392-402.

McKey D. 1974. Adaptive patterns in alkaloid physiology. American Naturalist 108: 305-320.

Nabity PD, Zavala JA, DeLucia EH. 2009. Indirect suppression of photosynthesis on individual leaves by arthropod herbivory. Annals of Botany 103: 655-663.

Nabity PD, Hillstrom ML, Lindroth RL, DeLucia E.H. 2012. Elevated CO_2 interacts with herbivory to alter chlorophyll fluorescence and leaf temperature in *Betula papyrifera* and *Populus tremuloides*. Oecologia.

Sack L, Holbrook NM. 2006. Leaf hydraulics. Annual Review of Plant Biology 57: 361–381.

Shi Q, Li C, Zhang F. 2006. Nicotine synthesis in *Nicotiana tabacum* L. induced by mechanical wounding is regulated by auxin. Journal of Experimental Botany 57: 2899-2907.

Steppuhn A, Gase K, Krock B, Halitschke R, Baldwin IT. 2004 Nicotine's defensive function in nature. PLoS Biology 2:1074-1080.

Tang JY, Zielinski RE, Zangerl AR, Crofts AR, Berenbaum MR, DeLucia EH. 2006. The differential effects of herbivory by first and fourth instars of *Trichoplusia ni* (Lepidoptera: Noctuidae) on photosynthesis in *Arabidopsis thaliana*. Journal of Experimental Botany 57: 527–536.

Tang JY, Zielinski R, Aldea M, DeLucia EH. 2009. Spatial association of photosynthesis and chemical defense in *Arabidopsis thaliana* following herbivory by *Trichoplusia ni*. Physiologia Plantarum 137: 115-124.

Thivierge K, Prado A, Driscoll BT, Bonneil E, Thibault P, Bede JC. 2010. Caterpillar and salivary specific modification of plant proteins. Journal of Proteome Research 9: 5887-5895.

Van Dam NM, Horn M, Mares M, Baldwin IT. 2001. Ontogeny constrains systemic protease inhibitor response in *Nicotiana attenuata*. Journal of Chemical Ecology 27: 547-568.

Voelckel C, Baldwin IT. 2004. Herbivore-induced plant vaccination. Part II. Array studies reveal the transience of herbivore-specific transcriptional imprints and a distinct imprint from stress combinations. Plant Journal 38: 650-663.

Walling LL. 2000. The myriad plant responses to herbivores. Journal of Plant Growth and Regulation 19: 195-216.

Wang L, Halitschke R, Kang J, Berg A, Harnish F, Baldwin IT. 2007. Independently silencing two members of JAR family impairs trypsin protease inhibitors activities but not nicotine accumulations. Planta 226: 159-167.

Wang L, Allmann S, Wu J, Baldwin IT. 2008. Comparisons of LIPOXYGENASE3- and JASMONATE RESISTANT4/6-silenced plants reveal that jasmonic acid and jasmonic acid-amino acid conjugates play different roles in herbivore resistance of *Nicotiana attenuata*. Plant Physiology 146: 904-915.

Welter SC. 1989. Arthropod impact on plant gas exchange. In *Insect–plant interactions* (ed E.A. Bernays) pp. 135-151. CRC Press, Boca Raton, FL.

Zangerl AR, Arntz AM, Berenbaum MR. 1997. Physiological price of an induced chemical defense: photosynthesis, respiration, biosynthesis, and growth. Oecologia 109: 433-441.

Zangerl AR, Hamilton JG, Miller TJ, Crofts AR, Oxborough K, Berenbaum MR, DeLucia EH. 2002. Impact of folivory on photosynthesis is greater than the sum of its holes. Proceedings of the National Academy of Sciences USA 99: 1088–1091.

Zavala JA, Baldwin IT. 2004. Fitness benefits of trypsin proteinase inhibitor expression in *Nicotiana attenuata* are greater than their costs when plants are attacked. BMC Ecology 4:11.

Zavala JA, Baldwin IT. 2006. Jasmonic acid signaling and herbivore resistance traits constrain regrowth after herbivore attack in *Nicotiana attenuata*. Plant, Cell and Environment 29: 1751–1760.

Zavala JA, Patankar AG, Gase K, Baldwin IT. 2004. Constitutive and inducible trypsin proteinase inhibitor production incurs large fitness costs in *Nicotiana attenuata*. Proceedings of the National Academy of Sciences USA 101: 1607-1612.

TABLES

Table 4.1. Chlorophyll fluorescence, gas exchange, and defense parameters in *Nicotiana attenuata* immediately after one day herbivory by *Manduca sexta* on wild-type and JA-defense suppressed (as-LOX) plants. Different letters denotes differences among treatments at P ≤ 0.05 level of significance.

	Wild type		asLOX	
	- herbivore	+ herbivore	- herbivore	+ herbivore
Chlorophyll fluorescence				
Propagated damage to F_v/F_m				
% of remaining leaf	---	2.9 ± 0.2a	---	2.3 ± 0.3b*
total area (mm^2)	---	66 ± 5a	---	52 ± 7b*
Propagated damage to F_q'/F_m'				
% of remaining leaf	---	9.0 ± 1.9a	---	4.8 ± 0.7b*
total area (mm^2)	---	206 ± 44a	---	109 ± 16b*
Gas exchange				
CO_2 assimilation (μmol m^{-2}s^{-1})	8.4 ± 0.1a	8.0 ± 0.2b*	8.4 ± 0.1Aa	8.1 ± 0.3b*
Stomatal conductance (mmol m^{-2}s^{-1})	0.233 ± 0.007a	0.222 ± 0.016a	0.214 ± 0.015a	0.181 ± 0.012b*
Intercellular CO_2 (C_i)	295 ± 2a	298 ± 3a	292 ± 4ab	281 ± 3b
Respiration	-0.63 ± 0.06a	-0.66 ± 0.09a	-0.47 ± 0.05b*	-0.55 ± 0.05ab
Defense metabolites				
JA (nmol mg FW^{-1})	51 ± 6a	107 ± 15b	49 ± 4a	58 ± 5a
TPI (nmol mg protein^{-1})	1.3 ± 0.1a	4.4 ± 0.4b	0.4 ± 0.1c	0.4 ± 0.1c
Nicotine (mg g FW^{-1})	0.58 ± 0.04a	0.61 ± 0.03a	0.43 ± 0.02b	0.38 ± 0.03b

* indicates significance at P ≤ 0.1

Table 4.2. Correlation coefficients (r) for the relationship of CO_2 assimilation (PS) or maximal electron transport efficiency (F_v/F_m) compared to defense metabolites jasmonic acid (JA), trypsin protease inhibitor (TPI), and nicotine for each time point assessed following three day feeding.

	3d		5d		7d		Summary	
	PS	F_v/F_m	PS	F_v/F_m	PS	F_v/F_m	PS	F_v/F_m
JA	-0.40$	0.67; **	-0.54**	0.54**	-0.13	NA	0.01	0.63***
TPI	0.58**	0.58; **	-0.50$	0.60*	0.17	NA	0.09	0.52**
Nicotine	0.44$	0.52; *	-0.53**	0.38$	-0.60**	NA	-0.10	0.42**

Correlations significant at the $P \leq 0.001$, $P \leq 0.01$, $P \leq 0.05$, $P \leq 0.1$ are depicted by ***, **, * and $, respectively.

FIGURES

Figure 4.1. Representative chlorophyll fluorescence images for maximal efficiency of photosystem II (F_v/F_m) and operating efficiency of photosystem II (F_q'/F_m') for wild-type and JA-defense modified (asLOX) *Nicotiana attenuata* leaves challenged by *Manduca sexta* herbivory for three days. The difference between genotypes in the percent of remaining leaf tissue that was reduced > 5% for F_v/F_m and > 10 % for F_q'/F_m' is denoted by * at $P \le 0.05$ level of significance.
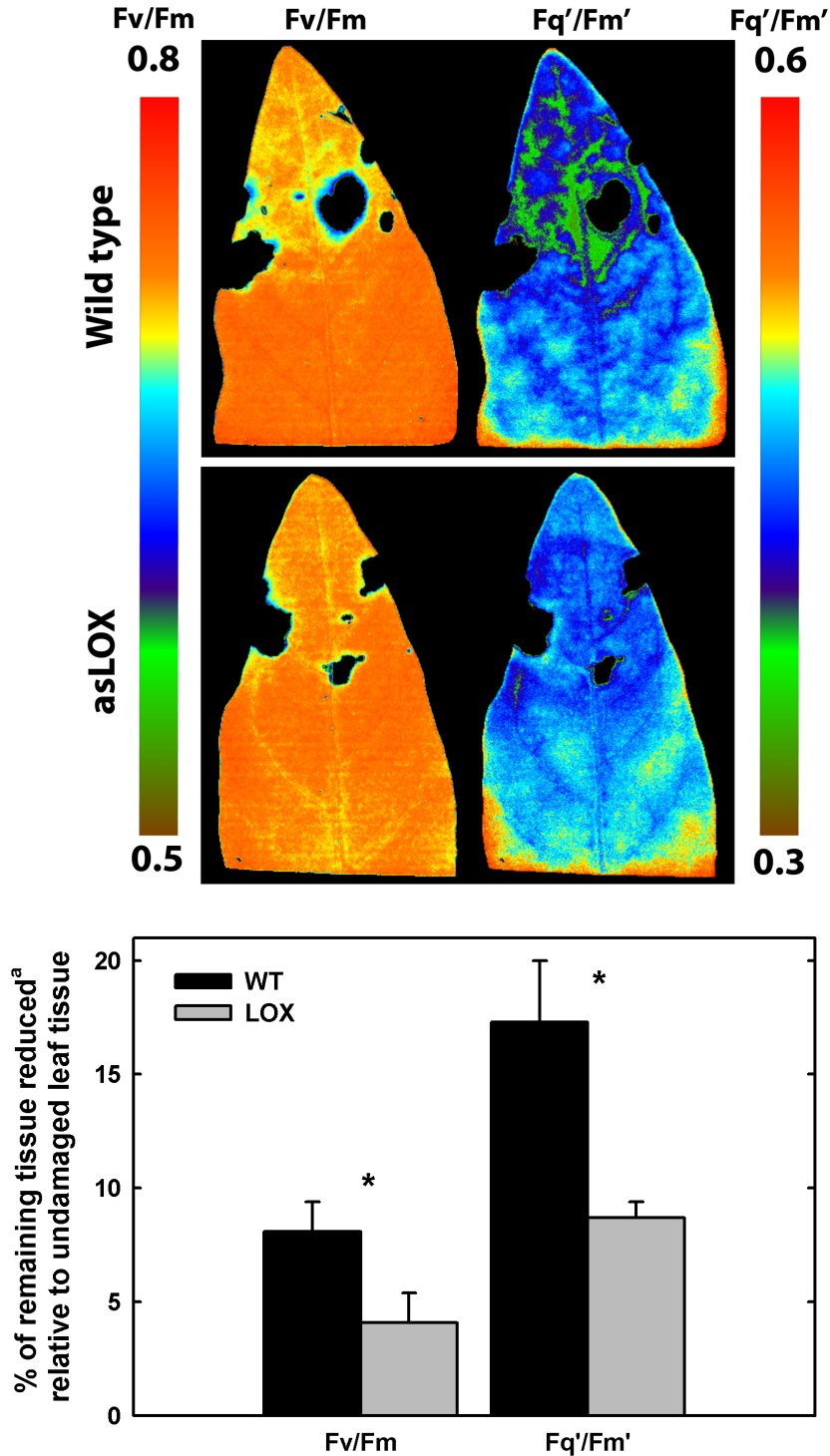
Figure 4.2. CO_2 assimilation of wild-type (top) and JA-defense modified asLOX (bottom) *Nicotiana attenuata* leaves challenged by *Manduca sexta* herbivory for three days. The corresponding intercellular $[CO_2]$ and stomatal conductance are also shown (right). * denotes treatment difference within a genotype at $P \leq 0.05$ level of significance unless otherwise indicated.
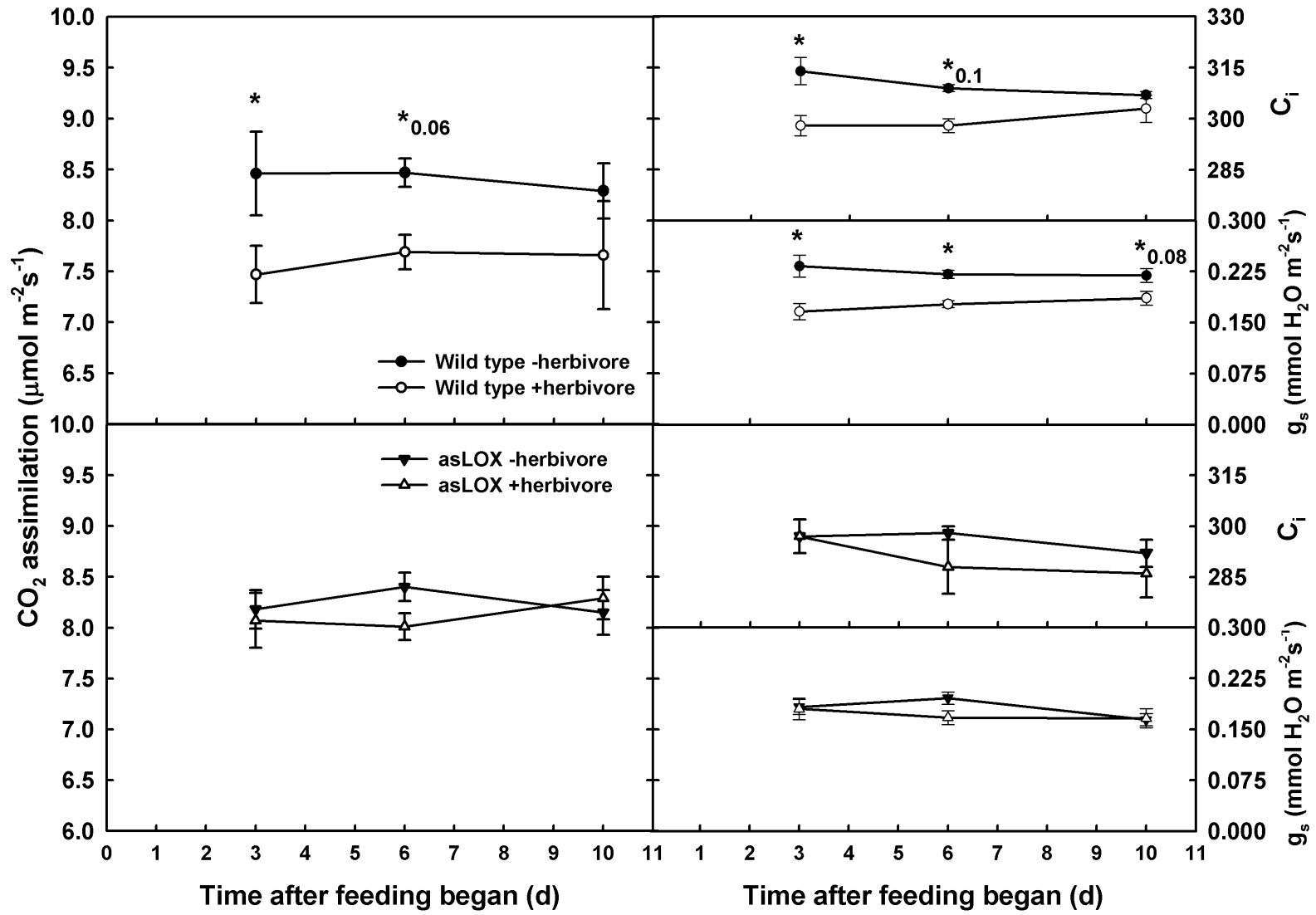
Figure 4.3. Jasmonic acid, TPI, and nicotine content of wild-type and JA-defense modified asLOX *Nicotiana attenuata* leaves challenged by *Manduca sexta* herbivory. Insects were removed after three days feeding and tissues were harvested 3, 5, and 10 days after feeding began, i.e., 0, 2, and 7-day recovery time. Different letters denotes differences among treatments at P ≤ 0.05 level of significance.
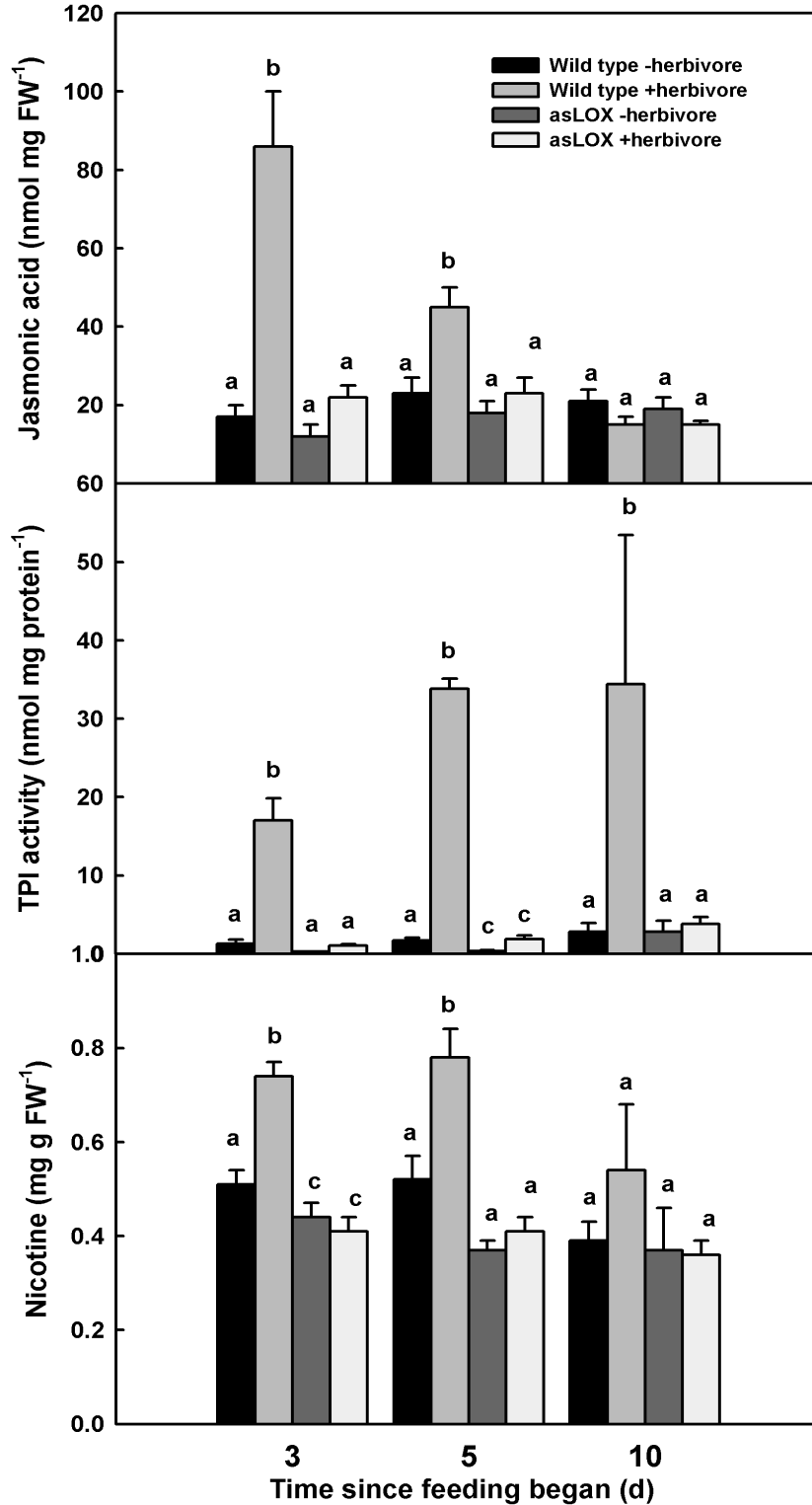
CHAPTER 5

PHYSIOLOGICAL AND GENOMIC BASIS FOR ENDOPARASITE CONTROL

OVER PLANT METABOLISM

ABSTRACT

Endoparasitism by gall forming insects dramatically alters plant phenotype by generating morphological and histological structures such that the insect benefits from induced changes within the host. Because these changes are often linked to insect fitness, they are hypothesized to serve as an extension of the parasite phenotype. To date, no morphologies benefit host physiology; however, we identified that the gall forming insect parasite, *Daktulosphaira vitifoliae*, induces adaxial leaf-side stomata formation where no stomata typically occur on wild and cultivated-grape leaves. We tested the extended phenotype hypothesis by characterizing the function of the phylloxera-induced stomata and tracing transport of assimilated carbon. Because inducible stomata suggest a significant manipulation of primary metabolism, we also characterized the gall transcriptome to identify the level of global reconfiguration to primary metabolism and the subsequent changes in downstream secondary metabolism. Phylloxera feeding induced stomata in proximity to the insect and the sink strength of the gall drove importation of the assimilated carbon. Gene expression related to photosynthesis decreased whereas gene expression for transport, glycolysis, and fermentation increased in leaf-gall tissues. This shift from an autotrophic to heterotrophic profile occurred concurrently with decreased gene expression for non-mevalonate and terpenoid synthesis and increased gene expression in shikimate and phenylpropanoid biosynthesis, secondary systems that alter defense status in grapes. These data report the first occurrence of functional, insect-induced stomata in nature,

provide physiological and genomic support that phylloxera globally reprogram grape leaf development and function to serve as an extended phenotype, and link genomic manipulation of metabolism to defense signaling in gall forming insects.

INTRODUCTION

Plant parasitism by virus, bacteria, or insects results in abnormal tissue growth and altered external morphologies often through tumor-like gall formation. Species-specific feeding behaviors of insects determine the type of induced morphologies and result in a range of structures on stems or leaves that includes extra-floral nectaries, spines, trichomes, and excretions; the functions of which are associated with enhanced parasite fitness (Price 1987, Waring and Price 1989, Stone et al. 2002, Wool 2004, Raman et al. 2005). As such, these attributes have led to the hypothesis that gall induction is controlled by and functions as an extension of the parasite phenotype (Stone and Schonrogge 2003). The mechanisms for host transformation are known for few bacterial species (Deeken et al. 2006, Stes et al. 2011); however, there is a lack of understanding for how insect parasites initiate and maintain control over plant development.

Gall forming insects are sedentary and as a result directly compete for mobilized nutrients with meristems or developing reproductive structures that function as plant sinks. This competitive environment drives the evolution of the galling habit from leaf edge to midvein (Inbar et al. 2004) and, among parasites, favors the individual closest to source tissue (Larson and Whitham 1997, Compson et al. 2011). The sink competition model emphasizes a selective pressure for the parasite to become a stronger sink or to manipulate photosynthesis and enhance source strength. Stimulated plant growth through gall-tissue formation and differentiation

succeeds as a manner to enhance the sink demand of the parasite whereas enhanced source strength is less documented (but see Fay et al. 1993, Dorchin et al. 2006).

The fluid-feeding aphid phylloxera, *Daktulosphaira vitifoliae* Fitch, is a globally distributed endoparasite of grapes (*Vitis* spp) that induces nutrient-enriched galls on leaves or roots, the latter which increases susceptibility to secondary pests that ultimately kill the vine (Granett et al. 2001). When introduced to naïve *V. vinifera* in Europe in the 1860s, phylloxera nearly caused the collapse of global grape production, and again threatened viticulture in California in the 1980s after overcoming resistant hybrid rootstocks (AxR#1; see Granett et al. 2001). Phylloxera attack on susceptible, cultivated *V. vinifera* may produce hundreds of competing sinks within the same leaf; however, native *Vitis* incur variable levels of leaf-galling depending on the *Vitis* species attacked and climate (Downie et al. 2000). Gall tissues are enriched in starch (Witiak 2006) and amino acids relative to un-attacked leaf tissue (Warick and Hildebrandt 1966). Unlike other phloem-feeding Aphidoidea that rely on N-fixing bacteria for nutrients, grape phylloxera house no described endosymbionts and feed from the parenchyma (Vorwerk et al. 2007). As such, they likely attain carbon from starch degradation and nitrogen from amino acids; however, the current understanding of the regulation of these processes is largely anecdotal.

In this study I investigated the manipulation of source/sink dynamics in the extensively characterized grape-phylloxera system and, in the context of the extended phenotype hypothesis, describe a new functional morphology of benefit to host physiology that is induced by gall forming insects. I also sequenced the gall transcriptome to test if large-scale reprogramming of gene expression drives the manifestation of the extended phenotype by altering sink/source

identity. These data represent the first examination of insect-induced stomata in nature and the first transcriptomic assessment of insect gall transformation in plants.

MATERIALS AND METHODS

Plant and Insect Material

Vitis vinifera cv. Frontenac vines were established in perpetual colony within a glasshouse to characterize the stomata with greater control over environment, and grown under field conditions for a single season experiment to assess function under typical vineyard conditions. Glasshouse vines were cloned from field cuttings from a single vine growing at the University of Illinois Fruit Research Farms and grown in 10 liter pots filled with soilless media (LC1 Sunshine, SunGro Horticulture, Bellevue, WA). Vines were maintained with monthly applications of 10 % NPK (w/v) and watered when necessary. Local *D. vitifoliae* were colonized on vines, and both plants and insects were maintained within a glasshouse with supplemental lighting (28:22 ± 2 °C, 16:8 L:D). Field plots of *V. vinifera* cv. Frontenac vines (1x vines; Double A Vineyards, NY) were planted prior to spring bud break, watered with 200 ppm N amendment for 1 month to encourage vegetative growth, and thereafter watered when needed. Local *D. vitifoliae* were collected from infested vineyards and allowed to colonize vines (in May).

Histology and Imaging

Phylloxera infested vines were surveyed to determine the occurrence and structure of leaves with induced-adaxial stomata. Epidermal peels (Figure 5.1) were prepared by painting cellulose acetate (nail varnish) on to leaf surfaces and then plating the imprint for microscopy. To assess stomatal number, impressions of the galled and non-galled surfaces of galled and non-

galled leaves (n = 5) were made using dental resin (President Plus, Coltene/Whaledent Inc, Cuyahoga Falls, OH, USA). Digital renderings of the impression surface were profiled using an optical profilometer (Nanofocus usurf explorer, Nanofocus, Glen Allen, VA, USA). Cell number was counted using the Motif Operator (usoft Analysis Premium software, Nanofocus) Intact leaf and gall tissues were harvested from vines and immediately submerged in 10 % neutral buffered formalin for > 1 day, serially dehydrated in ethanol, and embedded in paraffin. Tissue cross sections (Figure 5.2) were made by microtome (Leica RM2255, Leica Microsystems Inc, Buffalo Grove, IL) and then stained following standard protocols at the Core Facilities Histology laboratory in the Institute for Genomic Biology, University of Illinois at Urbana-Champaign.

Gas exchange

To characterize how the galling habit alters leaf photosynthesis, gas exchange was measured on second-generation galls of similar size but from separate field-grown vines using a portable infrared gas analyzer (LI6400 IRGA, Licor, Lincoln, NE). Leaves (n = 10) were identified with a single gall and surveyed for both daytime carbon uptake and nighttime respiration on both gall and adjacent non-galled leaf area. Dual-sided leaf measurements were measured at saturating light after the leaf reached a steady state within the 6cm^2 cuvette (25 ± 2 °C, ~50 % RH). Adaxial leaf carbon fluxes were then measured by taping over the sample manifold chamber (Licor, Lincoln, NE), inverting the leaf, and sampling over time (one measurement recorded every 10 seconds for 2 minutes) to enhance the signal-to-noise-ratio. All respiration measures were sampled over time and average values were used for comparisons. These field surveys were completed within one day and repeated the following day on a different cohort of leaves (in June).

CO$_2$ labeling

To assess the contribution of adaxial CO$_2$ influx into galls, greenhouse-grown vines were used to pulse adaxial and abaxial leaf sides with ^{13}C-enriched CO$_2$. Enriched CO$_2$ was applied to separate leaves using a modified gas exchange system. The system was modified for one-sided leaf gas exchange as described, and the sample and reference gas lines were redirected to include airflow through an adjacent 50 mL vial. Leaves (n=4) were dark-adapted (>20 minutes) to determine abaxial (plant) or adaxial (plant+insect) respiration and then light-adapted to reach steady state (PAR = 1500, 29 ± 1 °C, RH ~ 60 %). Once leaves were light adapted 1 mL of 5 % acetic acid in water was injected into the 50 mL vial containing 20 mg of ^{13}C sodium carbonate (IconIsotopes, Summit, NJ). This released a pulse of approximately 800 ppm labeled CO$_2$ that lasted in the gas exchange system for approximately four minutes. Subsequent pulses of decreasing concentrations were applied with additional 1 mL injections after the previous pulse disappeared and conditions returned to steady state. Each leaf side was labeled with four pulses over 10 minutes. We harvested labeled leaves after six hours because preliminary labeling experiments indicated ^{13}CO$_2$ was present in all tissues. After one and two days after labeling, leaf and gall tissue declined in δ^{13}C values whereas insect values remained similar suggesting the labeled was respired out of leaf tissue. Insect, gall, and leaf tissues from labeled and adjacent unlabeled areas on the same leaf were separated by tissue type. Leaves were divided further into two tissue types: tissue within a 4 mm diameter circle centered on the gall where the stomata occur and remaining leaf tissue lacking adaxial stomata.

Tissues exposed to ^{13}CO$_2$ were separated by type, insects and eggs were counted, and all tissues were oven-dried at 70° C. Tissues were weighed for final dry mass, ground to powder, and analyzed using an Elemental Combustion System (model 4010, Costech Analytical

Technologies, Valencia, CA) coupled to a Delta V isotope ratio mass spectrometer

(ThermoFisher Scientific, Waltham, MA).

RNA extraction and sequencing

To assess the transcriptome of mature sinks, galls containing nymphs of reproductive age

and undamaged leaves of similar age were harvested from separate leaves of separate vines and

pooled (n=10) for each biological replicate (n=3). Tissues were flash-frozen in liquid N_2 and

stored at -80°C for further processing. Insects were removed from gall tissues prior to RNA

extraction.

Total RNA was isolated from frozen tissues using Spectrum Plant Total RNA kit (Sigma-

Aldrich Co). RNA quality and quantity were determined by spectrophotometry (Nanodrop 1000,

ThermoFisher Scientific, Waltham, MA) and a denaturing agarose gel with ethidium bromide

staining. Construction of RNAseq libraries and sequencing on the Illumina HiSeq2000

instrument were carried out at the W.M.Keck Center for Comparative and Functional Genomics,

University of Illinois at Urbana-Champaign. One μg of DNAse treated total RNA per sample

was used to prepare individually barcoded RNAseq libraires with the TruSeq RNA Sample Prep

kit (Illumina, San Diego, CA). Libraries were pooled in equimolar concentration and each pool

was sequenced on one lane on a HiSeq2000 for 100 cycles using version 2 chemistry according

to the manufacturer's protocols (Illumina, San Diego, CA). Reads were demultiplexed using

Casava 1.7.

Bioinformatics

Reads were aligned to the *V. vinifera* transcriptome (version 12x; Phytozome v.7, JGI)

following a conservative RNAseq read assessment (C. Yendrek pers. comm). Briefly, raw reads

were aligned to the reference transcriptome using two mapping programs: CLC Genomic

Workbench (CLCBio) or Novoalign. A minimum total read count for each tissue was implemented (min = 50) and then differential expression was analyzed for each mapping using two discrete probability distribution-based methods DESeq (Anders and Huber 2010) and edgeR (Robinson et al. 2009). Differentially expressed genes (P<0.05) were combined from each analysis and then combined from each mapping to generate a single gene list. These differentially expressed genes were then merged with *Arabidopsis thaliana* TAIR v9 identifiers. Fold changes from unique *V. vinifera* transcripts that mapped onto duplicate *A. thaliana* genes were averaged, and the remaining genes were placed into functional categories based on the Mapman visualization toolkit (Thimm et al. 2004). Modified pathways (Figures 5.6 - 5.8) were redrawn from the resulting data. This process was repeated by varying minimum total read counts (5 and 25) and this resulted in similar overall expression patterns; however, I only report gene expression that had a minimum count of 50. Our combined gene list produced 4038 DE genes of which 337 did not map to *Arabidopsis* gene IDs and 951 were duplicates. The *V. vinifera* transcript IDs (12x; Phytozome v.7) and their corresponding *Arabidopsis* IDs (TAIR v.9) are listed in Table 5.1S.

Data Analysis

Gas exchange parameters and $\delta^{13}C$ values of tissues within the same leaf were blocked by machine (LI-6400) for field measurements and analyzed by repeated measures ANOVA (Proc Mixed 9.1, SAS Institute, Cary, NC). Elemental content was log transformed prior to analysis to correct for non-normality. Regression analyses were conducted by linear regression (Proc Reg, SAS Institute). A Fisher's exact test (Proc Freq, SAS Institute) was used to assess if functional categories assigned by Mapman for transcripts were significantly different relative to the overall gall expression patterns.

RESULTS

Vitis species are hypostomal where stomata occur only on abaxial leaf sides (Rosen 1916, Sterling 1952, Pratt 1974, Witiak 2006); however, I observed gall formation by grape phylloxera created adaxial leaf-side stomata (Figure 5.1). These adaxial stomata occurred in a gradient of increasing density with proximity to the developing gall and parasite for both cultivated and wild grape (Table 5.1, Figure 5.1). Cross-sections of leaf and gall tissue indicated that these stomata open to intercellular air spaces within the palisade layer whereas abaxial stomata open to diffuse mesophyll typical of photosynthetic organisms (Figure 5.2).

Assessments of gas exchange on field- and greenhouse-grown vines confirmed induced stomata actively assimilated CO_2 but the degree of photosynthetic enhancement to the leaf depended on the background CO_2 flux (i.e. signal:leaf area and number of insects respiring gall^{-1}) and the degree of gall-induced leaf distortion. In field-grown plants net CO_2 uptake per unit of leaf area declined with a single gall whereas respiration of the galled area increased relative to adjacent undamaged tissue (uptake: $F = 6.89$ df $= 1,7$ $P = 0.03$; respiration: $F = 20.53$ df $= 1,6$ $P = 0.004$; Figure 5.3). However, this includes non-photosynthetically active leaf material (approx. $0.1cm^2$ as determined from the side of estimated cylindrical gall surface area) that, if accounted for, increased CO_2 uptake of galled areas so they did not differ from non-galled tissue ($F = 4.58$ df $= 1,7$ $P = 0.07$). Similarly, respiration per unit dry mass did not differ between galled and non-galled leaf tissue ($t = 0$ df $= 12$, $P = 0.9$). Stomatal conductance (g_s) and transpiration (E) of adaxial leaf-sides of galls relative to adjacent non-galled tissues were greater during the day (g_s: $F = 35.56$ df $= 1$ $P < 0.001$; E: $F = 41.28$ df $= 1,7$ $P < 0.001$) but did not differ at night (g_s: $F =$

3.75 df = 1,6 P = 0.1; E: F = 3.84 df = 1 P = 0.1) indicating the flux of water through adaxial

stomata functions diurnally as in abaxial stomata.

The number of insects within each gall did not relate to gall size ($R^2 = 0.15$, F = 2.19, P =

0.16) nor did gall size relate to the nightly adaxial CO_2 flux ($R^2 = 0.04$, F = 0.5, P = 0.5).

However, the number of insects within each gall did relate to adaxial CO_2 output (Figure 5.4).

While the apparent efflux is minimal and within the error of the machine (± 0.3ppm), this

relationship allowed me to estimate how much adaxial CO_2 resulted from plant material (Figure

5.5).

The photosynthetic capacity of the leaf determined the ultimate uptake of $^{13}CO_2$ (Figure

5.5A) whereas respiration demands of gall tissue determined the translocation of fixed carbon

(Figure 5.5B). Six hours after $^{13}CO_2$ pulses were applied to the abaxial epidermis the $\delta^{13}C$ value

of leaf and gall increased but the $\delta^{13}C$ value of insect did not increase relative to unlabeled

tissues within the same leaf. Similarly adaxial application increased $\delta^{13}C$ values in leaf where

induced adaxial stomata occurred and in the gall but did not alter $\delta^{13}C$ values in leaf tissue with

no adaxial stomata (data not shown) or insect (Figure 5.5C). Labeling did not alter elemental

content of the leaf but tissue types contained different levels of % C (F = 259, df = 3,9, P <

0.001; leaf = 45.0 ± 0.4, gall = 43.7 ± 0.2 insect = 57.1 ± 0.4) and % N (F= 121, df = 3,9, P <

0.001; leaf = 3.6 ± 0.2, gall = 2.4 ± 0.2 insect = 7.1 ± 0.1).

The transcriptomic survey of gall function identified 2750 DE genes that were

significantly represented in 15 functional categories including photosynthesis, fermentation, and

secondary metabolism (Table 5.2). Light harvesting and carbon assimilation genes strongly

decreased whereas sucrose mobilization, glycolysis, and fermentation transcripts generally

increased in abundance in gall tissue (Figure 5.6). Transcripts encoding amino acid, oligopeptide,

and water transporters also increased (Table 5.3). Secondary metabolism transcripts generally increased for shikimate and phenylpropanoid biosynthetic pathways but generally decreased for non-mevalonate and terpenoid biosynthetic pathways with few exceptions: two terpenoid biosynthesis genes, geranyllinalool synthase and myrcene synthase, increased (Figure 5.7, Table 5.4). Biotic stress related transcripts for jasmonic acid and ethylene signaling increased in galls as well as an overall gene expression pattern favoring SA degradation (Figure 5.8; Table 5.5).

DISCUSSION

Feeding by the insect-parasite phylloxera on grape induced adaxial stomata that assimilated carbon and facilitated photosynthate transport to local sinks. Isotopically labeled CO_2 entered leaf stomata relative to photosynthetic capacity and the respiratory output or sink demand of the gall drove transport of labeled assimilate to the nearest sink. This pathway links adaxial stomata to attenuation of sink strength of developing leaf-gall tissue and thereby enhanced parasite fitness. As a result, these stomata serve as an extended phenotype of phylloxera and provide the first evidence of functional insect-induced stomata in nature. Stomata display varying levels of phenotypic plasticity because they optimize the direct cost of enhancing fitness (i.e. carbon assimilation) while maintaining plant water status (i.e. transpiration); yet, abiotic factors largely drive stomatal patterning and development across plants (Woodward 1987, Casson and Hetherington 2010). Parasite-induced stomata link biotic and abiotic control over this morphology and indicate the galling habit may also regulate adaptive loci that genetically control stomata (Hancock et al. 2011).

Gall formation distorts photosynthetic leaf tissues through aberrant cell growth and reduced photosynthesis at the leaf level in *V. vinifera* during previous examinations (Riling and

Steffan 1978, McCleod 1990). Although these studies did not specify how many galls were included in the gas cuvette, I also observed a reduction in CO_2 uptake per unit leaf area when a single gall was examined. However, if the leaf area is corrected for the non-photosynthetic area where the gall encloses the insect, or if respiration from insects inhabiting the gall is negated from the CO_2 flux, then a single gall does not reduce photosynthesis at the leaf level. This relationship might be expected as phylloxera coevolved with native grape species. To this end, leaves of native *Vitis* species show considerable intra and interspecific variability in the degree of gall distortion (Downie et al. 2000), making it likely that 1) grape phylloxera gall formation achieves densities that do not reduce the fecundity of native grapes, and 2) native grapes are not severely damaged by leaf galling. Like previous studies, this current one examined the leaf response of cultivated (non-native) *V. vinifera*, yet preliminary assessments of *V. riparia* show leaf galls do not reduce the operating efficiency of photosystem II under low or high light but tend to reduce non-photochemical quenching under high light (unpublished data). This might be expected given that formation of adaxial stomata can enhance cooling through transpiration and thereby facilitate heat dissipation in and around tissues that are deficient in many photosynthetic pigments (Blanchfield et al. 2006). Future photosynthetic surveys of galled native species may elucidate the degree of photosynthetic alteration grape phylloxera imposes.

The transcriptome of mature grape gall tissue lends further support for parasite manipulation of host genes because of the large-scale reconfiguration of metabolism from an autotrophic to heterotrophic profile. We observed an overall reduction in gene expression related to photosynthesis, but increases in gene expression for sugar mobilization, glycolysis, and fermentation. Transcripts unique to heterotrophy strongly increased. For example, phosphoglycerate mutase that converts 3-phosphoglycerate to 2-phosphoglycerate and enolase

that converts 2phosphoglycerate to phosphoenolpyruvate both increased in expression relative to leaf tissue. The enhanced C transport to gall tissue is supported by an increase in the C:N ratio despite decreased C and N content in leaf gall tissue. Previous work found N content tended to be lower in gall tissue but depended on growth status; faster-growing cells contained higher N (Warick and Hildebrandt 1966). Because we sampled mature gall tissue, the growth cycle may be in the senescent stages. Regardless, we observed general up regulation of amino acid (AA) and oligopeptide transporters that is associated with amino acid-enrichment in leaf gall tissue (Warick and Hildebrandt 1966) and in roots (Kellow et al. 2004). This enrichment is expected in sink tissue where it is facilitated by AA-enriched phloem unloading. This finding is also consistent with the lower N content of leaf gall tissue because some amino acids decrease (e.g., glutamine, leucine) whereas other substantially increase in leaf gall tissue (e.g., alanine, methionine; Warick and Hildebrandt 1966).

Interestingly we observed a strong up regulation of ethylene signaling and synthesis that may feedback to reduce N content. Aberrant cell growth yields clustered cells with little air space (Figure 5.2) that may lead to hypoxia, stimulate ethylene synthesis, and feedback to inhibit nitrate reductase. Similar shifts in solutes and transcripts occur in *Agrobacterium tumefaciens* galls (Deeken et al. 2006), and indicate that N is not synthesized in the gall but imported via oligopeptide transporters (Cao et al. 2011), the transport of which is likely mediated by glycolysis- and PEP dephosphorylation-generated ATP.

The shift in primary metabolism toward heterotrophic energy production is consistent well with the up regulation of transcripts for cell wall synthesis, and the pathway-specific regulation of secondary metabolism. Transcripts for enzymes that are involved in the biosynthesis of both sugars and phenolics such as laccases or those involved in lignin/lignan

biosynthesis increased and provide transcriptional support to development of the gall structure. Transcripts encoding shikimate and phenylpropanoid biosynthesis increased whereas non-mevalonate and its downstream pathways decreased (Figure 5.7). This pattern may be expected if low oxygen environments within galls favor PEP production over the oxygen-dependent TCA cycle. Excess mobile sugars may also feed forward to affect synthesis pathways and increase metabolites such as anthocyanin (Belhadj et al. 2006). I also observed universal suppression in genes encoding photosynthetic pigments such as carotenoids and chlorophylls, which decrease under phylloxera attack (Blanchfield et al. 2006). Of the terpenes, geranyllinalool (GLL) synthase was strongly up regulated. This enzyme synthesizes GLL that composes up to 95% of terpenes found in other sink tissue such as flower and berry (Martin et al. 2009).

The physiological and transcriptomic data suggest phylloxera is uniquely adapted to the gall lifestyle. Feeding from the parenchyma reduces the need for N-producing symbionts but requires C and N mobilization from the plant, which our transcriptional evidence and observed physiology indicate the leaf supplies. Beyond regulating nutritional status, however, phylloxera must also avoid eliciting defenses. Root feeding phylloxera may induce phenolic accumulation in damaged cells (Kellow et al. 2004) but often elicit the hypersensitive response (HR) on resistant tissues (Blank et al. 2009). Root galls also emit a range of volatiles including hexanal and hex-2-enal – both LOX-derived volatiles – methyl salicylate, and several volatiles originating from phenylpropanoid and mevalonate biosynthesis (Lawo et al. 2011). Although we examined leaf galls, our data transcriptionally support the synthesis of these metabolites and suggest phylloxera regulate gene expression within the leaf well beyond carbon metabolism.

Insect feeding elicits defenses specific to the feeding mechanism (piercing-sucking vs chewing) and plant host. Among the few galling insects investigated flies and moths do not

induce JA in monocots (Tooker and DeMoraes 2008). However, we observed a strong increase in gene expression for JA (LOX)-defense signaling and a similar up regulation in SA-carboxyl-methytransferases that degrade SA into methylated SA, a mobile signal. Our data support an active JA defense signaling is active but to an unknown degree given the up regulation of several JAZ domain genes that encode for repressors of JA-regulated transcription (Santner 2007). JA up regulation also occurred concurrent with up regulation for the degradation of salicylic acid that, as the general defense response by Aphidoidea attack (Thaler et al 2010), suggests SA defenses are being suppressed. Necrotrophic pathogens (e.g., mildews) induce JA signaling (e.g., Hamiduzzaman et al. 2005, Trouvelot et al. 2008,) so it is possible that phylloxera are inducing defense signaling for protection, although foliar JA application decreased fecundity of root feeding forms (Omer et al. 2000). Methylated JA also induces stilbenes, anthocyanins, and piceids (Belhadj et al. 2006, Faurie et al. 2009) and increases SA in grape (Repka et al. 2004). The interactions of these hormones make it difficult to extend the parasite phenotype to include manipulation of defense signaling and metabolism, at least until additional data on the metabolite pools are known. Given that methylated SA compromises parasitoid seeking behavior (Snoeren et al. 2010) but enhances predatory mite detection ability (De Boer and Dicke 2004), the role SA in phylloxera-grape interactions is unknown. It is important to note that preliminary sequencing of the phylloxera transcriptome identified expression patterns for 35 total detoxification enzymes (unpublished data). This value represents the lowest number of detoxification genes across insect genomes to date (Schuler 2011) and suggests it is highly likely the insect's defensive phenotype includes the leaf gall.

To the best of our knowledge we described the first occurrence of functional, insect induced stomata in nature and linked their physiological and genomic regulation to enhancing

parasite fitness. Transcriptional data are not without limitations; however, our conservative approach to define and visualize DE genes in combination with extensive physiological and prior anecdotal evidence suggests this global reconfiguration is real. Previous studies indicate that photosynthesis declines when phylloxera parasitize grape leaves (Rilling and Steffan 1978, McLeod 1990), yet this may depend on the susceptibility of the leaf to gall formation and the density of attack. Our data suggest that a single gall did not reduce photosynthesis when we accounted for the area of non-photosynthetic tissue. To avoid selection pressure that favors enhancing defenses, we would expect photosynthetic suppression within a host to be minimized as occurs when plants tolerate herbivores (Agrawal 2000). The formation of stomata as an extended phenotype attenuated sink strength and thereby may reduce interspecific competition that occurs with natural sinks (Larson and Whitham 1997) or intraspecific competition that results from insects colonizing the same leaf (Compson et al. 2011). Because stomata constitute a morphology that is physiologically important to the host, this attenuation of phylloxera feeding optimizes the parasitic lifestyle as a unique example of coevolved compatibility.

LITERATURE CITED

Agrawal AA. 2000. Overcompensation of plants in response to herbivory and the by-product benefits of mutualism. Trends in Plant Science 5: 309-313.

Anders S, Huber W. 2010. Differential expression analysis for sequence count data. Genome Biology 11: R106.

Belhadj A, Telef N, Saigne C, Cluzet S, Barrieu F, Hamdi S, Merillon JM. 2008. Effect of methyl jasmonate in combination with carbohydrates on gene expression of PR proteins, stilbene, and anthocyanin accumulation in grapevine cell cultures. Plant Physiology and Biochemistry 46: 493-499.

Blanchfield, AL, Robinson SA, Renzullo LJ, Powell KS. 2006. Phylloxera-infested grapevines have reduced chlorophyll and increased photoprotective pigment content – can leaf pigment composition aid pest detection? Funct Plant Biol. 33: 507-514.

Blank L, Wolf T, Elmert K, Schroder MB. 2009. Differential gene expression during hypersensitive response in phylloxera-resistant rootstock 'Borner' using custom oligonucleotide arrays. Journal of Plant Interactions 4: 261-269.

Bronner R. 1992. The role of nutritive cells in the nutrition of cynipids and cecidomyiids. In Biology of Insect-induced Galls (eds) Shorthouse JD, Rofritsch O, Oxford University Press, New York pp 118-140.

Cao J, Huang J, Yang Y, Hu X. 2011. Analyses of the oligopeptide transporter gene family in polar and grape. BMC Genomics 12: 465.

Casson SA, Hetherington AM. 2010. Environmental regulation of stomatal development. Current Opinion in Plant Biology 13: 90-95.

Compson ZG, Larson KC, Zinkgraf MS, Whitham TG. 2011. A genetic basis for the manipulation of sink-source relationships by the galling aphid *Pemphigus batae*. Oecologia 167: 711-721.

De Boer JG, Dicke M. 2004. The role of methyl salicylate in prey searching behavior of the predatory mite *Phytoseiulus persimilis*. Journal of Chemical Ecology 30: 255-271.

Deeken R, Engelmann JC, Efetova M, Czirjak T, Muller T, Kaiser WM, Tiertz O, Krischke M, Mueller MJ, Palme K, Dandekar T, Hedrich R. 2006. An integrated view of gene expression and solute profiles of *Arabidopsis* tumors: a genome-wide approach. The Plant Cell 18: 3617-3634.

Dorchin N, Cramer MD, Hoffmann JH. 2006. Photosynthesis and sink activity of wasp-induced galls in *Acacia pycnantha*. Ecology 87: 1781–1791.

Downie DA, Granett J, Fisher JR. 2000. Distribution and abundance of leaf galling and foliar sexual morphs of grape phylloxera (Hemiptera: Phylloxeridae) and *Vitis* species in the central and eastern United States. Environmental Entomology 29: 979-986.

Faurie B, Cluzet S, Merillon JM. 2009. Implication of signaling pathways involving calcium, phosphorylation and active oxygen species in methyl jasmonate-induced defense responses in grapevine cell cultures. Journal of Plant Physiology 166: 1863-1877.

Fay PA, Hartnett DC, Knapp AK. 1993. Increased photosynthesis and water potentials in *Silphium integrifolium* galled by cynipid wasps. Oecologia 93: 114-120.

Granett J, Walker MA, Kocsis L, Omer AD. 2001. Biology and management of grape phylloxera. Annual Review of Entomology 46: 387-412.

Hamiduzzaman MM, Jakab G, Barnavon L, Neuhaus JM, Mauch-Mani B. 2005. Beta-aminobutyric acid-induced resistance against downy mildew in grapevine acts through the potentiation of callose formation and jasmonic acid signaling. Molecular Plant and Microbe Interactions 18: 819-829.

Hancock AM, Brachi B, Faure N, Horton MW, Jarymowycz LB, Sperone FG, Toomajian C, Roux F, Bergelson J. 2011. Adaptation to climate across the *Arabidopsis thaliana* genome. Science 334: 83-86.

Inbar M, Wink M, Wool D. 2004. The evolution of host plant manipulation by insects: molecular and ecological evidence from gall-forming aphids on *Pistacia*. Molecular Phylogenetics and Evolution 32: 504-511.

Kellow AV, Sedgley M, Van Heeswijck R. 2004. Interaction between *Vitis vinifera* and grape phylloxera: changes in root tissue during nodosity formation. Annals of Botany 93: 581-590.

Larson KC, Whitham TG. 1997. Competition between gall aphids and natural plant sinks: plant architecture affects resistance to galling. Oecologia 109: 575-582.

Lawo NC, Weingart GJ, Schumacher R, Forneck A. 2011. The volatile metabolome of grapevine roots: first insights into the metabolic response upon phylloxera attack. Plant Physiology and Biochemistry 49: 1059-1063.

Martin DM, Toub O, Chiang A, Lo BC, Ohse S, Lund ST, Bohlmann J. 2009. The bouquet of grapevine (*Vitis vinifera* L. cv. Cabernet Sauvignon) flowers arises from the biosynthesis of sesquiterpenes in pollen grains. Proceedings of the National Academy of Sciences USA 106: 7245-7250.

Mcleod, JM. 1990. Damage assessment and biology of foliar grape phylloxera (Homoptera: Phylloxeridae) in Ohio. PhD Dissertation. The Ohio State University.

Omer AD, Thaler JS, Granett J, Karban R. 2000. Jasmonic acid induced resistance in grapevines to a root and leaf feeder. Journal of Economic Entomology 93: 840-845.

Owen DA. 1891. Some strange developments upon *Carya alba* caused by phylloxera. Proceedings of the Indiana Academy of Sciences p76.

Pratt C. 1974. Vegetative anatomy of cultivated grapes – a review. American Journal of Enology and Viticulture 25: 131-150.

Price PW. 1987. Adaptive nature of insect galls. Environmental Entomology 16: 15-24.

Raman, A, Schaefer CW, Withers TM (eds). 2005. Biology, ecology, and evolution of gall-inducing arthropods. Science Publishers, Inc, Plymouth, UK. Vol 1.

Repka V, Fischerova I, Silharova K. 2004. Methyl jasmonate is a potent elicitor of multiple defense responses in grapevine leaves and cell suspension cultures. Biologia Plantarum 48: 273-283.

Rilling G, Steffan H. 1978. Experiments on the CO_2 fixation and the assimilate import by leaf galls on phylloxera (*Dactylosphaera vitifolii* Shimer) on grapevine (*Vitis rupestris* 187G). Angewandte Botanik 52: 343-354.

Robinson MD, McCarthy DJ, Smyth GK. 2009. edgeR: a Bioconductor package for differential expression analysis of digital gene expression data. Bioinformatics 26: 139-140.

Rosen HR. 1916. The development of the *Phylloxera vastatrix* leaf gall. American Journal of Botany 3: 337-360.

Santner A. 2007. The JAZ proteins link jasmonate perception with transcriptional changes. The Plant Cell 19: 3839-3842.

Schuler MA. 2011. P450s in plant-insect interactions. Biochimica et Biophysica Acta 1814: 36-45.

Snoeren TAL, Mumm R, Poelman EH, Yang Y, Pichersky E, Dicke M. 2010. The herbivore-induced plant volatile methyl salicylate negatively affects attraction of the parasitoid *Diadegma semiclausum*. Journal of Chemical Ecology 36: 479-489.

Sterling C. 1952. Ontogeny of the phylloxera gall of grape leaf. American Journal of Botany 39: 6-15.

Stone GN, Schonrogge K. 2003. The adaptive significance of insect gall morphology. Trends in Ecology and Evolution. 18: 512-522.

Stone GN, Schonrogge K, Atkinson RJ, Bellido D, Pujade-Villar J. 2002. The population biology of oak gall wasps (Hymenoptera: Cynipidae). Annual Review of Entomology 47: 633-668.

Stes E, Vandeputte OM, El Jaziri M, Holsters M, Vereecke D. 2011. A successful bacterial coup d'état: how *Rhodococcus fascians* redirects plant development. Annual Review of Phytopathology 49: 69-86.

Thaler JS, Agrawal AA, Halitschke R. 2010 Salicylate-mediated interactions between pathogens and herbivores. Ecology 91: 1075-1082.

Thimm O, Blasing O, Gibon Y, Nagel A, Meyer S, Kruger P, Selbig J, Muller LA, Rhee SY, Stitt M. 2004. MAPMAN: a user-driven toll to display genomics data sets onto diagrams of metabolic pathways and other biological processes. Plant Journal 37: 914-939.

Tooker JF, DeMoraes CM. 2008. Gall insects and indirect plant defenses: a case of active manipulation? Plant Signaling and Behavior 3: 503-504.

Trouvelot S, Varnier AL, Allegre M, Mercier L, Baillieul F, Arnould C, Gianinazzi-Pearson V, Klarzynski O, Joubert JM, Pugin A. 2008. A beta-1,3-glucan sulfate induces resistance in grapevine against *Plasmopara viticola* through priming defense responses. Including HR-like cell death. Molecular Plant Microbe Interactions 21: 232-243.

Vorwerk S, Martinez-Torres D, Forneck A. 2007. *Pantoea agglomerans*-associated bacteria in grape phylloxera (*Daktulosphaira vitifoliae* Fitch). Agricultural and Forest Entomology 9: 57-64.

Waring GL, Price PW. 1989. Parasitoid pressure and the radiation of a gall forming group (Cecidomyiidae: *Asphondylia* spp) on creosote bush (*Larrea tridentata*). Oecologia 79: 293-299.

Warick RP, Hildebrandt AC. 1966. Free amino acid contents of stem and phylloxera gall tissue cultures of grape. Plant Physiology 41: 573-578.

Witiak SM. 2006. Hormonal and molecular investigations of phylloxera leaf gall development. Thesis. Pennsylvania State University.

Woodward FI. 1987. Stomatal numbers are sensitive to increases in CO_2 from pre-industrial levels. Nature 327: 617-618.

Wool, D. 2004. Galling aphids: specialization, biological complexity, and variation. Annual Review of Entomology 49: 175-192.

TABLES

Table 5.1. Stomatal index (SI; ratio of stomata to epidermal cells) for *V. riparia* and *V. vinifera* in proximity to gall and in non-galled leaf tissue of galled leaves. Stomatal density (SD; number of stomata mm^{-2}) for non-galled areas of galled leaves was 115 ± 8 and 270 ± 56 for *V. riparia* and *V. vinifera*, respectively.

| Species | n | Distance from gall on adaxial side | | | Non-galled portion of galled leaf | |
		0-300 um	300-600 um	600-900 um	Adaxial	Abaxial
V. riparia	5	3.3 ± 0.7	1.1 ± 0.5	0.4 ± 0.2	0 ± 0	11.0 ± 0.5
V. vinifera	5	1.5 ± 0.3	0.4 ± 0.1	0.1 ± 0.1	0 ± 0	10.2 ± 0.7

Table 5.2. Total number of genes, number of differentially expressed (DE) genes, and the percent coverage for each functional category adopted from Mapman for categories that were significantly represented relative to the overall expression patterns.

Categories	Total genes	DE genes	% coverage
Fermentation	12	6	50
Secondary metabolism	210	99	47
PS	136	63	46
Cell wall	219	90	41
Stress	410	151	37
Miscellaneous	660	233	35
Metal handling	44	15	34
Hormone metabolism	272	91	33
Transport	578	177	31
Signaling	707	205	29
Not assigned	4062	640	16
RNA	1554	235	15
Protein	1832	261	14
DNA	320	38	12
Mitochondrial electron transport / ATP synthesis	89	5	6

Table 5.3. Arabidopsis (TAIR v.9) identifier, % change in gall tissue relative to leaf, and annotation for transcripts with corresponding function in carbon metabolism (graphically depicted in Figure 5.6).

TAIR v. 9	% change	Annotation
FIGURE 5.6A		
Light Reactions		
atcg00070	-67	PSII K protein
atcg00680	-72	encodes for CP47, subunit of the photosystem II reaction center.
atcg00280	-68	chloroplast gene encoding a CP43 subunit of the photosystem II reaction center.
at1g76450	-55	oxygen-evolving complex-related
at1g77090	-76	thylakoid lumenal 29.8 kDa protein
at5g02120	-58	OHP (ONE HELIX PROTEIN)
atcg00020	-77	Encodes chlorophyll binding protein D1
at2g06520	-64	PSBX (photosystem II subunit X)
at1g14150	-60	oxygen evolving enhancer 3 (PsbQ) family protein
at2g30570	-54	PSBW (PHOTOSYSTEM II REACTION CENTER W)
at4g28660	-61	PSB28 (PHOTOSYSTEM II REACTION CENTER PSB28 PROTEIN)
at1g03600	-52	photosystem II family protein
at3g01440	-65	oxygen evolving enhancer 3 (PsbQ) family protein
atcg00270	-69	PSII D2 protein
at5g51545	-63	LPA2 (low psii accumulation2)
at5g54270	-55	LHCB3 (LIGHT-HARVESTING CHLOROPHYLL B-BINDING PROTEIN 3)
at2g34430	-70	LHB1B1
at3g27690	-50	LHCB2.3
at1g15820	-59	LHCB6 (LIGHT HARVESTING COMPLEX PSII SUBUNIT 6)
atcg00590	-69	hypothetical protein
atcg00540	-61	Encodes cytochrome f apoprotein
atcg00480	-81	chloroplast-encoded gene for beta subunit of ATP synthase

Table 5.3. (continued)

TAIR v. 9	% change	Annotation
atcg00140	-66	ATPase III subunit
at4g09650	-66	ATPD (ATP SYNTHASE DELTA-SUBUNIT GENE)
atcg00340	-67	Encodes the D1 subunit of photosystem I and II reaction centers.
atcg00350	-70	Encodes psaA protein comprising the reaction center for photosystem I
at2g46820	-66	PSI-P (PHOTOSYSTEM I P SUBUNIT)
at1g03130	-67	PSAD-2 (photosystem I subunit D-2)
at1g19150	-67	LHCA6
at1g34000	-58	OHP2 (ONE-HELIX PROTEIN 2)
at1g02180	677	ferredoxin-related
at3g17670	-56	binding
at1g20020	-61	FNR2 (FERREDOXIN-NADP(+)-OXIDOREDUCTASE 2)

Calvin Cycle

TAIR v. 9	% change	Annotation
atcg00490	-83	large subunit of RUBISCO.
at2g39730	-71	RCA (RUBISCO ACTIVASE)
at1g14030	-63	ribulose-1,5 bisphosphate carboxylase oxygenase large subunit
at1g73110	-54	ribulose bisphosphate carboxylase/oxygenase activase, putative
at1g56190	-65	phosphoglycerate kinase, putative
at1g16300	1246	GAPCP-2
at3g26650	-78	GAPA (GLYCERALDEHYDE 3-PHOSPHATE DEHYDROGENASE A
at1g12900	-71	GAPA-2 (GLYCERALDEHYDE 3-PHOSPHATE DEHYDROGENASE A
at2g21330	-79	fructose-bisphosphate aldolase, putative
at2g01140	136	fructose-bisphosphate aldolase, putative
at4g26530	-56	fructose-bisphosphate aldolase, putative
at3g54050	-67	fructose-1,6-bisphosphatase, putative
at2g45290	362	transketolase, putative
at3g55800	-70	SBPASE (sedoheptulose-bisphosphatase)

Table 5.3. (continued)

TAIR v. 9	% change	Annotation
at3g04790	-63	ribose 5-phosphate isomerase-related

Starch

at5g19220	-75	APL1 (ADP GLUCOSE PYROPHOSPHORYLASE LARGE SUBUNIT 1)
at1g11720	-57	ATSS3 (starch synthase 3)
at4g18240	-65	ATSS4
at1g32900	-80	starch synthase, putative
at4g17090	-70	CT-BMY (CHLOROPLAST BETA-AMYLASE)
at4g00490	-58	BAM2 (BETA-AMYLASE 2)
at4g15210	-55	BAM5 (BETA-AMYLASE 5)
at1g69830	-68	AMY3 (ALPHA-AMYLASE-LIKE 3)
at5g64860	123	DPE1 (DISPROPORTIONATING ENZYME)

Transport

at5g05820	221	phosphate translocator-related
at5g46110	187	APE2 (ACCLIMATION OF PHOTOSYNTHESIS TO ENVIRONMENT 2)
at3g14410	-58	transporter-related
at1g61800	305	GPT2

FIGURE 5.6B

Electron transport

at4g05020	310	NDB2 (NAD(P)H dehydrogenase B2)
at4g21490	148	NDB3
at5g08740	-74	NDC1 (NAD(P)H dehydrogenase C1)
at2g29990	2400	NDA2 (ALTERNATIVE NAD(P)H DEHYDROGENASE 2)
at3g22370	1293	AOX1A (ALTERNATIVE OXIDASE 1A)

TCA

at5g58330	-59	malate dehydrogenase (NADP), chloroplast, putative

Table 5.3. (continued)

TAIR v. 9	% change	Annotation
at2g05710	736	aconitate hydratase, cytoplasmic, putative
at4g13430	98	IIL1 (ISOPROPYL MALATE ISOMERASE LARGE SUBUNIT 1);

Mitochondrial transport

TAIR v. 9	% change	Annotation
at4g39460	335	SAMC1 (S-ADENOSYLMETHIONINE CARRIER 1)
at4g28390	35547	AAC3 (ADP/ATP CARRIER 3)
at5g12860	-83	DiT1 (dicarboxylate transporter 1)
at5g24030	573	SLAH3 (SLAC1 HOMOLOGUE 3)
at2g17270	-68	mitochondrial substrate carrier family protein

Sugar transport

TAIR v. 9	% change	Annotation
at4g00370	-75	ANTR2; inorganic phosphate transmembrane transporter/
at5g59250	-69	sugar transporter family protein
at4g16480	-55	INT4 (INOSITOL TRANSPORTER 4);
at4g35300	153	TMT2 (TONOPLAST MONOSACCHARIDE TRANSPORTER2);
at1g71890	337	SUC5; carbohydrate transmembrane transporter
at1g77210	376	sugar transporter, putative
at4g36670	521	mannitol transporter, putative
at5g18840	523	sugar transporter, putative

Water transport

TAIR v. 9	% change	Annotation
at2g37170	240	PIP2B (PLASMA MEMBRANE INTRINSIC PROTEIN 2); water channel
at2g45960	367	PIP1B (NAMED PLASMA MEMBRANE INTRINSIC PROTEIN 1B);
at4g00430	155	PIP1;4 (PLASMA MEMBRANE INTRINSIC PROTEIN 1;4); water channel
at3g54820	1025	PIP2;5 (PLASMA MEMBRANE INTRINSIC PROTEIN 2;5); water channel
at4g01470	398	TIP1;3 (TONOPLAST INTRINSIC PROTEIN 1;3); urea transporter
at3g16240	295	DELTA-TIP; ammonia transporter/ methylammonium transporter
at2g25810	467	TIP4;1 (tonoplast intrinsic protein 4;1); water channel

Table 5.3. (continued)

TAIR v. 9	% change	Annotation
at2g36830	340	GAMMA-TIP (GAMMA TONOPLAST INTRINSIC PROTEIN);
at4g10380	126	NIP5;1; arsenite transmembrane transporter/ boron transporter/ water channel
at1g80760	1242	NIP6;1 (NOD26-LIKE INTRINSIC PROTEIN 6;1);
at4g18910	985	NIP1;2 (NOD26-LIKE INTRINSIC PROTEIN 1;2); arsenite transporter
Hexose pool		
at3g59480	1049	pfkB-type carbohydrate kinase family protein
at5g51830	139	pfkB-type carbohydrate kinase family protein
at5g11110	-81	ATSPS2F (SUCROSE PHOSPHATE SYNTHASE 2F);
at1g04920	-78	ATSPS3F (sucrose phosphate synthase 3F)
at2g35840	285	sucrose-phosphatase 1 (SPP1)
at1g73370	509	SUS6 (SUCROSE SYNTHASE 6); UDP-glycosyltransferase/ sucrose synthase
at3g43190	1380	SUS4; UDP-glycosyltransferase/ sucrose synthase/ transferase,
at4g34860	188	beta-fructofuranosidase, putative / invertase, saccharase, beta-fructosidase,
at1g56560	-58	beta-fructofuranosidase, putative / invertase, saccharase, beta-fructosidase,
at1g12240	1214	ATBETAFRUCT4; beta-fructofuranosidase/ hydrolase,
at1g62660	2389	beta-fructosidase (BFRUCT3) / beta-fructofuranosidase / invertase, vacuolar
at1g47840	201	HXK3 (HEXOKINASE 3); ATP binding / fructokinase/ glucokinase
Glycolysis		
at3g04120	-50	GAPC1 (GLYCERALDEHYDE-3-PHOSPHATE DEHYDROGENASE)
at2g24270	-65	ALDH11A3; 3-chloroallyl aldehyde dehydrogenase/ G3P dehydrogenase
at2g36460	259	fructose-bisphosphate aldolase, putative
at1g74030	631	enolase, putative
at5g08570	253	pyruvate kinase, putative
at3g52990	296	pyruvate kinase, putative
at3g14940	-56	ATPPC3 (PHOSPHOENOLPYRUVATE CARBOXYLASE 3);

Table 5.3. (continued)

TAIR v. 9	% change	Annotation
at1g22170	623	phosphoglycerate/bisphosphoglycerate mutase family protein
at5g56350	264	pyruvate kinase, putative
at3g22960	129	PKP-ALPHA; pyruvate kinase
at5g61580	-54	PFK4 (PHOSPHOFRUCTOKINASE 4); 6-phosphofructokinase
at5g22620	-63	phosphoglycerate/bisphosphoglycerate mutase family protein
at4g37870	125	PCK1 (PHOSPHOENOLPYRUVATE CARBOXYKINASE 1); ATP binding

Fermentation

at4g17260	245	L-lactate dehydrogenase, putative
at5g54960	-89	PDC2 (pyruvate decarboxylase-2); carboxy-lyase/
at1g77120	399	ADH1 (ALCOHOL DEHYDROGENASE 1); alcohol dehydrogenase
at3g48000	201	ALDH2B4 (ALDEHYDE DEHYDROGENASE 2B4);
at1g23800	192	ALDH2B7; 3-chloroallyl aldehyde dehydrogenase
at4g34240	-59	ALDH3I1 (ALDEHYDE DEHYDROGENASE 3

Cell wall synthesis

at1g12780	653	UGE1 (UDP-D-glucose/UDP-D-galactose 4-epimerase 1);
at4g10960	398	UGE5 (UDP-D-glucose/UDP-D-galactose 4-epimerase 5);
at3g29360	257	UDP-glucose 6-dehydrogenase, putative
at5g15490	242	UDP-glucose 6-dehydrogenase, putative
at1g02000	1597	GAE2 (UDP-D-GLUCURONATE 4-EPIMERASE 2);
at1g08200	120	AXS2 (UDP-D-APIOSE/UDP-D-XYLOSE SYNTHASE 2);
at3g53520	117	UXS1 (UDP-GLUCURONIC ACID DECARBOXYLASE 1);
at4g26260	3780	MIOX4; inositol oxygenase
at1g14520	155	MIOX1 (MYO-INISITOL OXYGENASE); inositol oxygenase/ oxidoreductase

Raffinose synthesis

at5g20250	111	DIN10 (DARK INDUCIBLE 10); hydrolase,

Table 5.3. (continued)

TAIR v. 9	% change	Annotation
at3g57520	-88	AtSIP2 (Arabidopsis thaliana seed imbibition 2); hydrolase,
at1g55740	1567	AtSIP1 (Arabidopsis thaliana seed imbibition 1); hydrolase,
at4g01970	29154	AtSTS (Arabidopsis thaliana stachyose synthase); galactinol-raffinose
at1g56600	204	AtGolS2 (Arabidopsis thaliana galactinol synthase 2); transferase,
at2g47180	352	AtGolS1 (Arabidopsis thaliana galactinol synthase 1); transferase,
at1g60470	-75	AtGolS4 (Arabidopsis thaliana galactinol synthase 4); transferase,

Not graphically depicted

Oligopeptide transport

at5g19640	-94	proton-dependent oligopeptide transport (POT) family protein
at1g68570	-74	proton-dependent oligopeptide transport (POT) family protein
at1g69870	-73	proton-dependent oligopeptide transport (POT) family protein
at4g16370	-67	ATOPT3 (OLIGOPEPTIDE TRANSPORTER); oligopeptide transporter
at4g26590	-61	OPT5 (OLIGOPEPTIDE TRANSPORTER 5); oligopeptide transporter
at3g54140	-53	PTR1 (PEPTIDE TRANSPORTER 1); dipeptide transporter
at5g62680	-53	proton-dependent oligopeptide transport (POT) family protein
at5g46050	172	PTR3 (PEPTIDE TRANSPORTER 3); dipeptide transporter
at1g52190	184	proton-dependent oligopeptide transport (POT) family protein
at1g72125	186	transporter
at1g59740	192	proton-dependent oligopeptide transport (POT) family protein
at3g45650	225	NAXT1 (NITRATE EXCRETION TRANSPORTER1);
at5g14940	289	proton-dependent oligopeptide transport (POT) family protein
at1g65730	410	YSL7 (YELLOW STRIPE LIKE 7); oligopeptide transporter
at4g10770	483	OPT7 (OLIGOPEPTIDE TRANSPORTER 7); oligopeptide transporter
at3g53960	952	proton-dependent oligopeptide transport (POT) family protein
at1g22540	999	proton-dependent oligopeptide transport (POT) family protein

Table 5.3. (continued)

TAIR v. 9	% change	Annotation
Amino acid transport		
at1g31830	-89	amino acid permease family protein
at2g41190	-71	amino acid transporter family protein
at5g40780	-61	LHT1; amino acid transmembrane transporter
at1g08230	18	amino acid transporter family protein
at5g41800	158	amino acid transporter family protein
at2g42005	171	amino acid transporter family protein
at3g28960	236	amino acid transporter family protein
at5g09220	271	AAP2 (AMINO ACID PERMEASE 2); amino acid transmembrane transporter
at5g23810	295	AAP7; amino acid transmembrane transporter
at3g56200	340	amino acid transporter family protein
at2g21050	402	amino acid permease, putative
at1g47670	402	amino acid transporter family protein
at2g39130	716	amino acid transporter family protein

Table 5.4. Arabidopsis (TAIR v.9) identifier, % change in gall tissue relative to leaf, and annotation for transcripts with corresponding function in secondary metabolism (graphically depicted in Figure 5.7).

TAIR v. 9	% change	Annotation
FIGURE 5.7		
Mevalonate biosynthesis		
at5g47720	-93	acetyl-CoA C-acyltransferase, putative / 3-ketoacyl-CoA thiolase, putative
at4g11820	128	MVA1; acetyl-CoA C-acetyltransferase/ hydroxymethylglutaryl-CoA synthase
at1g76490	305	HMG1 (HYDROXY METHYLGLUTARYL COA REDUCTASE 1);
Non-mevalonate biosynthesis		
at1g74470	-67	geranylgeranyl reductase
at4g15560	-96	CLA1 (CLOROPLASTOS ALTERADOS 1); 1-deoxy-D-xylulose-5-P synthase
at1g63970	-55	ISPF; 2-C-methyl-D-erythritol 2,4-cyclodiphosphate synthase
at4g34350	-63	HDR (4-HYDROXY-3-METHYLBUT-2-ENYL DIPHOSPHATE reductase
at4g36810	-58	GGPS1 (GERANYLGERANYL PYROPHOSPHATE SYNTHASE 1);
Terpenoid biosynthesis		
at5g23960	-74	TPS21 (TERPENE SYNTHASE 21); (-)-E-beta-caryophyllene synthase
at1g61120	636	TPS04 (TERPENE SYNTHASE 04); (E,E)-geranyllinalool synthase
at1g78950	-57	beta-amyrin synthase, putative
at4g16740	0	ATTPS03; (E)-beta-ocimene synthase/ myrcene synthase
at1g78510	-73	SPS1 (solanesyl diphosphate synthase 1); trans-octaprenyltranstransferase
at3g25820	-50	ATTPS-CIN (terpene synthase-like sequence-1,8-cineole);
Carotenoid biosynthesis		
at4g25700	-33	BETA-OHASE 1 (BETA-HYDROXYLASE 1); carotene beta-ring hydroxylase
at1g57770	-62	amine oxidase family
at5g49555	-73	amine oxidase-related
at5g17230	-79	phytoene synthase (PSY) geranylgeranyl-diphosphate geranylgeranyl transferase
at3g04870	-57	ZDS (ZETA-CAROTENE DESATURASE); carotene 7,8-desaturase

Table 5.4. (continued)

TAIR v. 9	% change	Annotation
at3g10230	-61	LYC (LYCOPENE CYCLASE); lycopene beta cyclase
at3g63520	-70	CCD1 (CAROTENOID CLEAVAGE DIOXYGENASE 1);
at2g21860	-57	violaxanthin de-epoxidase-related
at1g08550	-62	NPQ1 (NON-PHOTOCHEMICAL QUENCHING 1); violaxanthin de-epoxidase

Tocopherol biosynthesis

at5g36160	115	aminotransferase-related
at3g63410	-60	APG1 (ALBINO OR PALE GREEN MUTANT 1); methyltransferase
at4g32770	-61	VTE1 (VITAMIN E DEFICIENT 1); tocopherol cyclase
at1g64970	-69	G-TMT (GAMMA-TOCOPHEROL METHYLTRANSFERASE);

Chlorophyll biosynthesis

at1g58290	-69	HEMA1; glutamyl-tRNA reductase
at1g69740	-53	HEMB1; catalytic/ metal ion binding / porphobilinogen synthase
at5g08280	-54	HEMC (HYDROXYMETHYLBILANE SYNTHASE);
at2g26540	-67	HEMD; uroporphyrinogen-III synthase
at2g30390	-55	FC2 (FERROCHELATASE 2); ferrochelatase
at5g45930	-57	CHLI2 (MAGNESIUM CHELATASE I2); ATPase/ magnesium chelatase
at5g13630	-81	GUN5 (GENOMES UNCOUPLED 5); magnesium chelatase
at3g56940	-69	CRD1 (COPPER RESPONSE DEFECT 1); DNA binding /
at5g18660	-59	PCB2 (PALE-GREEN AND CHLOROPHYLL B REDUCED 2);
at1g44446	-72	CH1 (CHLORINA 1); chlorophyllide a oxygenase
at3g14110	-56	FLU (FLUORESCENT IN BLUE LIGHT); binding
at3g59400	-60	GUN4; enzyme binding / tetrapyrrole binding

Shikimate biosynthesis

at5g34930	151	arogenate dehydrogenase
at1g11790	822	ADT1 (arogenate dehydratase 1); arogenate dehydratase/ prephenate dehydratase

Table 5.4. (continued)

TAIR v. 9	% change	Annotation
at5g22630	655	ADT5 (arogenate dehydratase 5); arogenate dehydratase/ prephenate dehydratase
at1g22410	213	2-dehydro-3-deoxyphosphoheptonate aldolase,
at2g21940	434	shikimate kinase, putative
at2g16790	142	shikimate kinase family protein
at2g35500	-54	shikimate kinase-related
at3g06350	802	MEE32 (MATERNAL EFFECT EMBRYO ARREST 32); NADP, NADPH binding

Phenylpropanoid biosynthesis

at5g42830	143	transferase family protein
at1g32100	667	PRR1 (PINORESINOL REDUCTASE 1); pinoresinol reductase
at4g35160	-94	O-methyltransferase family 2 protein
at2g33590	1114	cinnamoyl-CoA reductase family
at5g01210	1184	transferase family protein
at1g20510	321	OPCL1 (OPC-8:0 COA LIGASE1); 4-coumarate-CoA ligase
at2g23910	852	cinnamoyl-CoA reductase-related

Simple phenol biosynthesis

at5g05390	248	LAC12 (laccase 12); laccase
at5g48100	154	TT10 (TRANSPARENT TESTA 10); copper ion binding / laccase
at2g46570	226	LAC6 (laccase 6); laccase
at5g09360	587	LAC14 (laccase 14); laccase
at5g60020	585	LAC17 (laccase 17); laccase
at5g03260	1446	LAC11 (laccase 11); laccase
at2g38080	456	IRX12 (IRREGULAR XYLEM 12); laccase

Lignin and lignin biosynthesis

at2g37040	810	pal1 (Phe ammonia lyase 1); phenylalanine ammonia-lyase
at3g53260	562	PAL2; phenylalanine ammonia-lyase

Table 5.4. (continued)

TAIR v. 9	% change	Annotation
at3g10340	441	PAL4 (Phenylalanine ammonia-lyase 4); ammonia ligase/ ammonia-lyase/ catalytic
at2g30490	975	C4H (CINNAMATE-4-HYDROXYLASE); trans-cinnamate 4-monooxygenase
at3g21240	313	4CL2 (4-COUMARATE:COA LIGASE 2); 4-coumarate-CoA ligase
at1g51680	10807	4CL1 (4-COUMARATE:COA LIGASE 1); 4-coumarate-CoA ligase
at3g62000	-57	O-methyltransferase family 3 protein
at4g34050	174	caffeoyl-CoA 3-O-methyltransferase, putative
at4g26220	240	caffeoyl-CoA 3-O-methyltransferase, putative
at1g15950	154	CCR1 (CINNAMOYL COA REDUCTASE 1); cinnamoyl-CoA reductase
at4g36220	399	FAH1 (FERULIC ACID 5-HYDROXYLASE 1); monooxygenase
at5g54160	-4	ATOMT1 (O-METHYLTRANSFERASE 1);
at4g37990	-66	ELI3-2 (ELICITOR-ACTIVATED GENE 3-2);
at4g39330	-38	CAD9 (CINNAMYL ALCOHOL DEHYDROGENASE 9);
at3g19450	1411	ATCAD4; cinnamyl-alcohol dehydrogenase
at4g37970	5009	CAD6 (CINNAMYL ALCOHOL DEHYDROGENASE 6); binding /

Chalcone biosynthesis

at1g53520	-62	chalcone-flavanone isomerase-related
at1g59960	-73	aldo/keto reductase, putative
at5g05270	508	chalcone-flavanone isomerase family protein
at5g13930	2352	TT4 (TRANSPARENT TESTA 4); naringenin-chalcone synthase
at3g55120	354	TT5 (TRANSPARENT TESTA 5); chalcone isomerase

Isoflavonoid biosynthesis

at1g75290	3925	oxidoreductase, acting on NADH or NADPH
at4g39230	347	isoflavone reductase, putative
at1g75280	-98	isoflavone reductase, putative

Flavonol biosynthesis

Table 5.4. (continued)

TAIR v. 9	% change	Annotation
at1g49390	347	oxidoreductase, 2OG-Fe(II) oxygenase family protein
at1g17020	-56	SRG1 (SENESCENCE-RELATED GENE 1); oxidoreductase,
at4g25300	-92	oxidoreductase, 2OG-Fe(II) oxygenase family protein
at3g21420	350	oxidoreductase, 2OG-Fe(II) oxygenase family protein
at2g45400	-97	BEN1; binding / catalytic/ coenzyme binding / oxidoreductase,

Anthocyanin biosynthesis

at5g05600	455	oxidoreductase, 2OG-Fe(II) oxygenase family protein
at2g22590	224	transferase, transferring glycosyl groups
at4g22880	1978	LDOX (LEUCOANTHOCYANIDIN DIOXYGENASE); leucocyanidin oxygenase
at5g49690	-80	UDP-glucoronosyl/UDP-glucosyl transferase family protein
at1g03495	625	transferase/ transferase, transferring acyl groups other than amino-acyl groups

Dihydroflavonol biosynthesis

at5g24530	141	DMR6 (DOWNY MILDEW RESISTANT 6); oxidoreductase
at4g01070	695	GT72B1; UDP-glucosyltransferase/ UDP-glycosyltransferase
at5g54010	3311	glycosyltransferase family protein
at4g12300	189	CYP706A4; electron carrier/ heme binding / iron ion binding /
at5g53990	23002	glycosyltransferase family protein
at5g42800	-99	DFR (DIHYDROFLAVONOL 4-REDUCTASE); dihydrokaempferol 4-reductase
at1g61720	2414	BAN (BANYULS); oxidoreductase
at4g35420	272	dihydroflavonol 4-reductase family / dihydrokaempferol 4-reductase family
at3g51240	-54	F3H (FLAVANONE 3-HYDROXYLASE); naringenin 3-dioxygenase
at5g07990	-42	TT7 (TRANSPARENT TESTA 7); flavonoid 3'-monooxygenase/ oxygen binding

Table 5.5. Arabidopsis (TAIR v.9) identifier, % change in gall tissue relative to leaf, and annotation for transcripts with corresponding function in biotic defense signaling (graphically depicted in Figure 5.8).

TAIR v. 9	% change	Annotation
FIGURE 5.8		
Salicylic acid signaling		
at4g36470	218	S-adenosyl-L-methionine:carboxyl methyltransferase family protein
at1g68040	-98	S-adenosyl-L-methionine:carboxyl methyltransferase family protein
at3g11480	449	BSMT1
at5g66430	507	S-adenosyl-L-methionine:carboxyl methyltransferase family protein
at5g04370	299	NAMT1
Jasmonic acid signaling		
at3g22400	-63	LOX5
at3g45140	-72	LOX2 (LIPOXYGENASE 2)
at1g67560	175	lipoxygenase family protein
at3g25780	334	AOC3 (ALLENE OXIDE CYCLASE 3)
at1g76690	225	OPR2
at1g76680	727	OPR1
not assigned	359	GSVIVT01015472001 3-ketoacyl-CoA synthase 11
at1g19640	345	JMT (JASMONIC ACID CARBOXYL METHYLTRANSFERASE)
not assigned	1962	GSVIVT01000967001 jasmonate-zim-domain protein 10
not assigned	1131	GSVIVT01021514001 jasmonate-zim-domain protein 8
not assigned	1988	GSVIVT01021516001 jasmonate-zim-domain protein 8
not assigned	1848	GSVIVT01021518001 jasmonate-zim-domain protein 8
Ethylene signaling		
at3g61510	1694	ACS1 (ACC SYNTHASE 1); 1-aminocyclopropane-1-carboxylate synthase
at4g11280	353	ACS6 (ACC SYNTHASE 6)
at2g19590	2111	ACO1 (ACC OXIDASE 1); 1-aminocyclopropane-1-carboxylate oxidase

Table 5.5. (continued)

TAIR v. 9	% change	Annotation
at3g23150	221	ETR2 (ethylene response 2); ethylene binding / glycogen synthase kinase
at3g23240	349	ERF1 (ETHYLENE RESPONSE FACTOR 1); DNA binding
at4g17500	452	ATERF-1 (ETHYLENE RESPONSIVE ELEMENT BINDING FACTOR 1
at5g44210	574	ERF9 (ERF DOMAIN PROTEIN 9); DNA binding / transcription repressor
at3g15210	143	ERF4 (ETHYLENE RESPONSIVE ELEMENT BINDING FACTOR 4);
at5g25190	146	ethylene-responsive element-binding protein, putative
at5g51190	866	AP2 domain-containing transcription factor, putative
at4g31980	-96	unknown protein
at4g20880	133	ethylene-responsive nuclear protein / ethylene-regulated protein (ERT2)
at2g31730	3641	ethylene-responsive protein, putative
at1g04380	2786	2-oxoglutarate-dependent dioxygenase, putative
at1g04350	1215	2-oxoglutarate-dependent dioxygenase, putative

Figure 5.1. *Vitis* leaves are hypostomatal having no stomata on the adaxial side (A) but gall formation generates stomata in increasing density at closer proximity to the gall (arrow; B). Abaxial tissue without or adjacent to galls have similar stomata patterning (Table 5.1).
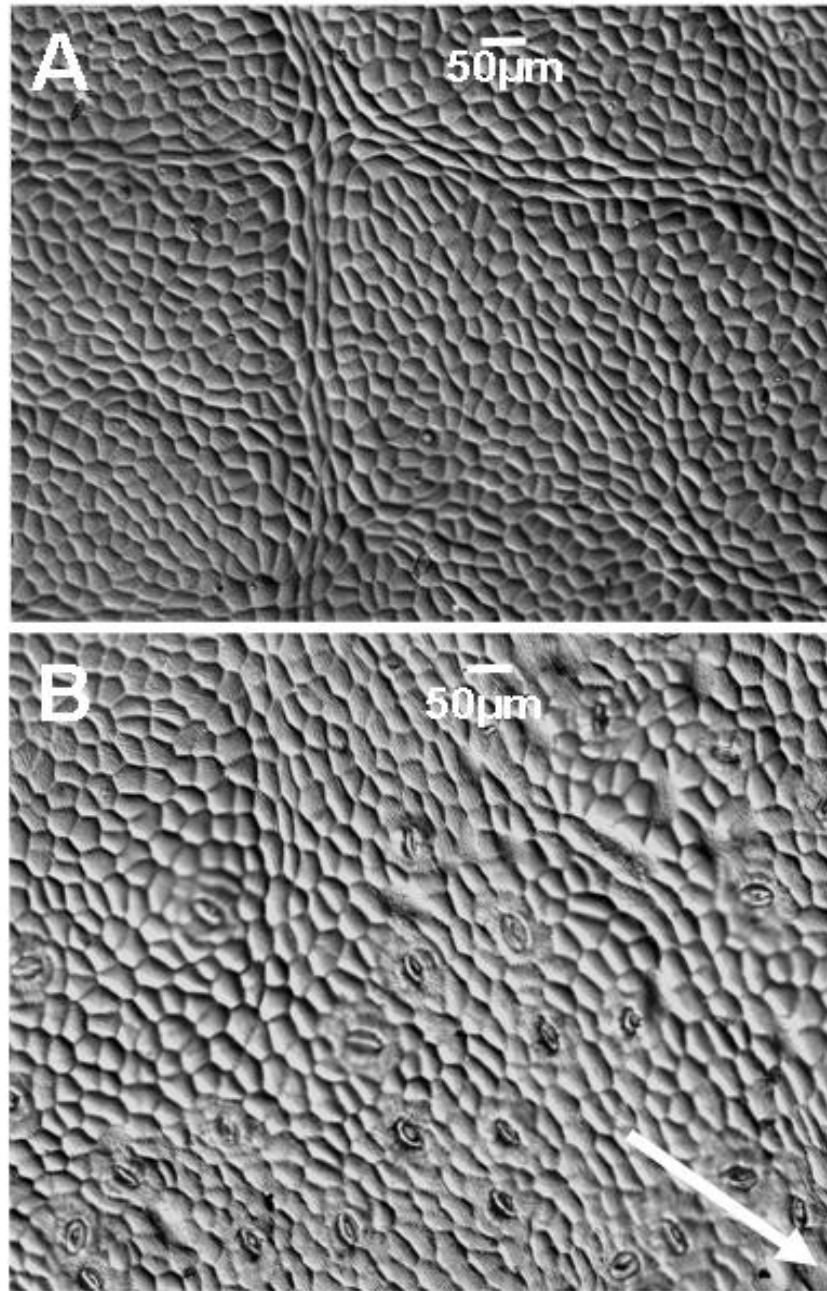
Figure 5.2. Tissue cross-sections for *V. vinifera* 'Frontenac' tissue that is undamaged (A) and with developed gall tissue (B). Stomata (s) typically form on the abaxial leaf-side (A) but gall formation generates adaxial stomata. Bar = 50 μm.
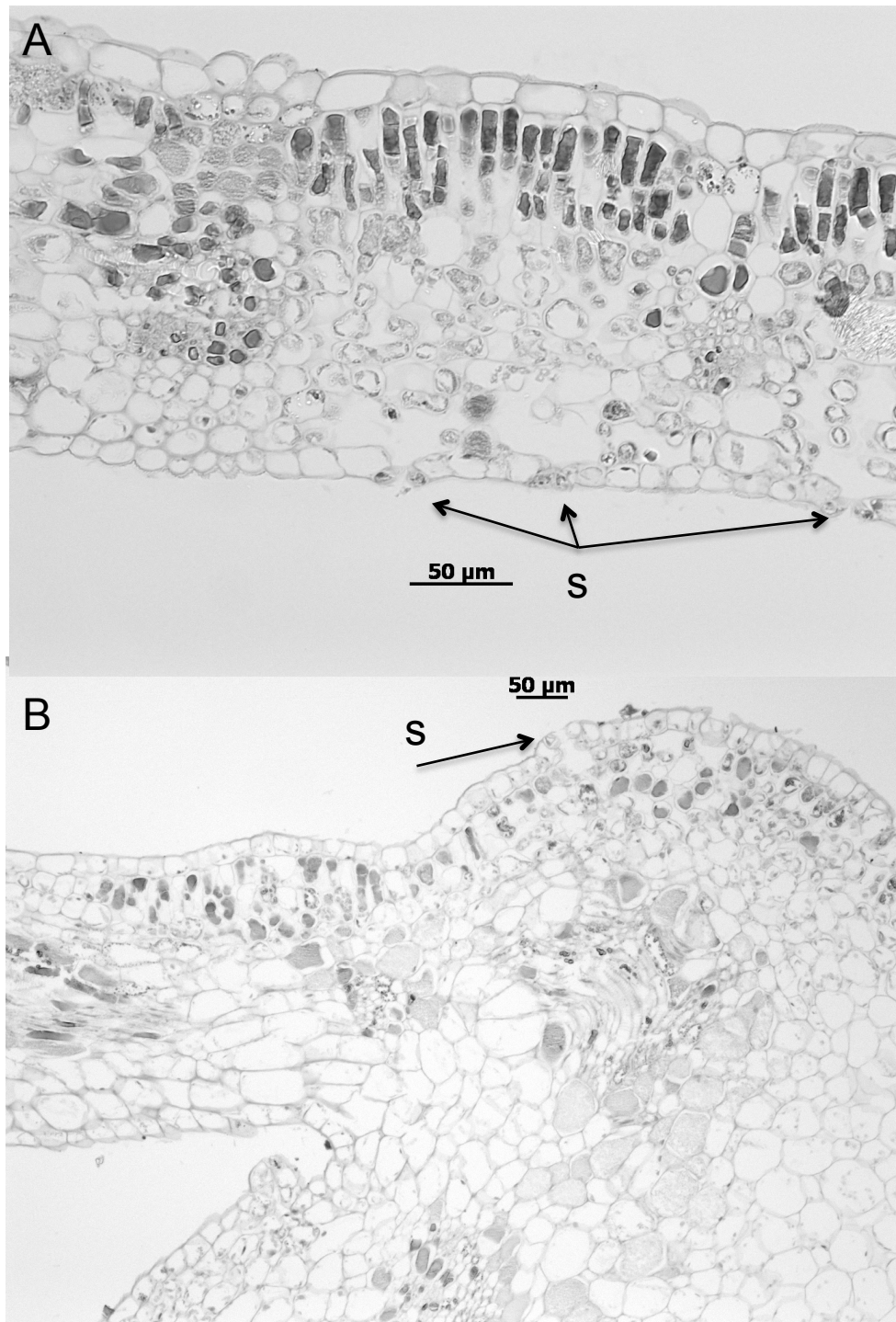
Figure 5.3. Net CO_2 uptake during the day (positive) and night (negative) of field-grown galled and non-galled adjacent leaf tissue. Fluxes include insect respiration. * denotes significant differences between tissue types at each time assessed.
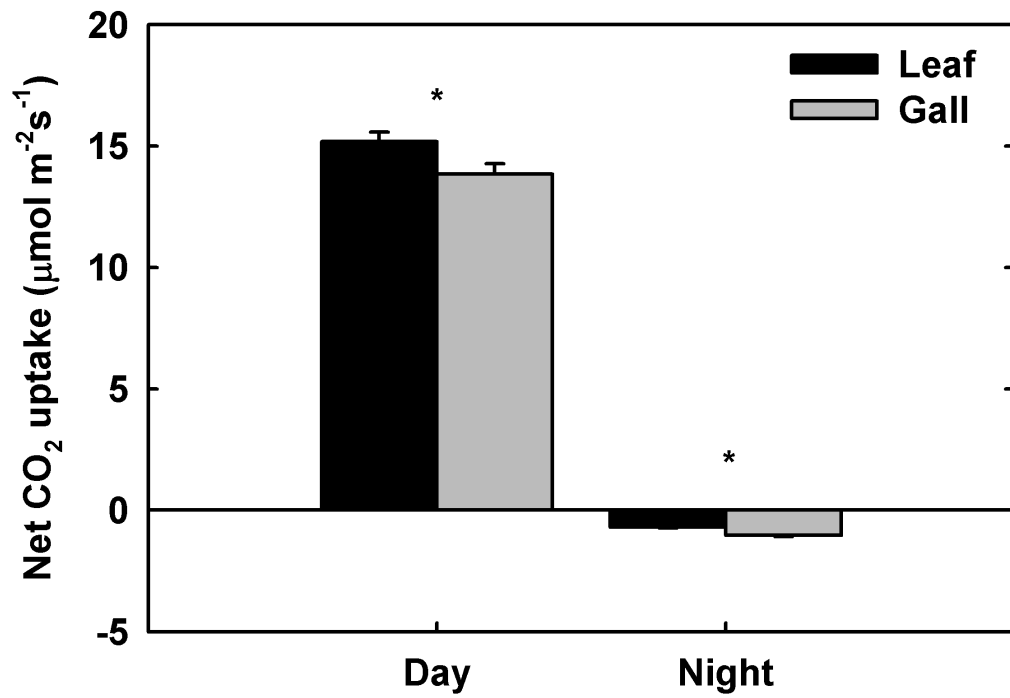
Figure 5.4. Nighttime adaxial CO_2 efflux related to the number of insects and eggs within the gall.
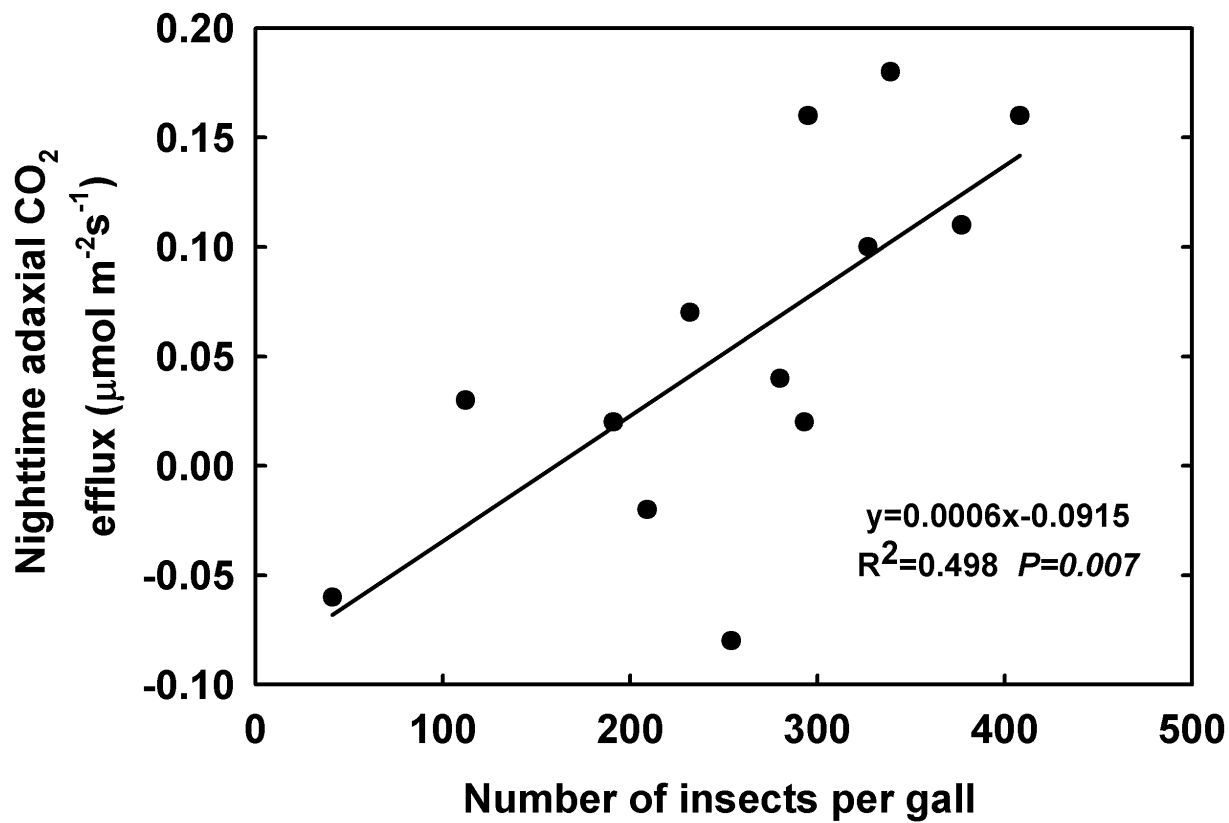

$$y=0.0006x-0.0915$$
$$R^2=0.498 \quad P=0.007$$

Figure 5.5. Post labeling $\delta^{13}C$ values of leaf tissue related to abaxial or adaxial CO_2 uptake (A), gall tissue related to abaxial or adaxial CO_2 efflux (B), and all tissue from the corresponding leaf, gall, and insect (C). Dashed lines denotes the $\delta^{13}C$ of unlabeled grape leaves ($-24.7 \pm 0.8\%_{oo}$). CO_2 flux from adaxial side was adjusted to remove insect respiration (see text). Graphical depiction of leaf sides and where label was applied (D).
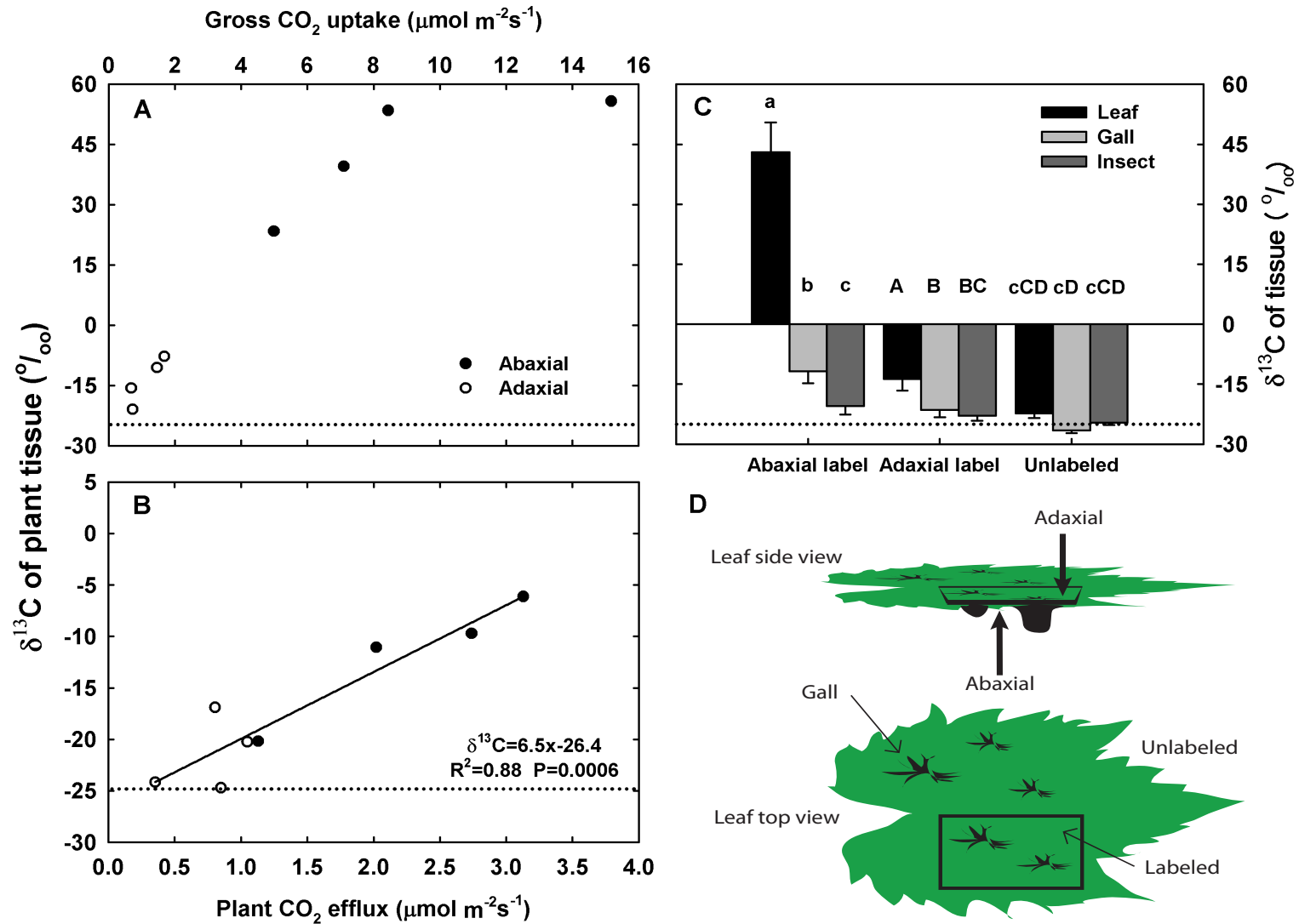
Figure 5.6. Graphical representation of the transcriptional shift from autotrophic to heterotrophic metabolism within a gall cell (A) and for inter- and intracellular metabolic processes (glycolysis, fermentation, respiration; B). Each orange or blue box represents a unique differentially expressed transcript encoding a protein/enzyme. Green boxes represent metabolites, yellow boxes represent metabolites involved in cell wall synthesis, and pink boxes represent processes.

Figure 5.7. Graphical representation of the transcriptional shift in secondary metabolism. Each orange or blue box represents a unique differentially expressed transcript encoding a protein/enzyme. Pink boxes represent major biosynthesis pathways/processes.
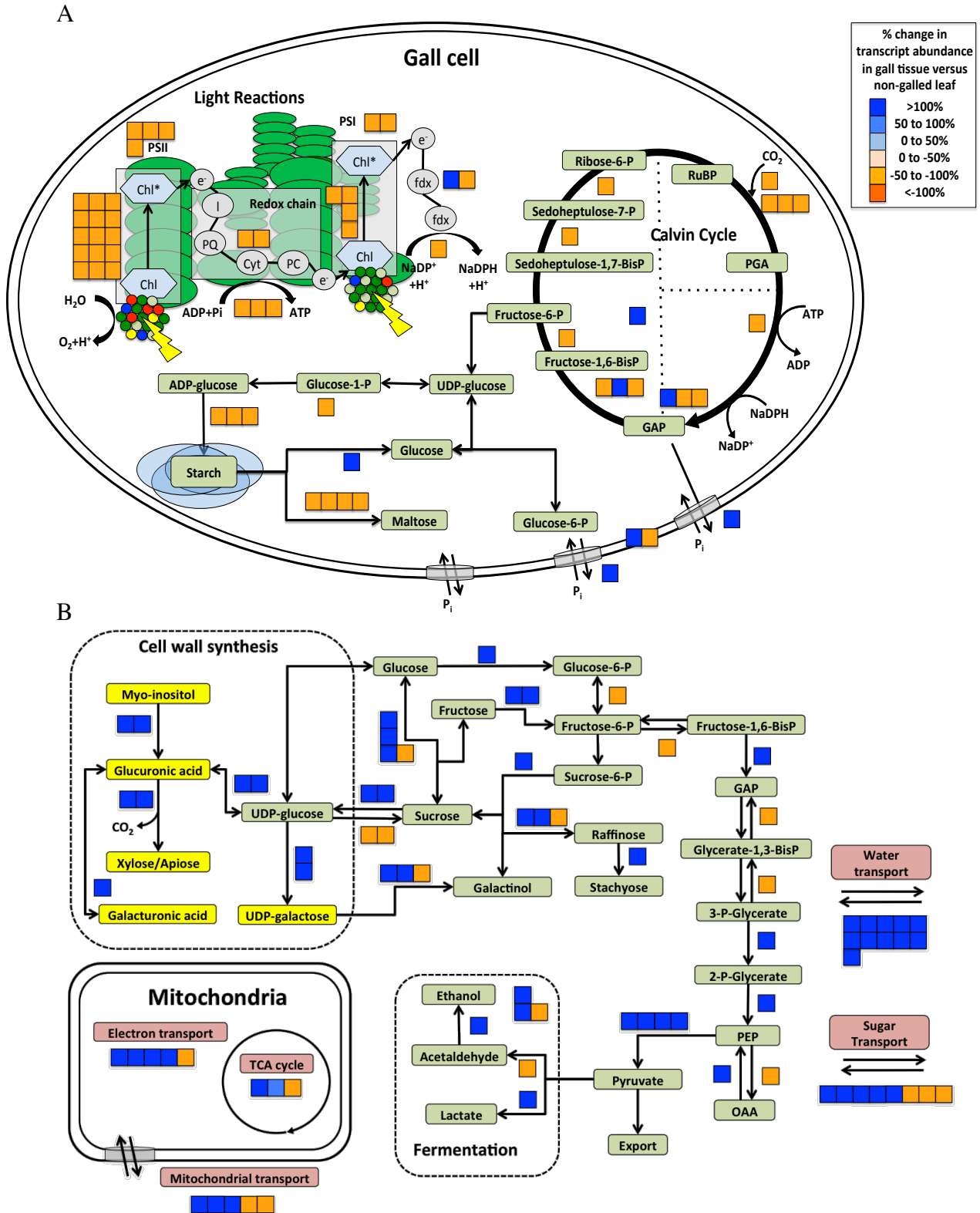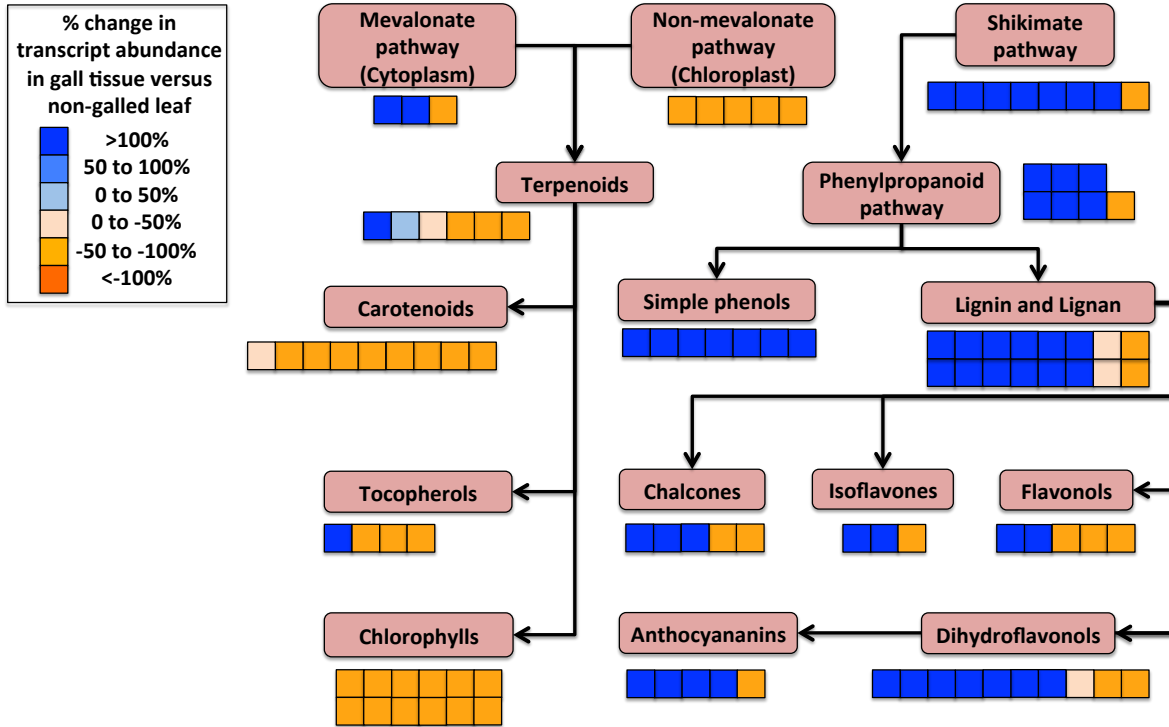
Figure 5.8. Graphical representation of the transcriptional shift in biotic defense signaling. Each orange or blue box represents a unique differentially expressed transcript encoding a protein/enzyme. Green boxes represent metabolites and enzymes whereas pink boxes represent processes.
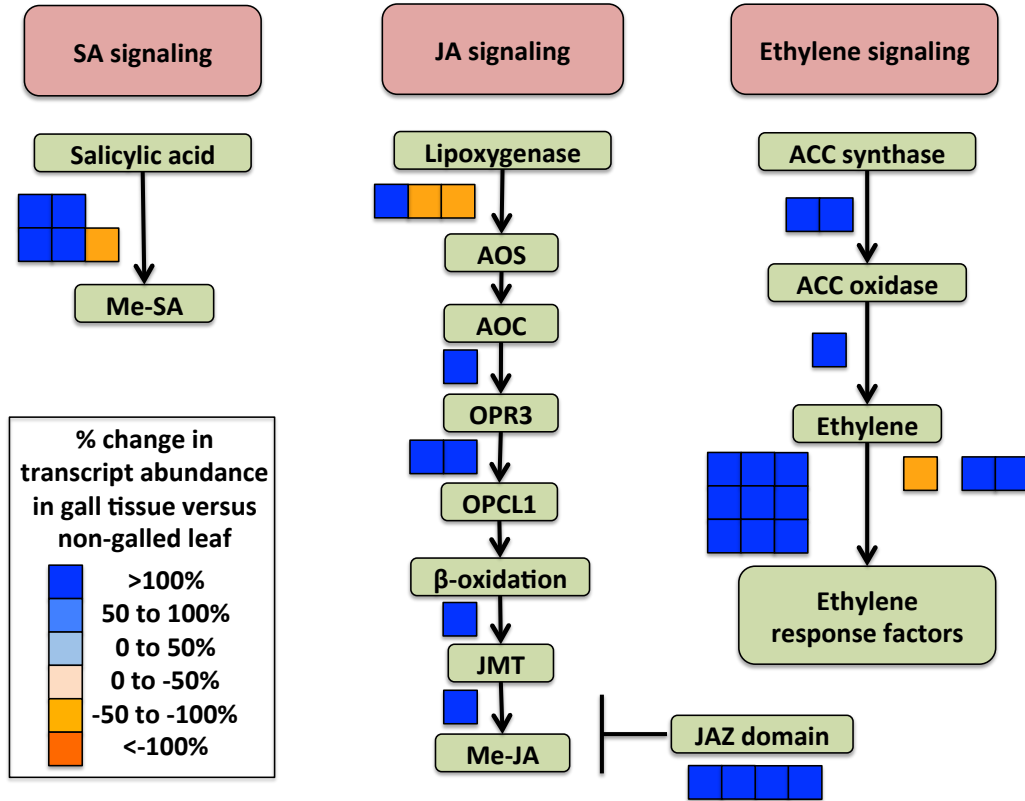
Table 5.1S. *Arabidopsis* (TAIR v.9) identifier and its corresponding *Vitis vinifera* transcript ID from release 12x (Phytozome v.7).

TAIR v. 9	Transcript ID	TAIR v. 9	Transcript ID
at1g02000	GSVIVT01031680001	at1g20020	GSVIVT01009925001
at1g02000	GSVIVT01018554001	at1g22170	GSVIVT01008997001
at1g02180	GSVIVT01018345001	at1g23800	GSVIVT01020227001
at1g03130	GSVIVT01017944001	at1g23800	GSVIVT01032500001
at1g03130	GSVIVT01001159001	at1g23800	GSVIVT01000602001
at1g03600	GSVIVT01030552001	at1g32900	GSVIVT01027437001
at1g04920	GSVIVT01020928001	at1g32900	GSVIVT01018618001
at1g08200	GSVIVT01036152001	at1g32900	GSVIVT01019680001
at1g08200	GSVIVT01015684001	at1g32900	GSVIVT01028521001
at1g08200	GSVIVT01031418001	at1g34000	GSVIVT01034578001
at1g08200	GSVIVT01038790001	at1g47840	GSVIVT01009899001
at1g11720	GSVIVT01012723001	at1g55740	GSVIVT01014778001
at1g11720	GSVIVT01004632001	at1g56190	GSVIVT01036773001
at1g12240	GSVIVT01006154001	at1g56560	GSVIVT01031267001
at1g12240	GSVIVT01001272001	at1g56600	GSVIVT01031278001
at1g12780	GSVIVT01019833001	at1g56600	GSVIVT01031280001
at1g12900	GSVIVT01032942001	at1g56600	GSVIVT01034938001
at1g14030	GSVIVT01003217001	at1g56600	GSVIVT01031285001
at1g14150	GSVIVT01019955001	at1g56600	GSVIVT01017634001
at1g14520	GSVIVT01016929001	at1g56600	GSVIVT01031282001
at1g14520	GSVIVT01016931001	at1g60470	GSVIVT01013763001
at1g15820	GSVIVT01029789001	at1g61800	GSVIVT01012648001
at1g16300	GSVIVT01036751001	at1g61800	GSVIVT01001996001
at1g19150	GSVIVT01015045001	at1g62660	GSVIVT01018625001
at1g20020	GSVIVT01018772001	at1g69830	GSVIVT01032922001

Table 5.1S. (continued)

TAIR v. 9	Transcript ID	TAIR v. 9	Transcript ID
at1g69830	GSVIVT01020069001	at2g29990	GSVIVT01005840001
at1g71890	GSVIVT01034886001	at2g30570	GSVIVT01000743001
at1g73110	GSVIVT01016062001	at2g30570	GSVIVT01036277001
at1g73370	GSVIVT01035210001	at2g34430	GSVIVT01028204001
at1g73370	GSVIVT01029388001	at2g34430	GSVIVT01021406001
at1g74030	GSVIVT01008197001	at2g34430	GSVIVT01021405001
at1g76450	GSVIVT01013427001	at2g35840	GSVIVT01029753001
at1g77090	GSVIVT01010018001	at2g35840	GSVIVT01022530001
at1g77120	GSVIVT01026505001	at2g36460	GSVIVT01033791001
at1g77120	GSVIVT01026507001	at2g36830	GSVIVT01025038001
at1g77120	GSVIVT01010024001	at2g36830	GSVIVT01033677001
at1g77120	GSVIVT01026510001	at2g37170	GSVIVT01016276001
at1g77120	GSVIVT01026508001	at2g37170	GSVIVT01025188001
at1g77120	GSVIVT01010027001	at2g39730	GSVIVT01024910001
at1g77210	GSVIVT01015332001	at2g39730	GSVIVT01016501001
at1g80760	GSVIVT01034224001	at2g39730	GSVIVT01034123001
at2g01140	GSVIVT01011810001	at2g45290	GSVIVT01027667001
at2g05710	GSVIVT01030588001	at2g45290	GSVIVT01018555001
at2g05710	GSVIVT01037657001	at2g45960	GSVIVT01023078001
at2g06520	GSVIVT01035449001	at2g45960	GSVIVT01024113001
at2g17270	GSVIVT01022311001	at2g46820	GSVIVT01027447001
at2g17270	GSVIVT01023867001	at2g47180	GSVIVT01028174001
at2g21330	GSVIVT01018820001	at2g47180	GSVIVT01028176001
at2g24270	GSVIVT01023590001	at2g47180	GSVIVT01031274001
at2g24270	GSVIVT01035891001	at2g47180	GSVIVT01031284001
at2g25810	GSVIVT01035640001	at3g01440	GSVIVT01014586001

Table 5.1S. (continued)

TAIR v. 9	Transcript ID	TAIR v. 9	Transcript ID
at3g04120	GSVIVT01037165001	at3g53520	GSVIVT01025596001
at3g04120	GSVIVT01037176001	at3g54050	GSVIVT01034034001
at3g04120	GSVIVT01010328001	at3g54050	GSVIVT01034037001
at3g04120	GSVIVT01037170001	at3g54820	GSVIVT01025681001
at3g04790	GSVIVT01021828001	at3g55800	GSVIVT01016373001
at3g14410	GSVIVT01027148001	at3g57520	GSVIVT01002784001
at3g14940	GSVIVT01020705001	at3g57520	GSVIVT01033305001
at3g14940	GSVIVT01014206001	at3g57520	GSVIVT01004662001
at3g16240	GSVIVT01017042001	at3g57520	GSVIVT01005620001
at3g17670	GSVIVT01029370001	at3g57520	GSVIVT01007597001
at3g22370	GSVIVT01022814001	at3g59480	GSVIVT01010790001
at3g22960	GSVIVT01037043001	at4g00370	GSVIVT01026946001
at3g22960	GSVIVT01018079001	at4g00430	GSVIVT01026944001
at3g22960	GSVIVT01003140001	at4g00430	GSVIVT01021012001
at3g26650	GSVIVT01001128001	at4g00430	GSVIVT01032861001
at3g27690	GSVIVT01014074001	at4g00430	GSVIVT01026942001
at3g27690	GSVIVT01030053001	at4g00490	GSVIVT01026922001
at3g29360	GSVIVT01011507001	at4g01470	GSVIVT01016615001
at3g43190	GSVIVT01015018001	at4g01970	GSVIVT01034980001
at3g48000	GSVIVT01007784001	at4g01970	GSVIVT01028143001
at3g48000	GSVIVT01020224001	at4g05020	GSVIVT01006114001
at3g52990	GSVIVT01033605001	at4g09650	GSVIVT01001595001
at3g52990	GSVIVT01033599001	at4g10380	GSVIVT01019729001
at3g52990	GSVIVT01033747001	at4g10960	GSVIVT01019547001
at3g52990	GSVIVT01034684001	at4g10960	GSVIVT01019545001
at3g53520	GSVIVT01025597001	at4g13430	GSVIVT01027922001

Table 5.1S. (continued)

TAIR v. 9	Transcript ID	TAIR v. 9	Transcript ID
at4g13430	GSVIVT01029978001	at4g37870	GSVIVT01003710001
at4g15210	GSVIVT01030642001	at4g37870	GSVIVT01005596001
at4g16480	GSVIVT01006723001	at4g39460	GSVIVT01022254001
at4g17090	GSVIVT01013272001	at4g39460	GSVIVT01001423001
at4g17260	GSVIVT01001303001	at5g02120	GSVIVT01034129001
at4g17260	GSVIVT01027640001	at5g05820	GSVIVT01024817001
at4g18240	GSVIVT01021404001	at5g08570	GSVIVT01034344001
at4g18240	GSVIVT01032233001	at5g08740	GSVIVT01022367001
at4g18910	GSVIVT01035178001	at5g11110	GSVIVT01035882001
at4g18910	GSVIVT01021274001	at5g12860	GSVIVT01025268001
at4g21490	GSVIVT01006508001	at5g15490	GSVIVT01007910001
at4g21490	GSVIVT01030007001	at5g15490	GSVIVT01012198001
at4g26260	GSVIVT01015266001	at5g18840	GSVIVT01022027001
at4g26530	GSVIVT01014837001	at5g18840	GSVIVT01017845001
at4g28390	GSVIVT01005827001	at5g18840	GSVIVT01017836001
at4g28390	GSVIVT01004268001	at5g18840	GSVIVT01017844001
at4g28390	GSVIVT01020575001	at5g19220	GSVIVT01017911001
at4g28660	GSVIVT01028434001	at5g20250	GSVIVT01015589001
at4g34240	GSVIVT01022356001	at5g22620	GSVIVT01005201001
at4g34860	GSVIVT01009904001	at5g22620	GSVIVT01031393001
at4g34860	GSVIVT01024105001	at5g24030	GSVIVT01028789001
at4g35300	GSVIVT01022309001	at5g46110	GSVIVT01012209001
at4g35300	GSVIVT01023868001	at5g46110	GSVIVT01021114001
at4g35300	GSVIVT01013414001	at5g46110	GSVIVT01012210001
at4g36670	GSVIVT01018988001	at5g51545	GSVIVT01018558001
at4g37870	GSVIVT01006166001	at5g51830	GSVIVT01018449001

Table 5.1S. (continued)

TAIR v. 9	Transcript ID	TAIR v. 9	Transcript ID
at5g51830	GSVIVT01027578001	atcg00280	GSVIVT01003327001
at5g54270	GSVIVT01003201001	atcg00280	GSVIVT01027074001
at5g54270	GSVIVT01014439001	atcg00280	GSVIVT01006662001
at5g54270	GSVIVT01003204001	atcg00340	GSVIVT01009295001
at5g54960	GSVIVT01021184001	atcg00340	GSVIVT01017483001
at5g54960	GSVIVT01004503001	atcg00350	GSVIVT01017484001
at5g54960	GSVIVT01005052001	atcg00350	GSVIVT01023733001
at5g54960	GSVIVT01003940001	atcg00350	GSVIVT01014968001
at5g56350	GSVIVT01033379001	atcg00480	GSVIVT01029711001
at5g56350	GSVIVT01025504001	atcg00480	GSVIVT01006210001
at5g58330	GSVIVT01016172001	atcg00480	GSVIVT01033373001
at5g59250	GSVIVT01024909001	atcg00490	GSVIVT01013856001
at5g61580	GSVIVT01013938001	atcg00490	GSVIVT01022403001
at5g64860	GSVIVT01022223001	atcg00540	GSVIVT01013928001
atcg00020	GSVIVT01016441001	atcg00540	GSVIVT01015185001
atcg00070	GSVIVT01037458001	atcg00590	GSVIVT01006217001
atcg00140	GSVIVT01021581001	atcg00680	GSVIVT01028641001
atcg00270	GSVIVT01010924001	atcg00680	GSVIVT01006503001
atcg00270	GSVIVT01029661001		

139

CHAPTER 6

SUMMARY

The research presented in this dissertation examined the leaf-level alterations in photosynthesis resulting from insect herbivory. I established a conceptual framework that identified four mechanisms for how photosynthesis in the remaining leaf tissue changes after (and during) an herbivore attack. Feeding damage reduces photosynthesis in remaining tissues by severing vasculature (Aldea et al. 2006, Tang et al. 2006), altering sink/source relationships (Dorchin et al. 2006, Patankar et al. 2011), releasing autotoxic metabolites (Zangerl et al. 2002, Gog et al. 2005), and suppressing photosynthetic gene expression and function upon the induction of defenses (Bilgin et al. 2010). These mechanisms are not mutually exclusive, however, and likely interact in ways where the ultimate cost to fitness is yet to be determined. As a first step toward elucidating significant components of these interactions, I examined leaf-level responses under conditions of climate change we expect to see in the year 2050. Then I examined two mechanisms in-depth by coupling ecophysiology with genetics. My goal in this dissertation was to visualize the manipulation of photosynthesis by herbivores that reduces plant function, and ultimately impacts fitness and ecosystem productivity.

Leaf architecture determines the magnitude and duration of photosynthetic suppression in remaining tissue and, as a result, may predict the response of these tissues to herbivore attack. Palmate leaves with multiple first-order veins decrease stomatal conductance minimally, if at all, whereas pinnate leaves of single first-order veins decrease conductance greatly when first order veins are severed (Sack et al. 2008). When leaves are compared among the few studies that use imaging technologies (Aldea et al. 2006, Chapter 3) using a meta-analysis, leaf type tends to interact with herbivore damage type (Figure 6.1). Galling herbivory reduces F_q'/F_m' in remaining

140

tisues more in palmate leaves (n = 3) than similar tissues in pinnate leaves (n = 8). Chewing

herbivory damages F_q'/F_m' in pinnate (n = 13) more than palmate leaves (n = 1), although more

data points are necessary to resolve statistical effects. These data convey the importance of

vascular redundancy to defoliation tolerance (Sack et al. 2008) and suppression of

photosynthesis in remaining visibly unaltered tissues but indicate the need for additional data

within and beyond temperate ecosystems.

Recent surveys of different damage types indicate that gall formation alters leaf function

with a great degree of species specificity. In eastern hardwood trees, F_q'/F_m' decreases a great

distance from the insect (Aldea et al. 2006) yet in aspen trees the propagated damage was

minimal (Chapter 3). However, gall formation repeatedly reduced leaf temperature in adjacent

tissues in these surveys, and again when I examined a local galling interaction in the phylloxera-

grape system (Figure 6.2). Accordingly then, how does the energy balance of a leaf change under

gall attack and what does this mean for the plant-insect interaction? Few investigations have

attempted to answer this question but the data indicate a strong link between insect fitness and

the microclimate of the leaf (see Pincebourde et al. 2006). Given that stomatal aperture will

decrease under increasing atmospheric $[CO_2]$ and reduce transpiration-driven nutrient flux to

developing sinks, warmer leaf temperatures will interact with sink demand to alter the selective

environment for galling insects, largely by altering competition among sinks.

The interdependence of the four mechanisms discussed in Chapter 1 increases the

difficulty in parsing out which mechanisms are driving alterations in remaining leaf tissue. One

way I addressed this complexity was by coupling spatial assessments of whole leaf-level

physiology with plants genetically suppressed in defense-signaling pathways. This simple design

allowed me to capture the herbivore-induced photosynthetic suppression associated with defense

signaling that has been suggested by transcriptomic evidence (see Bilgin et al. 2010) yet not physiologically realized. To this end, my research identified that a ubiquitous defense response in plants suppresses electron transport in remaining leaf tissue. While sequential synthesis and mobilization of defense metabolites maintained the suppression in photosynthesis, the initial wound signal (JA) correlated strongest with suppressed electron transport. This suggests JA and the upstream lipoxygenase-mediated signaling components regulate light harvesting at the transcriptional and physiological level, and then degrees of autotoxicity (with nicotine) and resource trade-offs (to TPIs) accounted for the remaining costs to photosynthesis. Current research links circadian-regulation pathways to JA signaling (Goodspeed et al. 2012) and increasing $[CO_2]$ to suppression of JA-signaling (Zavala et al. 2008), and reinforces the link between photosynthesis and jasmonic acid signaling in plants. Future studies will sort out the exact mechanisms that couple the trade-offs between photosynthesis and defense signaling, which are likely highly conserved and ubiquitously interactive (e.g., map kinases).

Phloem feeding and galling insects induce sinks by unloading phloem either to their midguts or to induced tissue growth The genetic basis for insect manipulation of sink identity was largely anecdotal until we assesed the gall transcriptome in Chapter 5. Given the extensive literature on the phylloxera-grape system (see Granett et al. 2001), especially on chemical profiles within gall tissue (e.g., Kellow et al. 2004, Lawo et al. 2011), the transcriptomic data provide strong support for 150 years of descriptive biology. Phylloxerids, thus far, appear unique in their ability to induce stomata (see Owen 1891), and may use this morphology to enhance transpiratory efflux and ultimately nutrient transport. This level of insect control is largely confirmed in the transcriptomic profile of gal tissue where an insect-induced tissue has enhanced expression patterns of plant nutrient transporters. The development of stomata evolved either

through the act of galling coopting a network that shares components of asymmetric cell division

or altering the hormonal mileu and thereby stimulating the stomatal lineage by yet unidentified

mechanisms. Given the data presented in Chapter 5, phylloxera likely induce gall formation

through a complex mix of hormones similar to *Rhodoccocus fascians* (Stes et al. 2011) and may

secrete a cysteine enriched signaling peptide to augment stomata development (Marshall et al.

2011), although additional stage-specific data are necessary to elucidate these pathways. It will

be interesting to pursue this interaction across *Vitis* species especially in the context of inter- and

intraspecific competition within a leaf given the apparent manipulation by phylloxera of both

sink and source dynamics.

LITERATURE CITED

Aldea M, Hamilton, JG, Resti JP, Zangerl AR, Berenbaum MR, Frank TD, DeLucia EH. 2006. Comparison of photosynthetic damage from arthropod herbivory and pathogen infection in understory hardwood samplings. Oecologia 149: 221-232.

Bilgin DD, Zavala JA, Zhu J, Clough SJ, Ort DR, DeLucia EH. 2010. Biotic stress globally down-regulates photosynthesis genes. Plant Cell and Environment. 33: 1597-1613.

Dorchin N, Cramer MD, Hoffmann JH. 2006. Photosynthesis and sink activity of wasp-induced galls in *Acacia pycnantha*. Ecology 87: 1781–1791.

Gog L, Berenbaum MR, DeLucia EH, Zangerl AR. 2005. Autotoxic effects of essential oils on photosynthesis in parsley, parsnip, and rough lemon. Chemoecology 15: 115–119.

Goodspeed D, Chehab EW, Min-Venditti A, Braam J, Covington MF. 2012. Arabidopsis synchronizes jasmonate-mediated defense with insect circadian behavior. Proceedings of the National Academy of Sciences, USA 109: 4674-4677.

Granett J, Walker MA, Kocsis L, Omer AD. 2001. Biology and management of grape phylloxera. Annual Review of Entomology 46: 387-412.

Kellow AV, Sedgley M, Van Heeswijck R. 2004. Interaction between *Vitis vinifera* and grape phylloxera: changes in root tissue during nodosity formation. Annals of Botany 93: 581-590.

Lawo NC, Weingart GJ, Schumacher R, Forneck A. 2011. The volatile metabolome of grapevine roots: first insights into the metabolic response upon phylloxera attack. Plant Physiology and Biochemistry 49: 1059-1063.

Marshall E, Costa LM, Gutierrez-Marcos J. 2011. Cysteine-rich peptides (CRPs) mediate diverse aspects of cell-cell communiation in plant reproduction and development. Journal of Experimental Botany 62: 1677-1686.

Owen DA. 1891. Some strange developments upon *Carya alba* caused by phylloxera. Proceedings of the Indiana Academy of Sciences p76.

Patankar R, Thomas SC, Smith SM. 2011. A gall-inducing arthropod drives declines in canopy photosynthesis. Oecologia 167: 701-709.

Pincebourde S, Frak E, Sinoquet H, Regnard JL, Casas J. 2006. Herbivory mitigation through increased water-use efficiency in a leaf-mining moth-apple tree relationship. Plant Cell and Environment 29: 2238-2247.

Sack L, Dietrich EM, Streeter CM, Sanchez-Gomez D, Holbrook NM. 2008. Leaf palmate venation and vascular redundancy confer tolerance of hydraulic disruption. Proceedings of the National Academy of Sciences USA 105: 1567-1572.

Stes E, Vandeputte OM, El Jaziri M, Holsters M, Vereecke D. 2011. A successful bacterial coup d'état: how *Rhodococcus fascians* redirects plant development. Annual Review of Phytopathology 49: 69-86.

Tang JY, Zielinski RE, Zangerl AR, Crofts AR, Berenbaum MR, DeLucia EH. 2006. The differential effects of herbivory by first and fourth instars of *Trichoplusia ni* (Lepidoptera: Noctuidae) on photosynthesis in *Arabidopsis thaliana*. Journal of Experimental Botany 57: 527–536.

Zangerl AR, Hamilton JG, Miller TJ Crofts AR, Oxborough K, Berenbaum MR, DeLucia EH. 2002. Impact of folivory on photosynthesis is greater than the sum of its holes. Proceedings of the National Academy of Sciences USA 99: 1088–1091.

Zavala JA, Casteel CL, DeLucia EH, Berenbaum MR. 2008. Anthropogenic increase in carbon dioxide compromises plant defense against invasive insects. Proceedings of the National Academy of Sciences USA 105: 5129-5133.

Figure 6.1. Box plots showing smallest and largest value, upper and lower quartile, and median percent change (when calculatable) in operating efficiency of photosystem II (F_q'/F_m') in remaining leaf tissue attacked by chewing or galling insects when compared using a metaanalysis of species categorized as having either pinnate or palmate venation. Data are from Aldea et al. 2006 and Chapter 3.
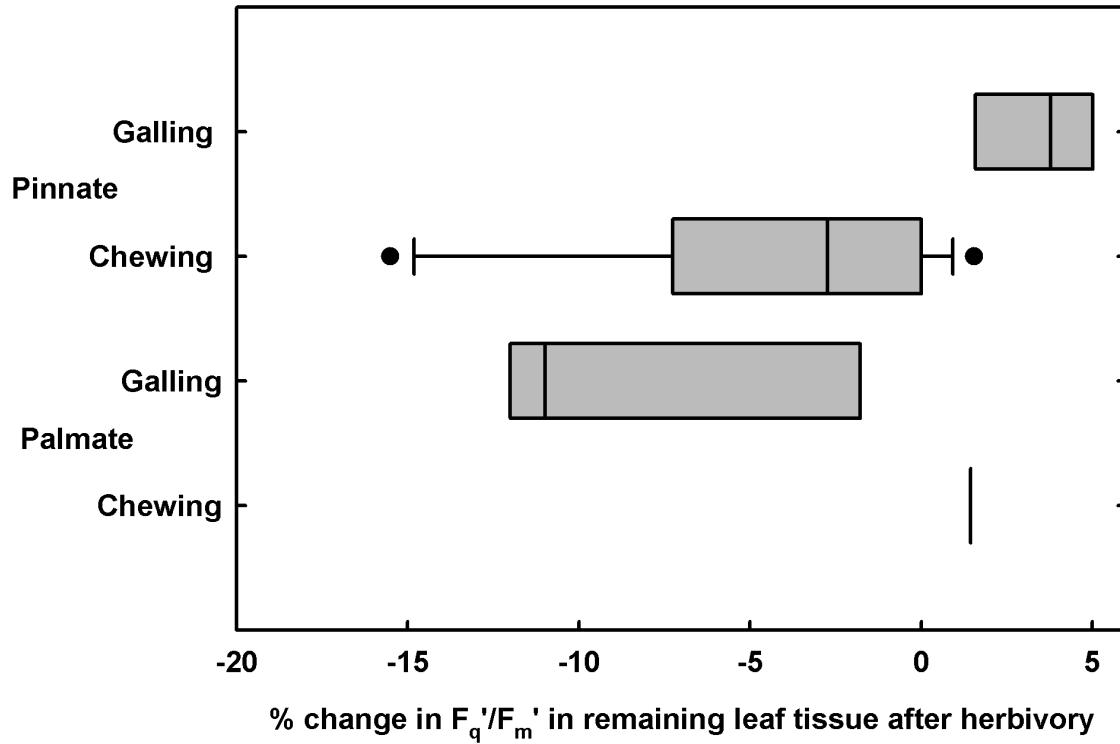
Figure 6.2. Phylloxera parasitism of grape reduced leaf temperature a minimal distance (< 1 mm); however the gall temperature was 0.5 ± 0.2 °C cooler than adjacent tissues (one sided paired t test, df = 5, P = 0.04).